Transcriptional Regulation of Yeast *CUP1* gene

by

Roshini Nilupama Wimalarathna

A dissertation submitted to the Graduate Faculty in Biology in partial fulfillment of the requirements for the degree of

Doctor of Philosophy

The City University of New York

2012

This manuscript has been read and accepted for the Graduate Faculty in Biology in satisfaction of the dissertation requirement for the degree of Doctor of Philosophy.

_____	_____
Date	Chair of Examination Committee
	Dr. Chang-Hui Shen, College of Staten Island
_____	_____
Date	Executive Officer
	Dr. Laurel A. Eckhardt
	Dr. Probal Banerjee, College of Staten Island
	Dr. Jimmie E. Fata, College of Staten Island
	Dr. Qi He, Brooklyn College
	Dr.Yu-Wen Hwang, NYS Institute for Basic Research
	Dr. Sujin Bao, Mount Sinai School of Medicine

Supervising Committee

The City University of New York

Abstract

Transcriptional Regulation of Yeast *CUP1* gene

by

Roshini Nilupama Wimalarathna

Adviser: Dr. Chang-Hui Shen

The yeast *CUP1* gene encodes a metallothionein required for cell growth at high copper concentrations. The induction of *CUP1* with copper results in activator-dependent nucleosome repositioning. To further understand the mechanism of *CUP1* activation, it is necessary to identify which chromatin remodeler(s) is/are involved in *CUP1* induction. Here, we demonstrated that both *ino80*Δ and *snf2*Δ cells grew well in the absence of copper, but were inviable in the presence of copper, indicating that they are required for *CUP1* expression. Furthermore, *CUP1* mRNA did not significantly increase in mutants lacking either remodeler in the presence of copper**,** suggesting that they regulate *CUP1* induction at the transcriptional level. Both *isw1Δ* and *rsc3Δ* cells displayed similar growth patterns as WT cells in the presence of copper. Further *CUP1* mRNA was significantly increasing in both *isw1Δ* and *rsc3Δ* cells showing similar pattern as WT cells. This observation suggests that ISW1 and RSC3 remodeling complexes have no positive effect in *CUP1* expression. We also demonstrated, using chromatin immunoprecipitation, that both INO80 and SWI/SNF are present at the promoter in the wild type cells and they were dependent on each other to be recruited to the *CUP1* promoter. Both chromatin remodeling activity and targeted histone acetylation were not observed in *ino80*Δ or

*snf2*Δ strains at the *CUP1* promoter. These results suggest that both INO80 and SWI/SNF directly participate in *CUP1* chromatin remodeling, and that histone acetylation is recruited after the arrival of chromatin remodelers. We also observed that more *pol*II was recruited to the *CUP1* promoter under inducing conditions and that such a recruitment was not observed in *ino80*Δ or *snf2*Δ strains. Furthermore, we observed that both Snf2p and Ino80p were activator-dependent. Our observations provide direct evidence for the involvement of both INO80 and SWI/SNF remodelers in *CUP1* activation. In light of these findings, we propose a working model for *CUP1* activation.

Acknowledgements

I respectfully express my deepest gratitude and appreciation to my mentor, Dr. Chang-Hui Shen, for his kindness, patience supervision and guidance during the entire project. I always believe that I was lucky to have such an encouraging, helpful and an understanding person as my mentor within these six years. I would also like to sincerely thank my examination committee, Dr Probal Banerjee, Dr. Jimmie E. Fata, Dr. Qi He, Dr. Yu-Wen Hwang and Dr. Sujin Bao for their helpful suggestions and discussions.

My affectionate gratitude goes to my dearest friends and lab partners for helping me in both personal and academic matters during these six years. My special thanks goes to graduate students, Paulina Konarzewska, Michelle Esposito, and Goldie Lazarus for being my family at the lab, and helping me to complete this project in many ways including, proof reading and covering some of my classes. Equally my deepest gratitude goes to Po Pan and Wei-Chun Tang for helping me in my research. I also like to extend my gratitude to Dr. Priya Ranjan for passing his scientific wisdom and knowledge.

I would like to give my deepest gratitude to College of Staten Island and Graduate center for providing me financial support for my graduate education and for giving me an excellent platform to improve my teaching and research skills. Equally my deepest gratitude goes to the members of Biology department at College of Staten Island for being supportive in all these years.

Last but not least, I would like to thank from the bottom of my heart to my parents, and husband Sanjeewaka Gunadasa for their understanding, encouragement, patience and continuous support. My special thanks go to my loving daughter, Tharushi Gunadasa for sacrificing her mother-daughter time to help me to achieve my goals. It would not have been possible to complete my Ph.D. this successfully, without the love and support of my family.

Roshini Nilupama Wimalarathna.

Table of Contents

List of Tables and Figures

Abbreviations

ATP	Adenosine- triphosphate
BAF	BRG1 or hbrm associated factor
BAP	Brahma associated proteins
CHD	Chromatin-helicase DNA binding protein
ChIP	Chromatin immuno precipitation
DEPC	Diethylpyrocarbonate
DNA	Deoxyribonucleic acd
dNTp's	Deoxynucleotriphosphate
dTTP	Deoxythymidine triphosphate
dUTP	Deoxyuridine triphosphate
EDTA	Ethylenediaminetetraacetic acid
EtBr	Ethidium bromide
HAT	Histone actyltransferases
HDAC	Histone deacetylases
HMT	Histone methyltransferas
ISWI	Imitation switch
KDAC	Lysine deacetylases
LB	Lysogeny Broth
MGB probe	Minor groove binder probe
ORF	Open reading frame
PBAF	Polybromo associated BAF

PBAP	Polybromo associated BAP
PCR	Polymerase chain reaction
PMSF	Phenylmethanesulfonylfluoride or phenylmethylsulfonyl fluoride
qPCR	Quantitative polymerase chain reaction
qRT-PCR	Real time quantitative polymerase chain reaction
RNA	Ribonucleic acid
ROX dye	Carboxy-X-rhodamine dye
RSC	Remodels the structure of chromatin
RT-PCR	Reverse transcriptase polymerase chain reaction
SAGA	Spt-Ada-Gcn5 acetyltransferase
SANT	SWI3, ADA2, N-CoP and TFIIIB domain
SC	Synthetic Complete
SDS	Sodium Dodecyl Sulphate
SLIDE	SANT like ISWI domain
SLIK	SAGA-like
SM	Spheroplast Medium
SWI/SNF	Switching deficient/ sucrose non fermenting
TAE	Tris- acetate ethylenediaminetetraacetic acid
TBE	Tris-borate- ethylenediaminetetraacetic acid buffer
TBP	TATA binding protein
TBS	Tris-buffered saline
TE	Tris- ethylenediaminetetraacetic acid
TES	Tris- ethylenediaminetetraacetic acid -sodium dodecyl sulphate buffer

TSA	Trichostatin A
UAS	Upstream activating sequence
UDG	Uracil DNA glycosylase
WT	Wild type

CHAPTER 1

1 Introduction

1.1 Chromatin Structure

Chromatin is the structure that the eukaryotic genome is packed into, the nucleus by allowing meters of DNA to fit into the small volume. The chromatin is composed of DNA and proteins, most of these proteins are histones. The nucleosome is the fundamental repeating unit of the chromatin. This vast amount of DNA wraps around histone proteins and gives rise to the nucleosome. Non-histone proteins are responsible for folding the thread of the nucleosome into the structures of higher order fibers (McGhee *et al*., 1980; Kornberg *et a*l., 1992).

1.1.1 Nucleosome and Histones (Core histones and Linker histones)

The nucleosome is 11-nm in diameter and 6-nm in height flat disk or cylinder (Figure 1.1). Individual nucleosomes can be obtained by treating chromatin with the endonuclease micrococcal nuclease**,** which is a DNA degrading enzyme. Crystallographic structure studies have revealed that 146 base pairs of DNA are wrapped in a left-handed superhelix 1.7 times around an octameric histone core (Luger *et al*., 1997).

This octameric histone core consist**s** of two copies of each of the histone molecules H2A, H2B, H3 and H4, with a total mass of about 100,000 dalton (Luger *et al*., 1997; Luger *et al*., 2003). Histone**s** H3 and H4 are highly conserved in all eukaryotes which suggested that their

functions are identical in all eukaryotes. Even though there is a very small species specific variation in the sequence of the H2A and H2B, they can also be recognized in all eukaryotes (McGhee *et al*., 1980). Each core histone contains an N- terminal domain that extends from the surface of the octomer (Figure 1.1). The histone tails are targets of the post-translational modifications. These modifications include lysine acetylation and methylation, serine phosphorylation, ubiquitination, sumoylation and ADP-ribosylation (Margueron *et al*., 2005).

The repeating nucleosome cores further arranges into higher-order structures and these higher order structures are stabilized by the linker histone, H1 (Graziano *et al*., 1994; Luger *et al*., 1998). The role of H1 is different from the core histones. Linker histones are present in half the amount of the core histones. The linker histone H1 binds the nucleosome at the entry and exit sites of the DNA (Figure 1.2). The H1 histones are larger than core histones and can be extracted more readily from chromatin by using a diluted salt solution. It has been less conserved during evolution than the core histones. The H1 molecule has a globular central region which is evolutionary conserved and an amino-terminal and a carboxyl-terminal, which are less conserved. The globular domain binds to a nucleosome and its arms extend to contact the histone core of adjacent nucleosomes and pull the adjacent nucleosomes together. The H1 histone thus plays a major role in arranging the nucleosomes into a regular repeating array (Thoma *et al*., 1979; Brown *et al*., 2001).

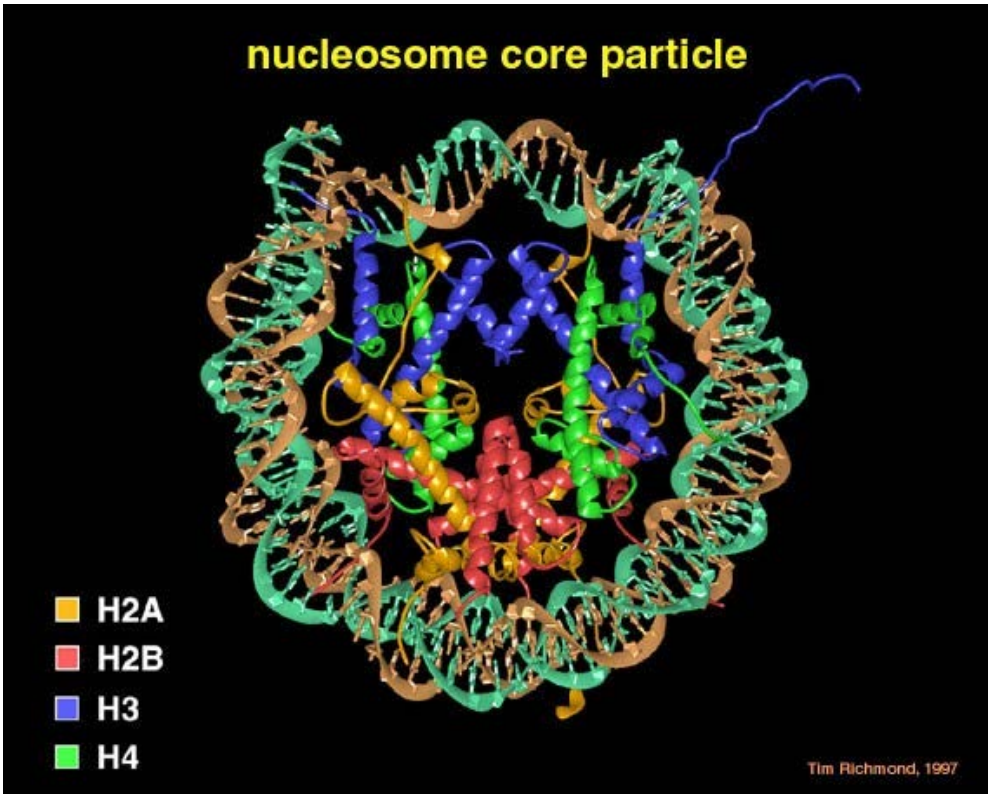

Figure 1.1 Nucleosome. The crystal structure of a nucleosome core particle, viewed down the super-helical axis. The nucleosome core particle**s** are colored in yellow (H2A), red (H2B), blue (H3) and green (H4) respectively and shows the extension of histone tails. Light blue and brown ribbon shows the DNA wrapped around the nucleosome core particles (Luger *et al*., 1997).

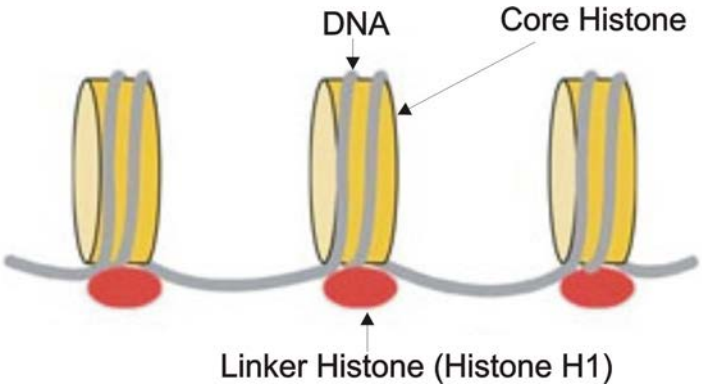

Figure 1.2 Schematic illustration of the position of histone H1 (Brown *et al*., 2001).

1.1.2 Higher order chromatin structure

The higher order structure describes how the 10-nm chromatin structure is packed into a nucleus. This higher order packaging of chromatin is one of the most interesting aspects of chromatin, even though it is still poorly understood today. A 2-nm DNA helix winds around the histones and form the nucleosomes. This gives rise to a 10-nm chromatin fiber which is called "beads on a string" at low ionic strengths (Figure 1.3). Histone H1 is not required for this 10-nm structure (Tremethick *et al*., 2007).

The next order of DNA organization in the chromatin is the packing of nucleosomes into the 30-nm chromatin fibers. This level of packaging requires histone H1. There are two different models that have been proposed for the arrangement of the 30-nm fibers. They are the solenoid model and the zigzag model. The higher-order chromatin structure is provided by the formation of looped domains. These looped domains may be formed and maintained by DNA-binding proteins. These DNA-binding proteins recognize the regions of specific nucleotide sequences and clamp the 30- nm chromatin fibers together (Alberts *et al*., 1989).

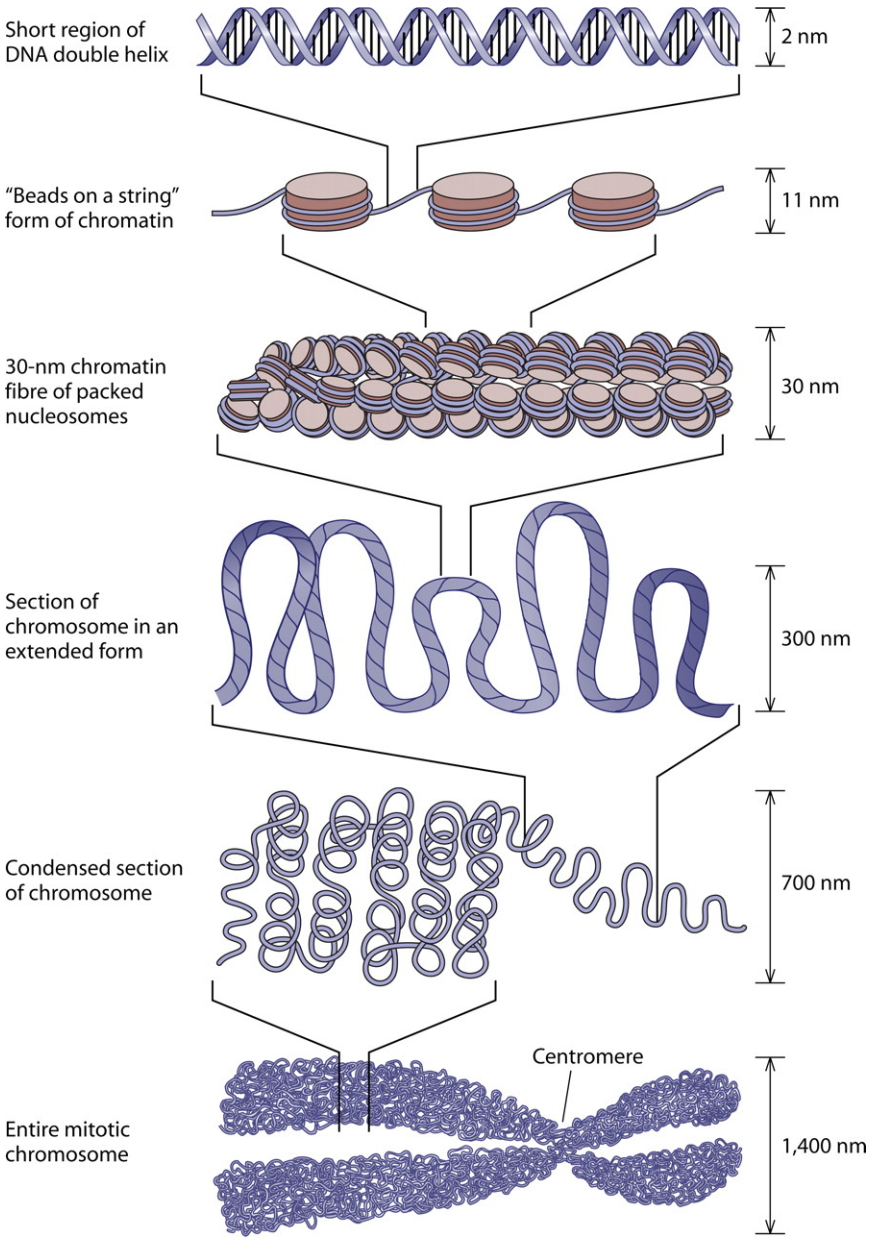

Figure 1.3 Schematic illustration of the packaging of chromatin into its higher order structure (Alberts *et al*., 1998).

1.2 Histone Modification

Although the chromatin structure helps to package a vast amount of DNA into the nucleus, this compaction creates a problem of accessing the DNA for many of the DNA template-based cellular activities, including transcription, replication and recombination. To overcome the repressive effects of chromatin in transcription by RNA polymerase II, the chromatin structure must be perturbed at promoter regions prior to, or during, transcriptional activation by sliding the nucleosomes or disrupting the nucleosomes. There are two types of enzymes that work on the nucleosomes and allow the access of the *trans-acting* factors. One type of these enzymes covalently modifies histone proteins by acetylation, deacetylation, methylation, phosphorylation, ubiquitination, sumoylation, ADP ribosylation, glycosylation, biotinylation and carbonylation. The first four types of modifications have been studied extensively compared to the other modifications. The second type of these enzymes uses ATP hydrolysis to reposition nucleosomes. These enzymes are called ATP-dependent remodeling complexes. These complexes use the free energy generated by ATP hydrolysis to move nucleosomes along DNA, and change the chromatin structure (Smith *et al*., 2005; Kim *et al*., 2006; Margueron *et al.*, 2005).

.2.1 Histone Acetylation and gene activation

It has been shown that acetylation of lysine residues on the core histones' N-terminal tails is normally associated with transcriptionally active genes. In general histone H3 Lys 9, Lys 14, Lys 18 and Lys 23, histone H4, Lys 5, Lys 8, Lys 12 and Lys 16, histone H2A Lys 5 and Lys 9, and histone H2B Lys 5, Lys 12, Lys 15 and Lys 20 are all targets for acetylation (Tsukiyama *et al*., 1999; Marmorstein *et al*., 2001; Roth *et al*., 2001). Histone acetyltransferases (HATs) are the enzymes responsible for the transfer of the ε-amino group of lysine residues. HATs consist of both large multi-subunit complexes and functionally transcriptional coactivators which are recruited to promoters by interaction with DNA-bound activator proteins (Utley *et al*., 1998).

Based on sequence similarity HATs can be grouped into families such as Hat1p, Gcn5p/PCAF, p300/CBP, MYST, p160,CIITA, Atf2p, $TAF_{II}250$, TFIIC, Nut1p, Elp3p, CDY, Hpa2p, TFIIB, MCM3AP, Eco1p and Ard1p (Yang *et al*., 2004; Peterson *et al*., 2004). In terms of subcellular location, HATs can be categorized into two types, Type A and Type B. Type A HATs are found in the nucleus. This type of HAT acetylates histone in chromatin context and may play important roles in the regulation of gene expression by functioning as transcriptional co-activators. Some examples of type A HATs include PCAF, CBP/p300, $TAF_{II}250$, ACTR, Tip60p, Esa1p and Elp3p (Ogryzko *et al*., 1996; Spencer *et al*., 2001; Kelly *et al*., 2000; Yamamoto *et al*., 1997; Mizzen *et al*., 1996; Clarke *et al*., 1999). Type B HATs can be found in the cytoplasm and are involved in the acetylation of nascent histone H3 and histone H4. Hat1p is the sole known type B HAT (Parthun *et al*., 2007; Brownell *et al*., 1996). However, recent

evidence has shown that Hat1p may function in multiple locations (Kelly *et al*., 2000; Poveda *et al*., 2004) and thus not precisely fit into this classification. The Gcn5p/PCAF family is one of the nuclear HATs, which consists of Gcn5p, PCAF and related proteins. Gcn5p was first identified as a type A HAT in *Tetrahymena thermophila* (Brownell *et al*., 1996). Later, the homologs of Gcn5p was found in human, mouse, *Schizosaccharomyces pombe* and *Drosophila melanogaster*, suggesting that its function is highly conserved throughout the eukaryotes (Candau *et al*., 1996; Xu *et al*., 1998; Smith *et al*., 1998; Sterner *et al*., 2000). Gcn5p primarily acetylates histone H3 Lys14 and histone H4 Lys 8 and Lys 16 (Kuo *et al*., 1996). Yeast Gcn5p is required for normal progression through the G2/ M boundary (Kreb *et al*., 2000) and mitotic gene expression (Wenzheng *et al*., 1998).

Histone acetylation can modulate gene transcription at two levels: global histone acetylation and promoter–specific histone acetylation. While global histone acetylation correlates with general transcription activity (Gottesfeld *et al*., 1997), promoter-specific acetylation is a critical mechanism for the control of specific gene activity (Vaissiere *et al*., 2008). In this study, our focus deals with promoter-specific level histone acetylation.

At the promoter-specific level, the induction of *CUP1* with copper in *Saccharomyces cerevisiae* resulted in the targeted acetylation of both H3 and H4 at the *CUP1* promoter. Nucleosomes containing upstream activating sequences and sequences farther upstream were the targets for acetylation (Shen *et al*., 2002).

It has also been shown that the levels of H3 and H4 histone acetylation at the *INO1* promoter and ORF (open reading frame) increased under inducing conditions (Esposito *et al*., 2010). Such an increase is not due to the increase of nucleosome number; instead, it is because the acetylation level per nucleosome increased significantly.

It requires the description of nucleosome repositioning and the changes of histone acetylation to understand the role of histone acetylation in the order of events during gene activation. Relatively few genes have obtained such detailed information including *CUP1* (Shen *et al*., 2001; Shen *et al*., 2002), *PHO5* (Svaren *et al*., 1997), *PHO8* (Reinke *et al*., 2001), *HO* (Cosma *et al*., 1999), and *INO1* (Esposito *et al*., 2010) genes. It has been shown that different roles of acetylation in the mechanisms of gene activation are possible. For example, histone acetylation is not required until a very late stage when a TATA-binding protein binds to the *TATA* box in *CUP1* induction, whereas histone acetylase is recruited by the chromatin remodeler at an early stage in *PHO8* and *HO* induction. As such, HATs could influence gene activation in different pathways.

1.2.2 Histone Deacetylation

Histone deacetylases (HDACs) oppose the effects of HATs by deacetylation the lysine residues. Histone deacetylation reverse the neutralized histone tails back to charged tails and thus promote the interactions between DNA and histone tails. Therefore, histone deacetylation causes condensation of chromatin fibers and gene repression. HDACs are also called lysine deacetylases (KDAC) (Figure 1.4).

HDAC proteins can be divided into four classes (in mammalian) based on their function and DNA sequence similarity. The first and second class of HDACs belong to the classical HDACs and their activities are inhibited by trichostatin A (TSA). The third class of HDACs is a family of NAD+-dependent proteins which are not affected by TSA. HDAC1, HDAC2, HDAC3 and HDAC8 all belong to class I. The HDAC1, HDAC2 and HDAC8 are primarily found in the nucleus, while, HDAC3 is found in both the nucleus and the cytoplasm. HDAC4, HDAC5, HDAC6, HDAC7, HDAC9a, HDAC9b and HDAC10 belong to class II. They can be shuttled in and out of the nucleus in response to certain cellular signals (Longworth *et al*., 2006; de Ruijter *et al*., 2003). HDAC6 is mainly localized in the cytoplasm. The Sirtuins in mammals which are SIRT1, SIRT2, SIRT3, SIRT4, SIRT5, SIRT6 and SIRT7 belongs to class III. Further, HDAC11 is the only HDAC that belongs to class IV (Fischle *et al*., 2002; Hubbert *et al*., 2002). It is localized in the nucleus; however, it has been shown that it can be co-precipitated with the cytoplasmically localized HDAC6. HDAC11 contains a catalytic domain situated at the N-terminus, with proven HDAC activity that can be inhibited by trapoxin (a TSA analogue) (Gao *et al*., 2002).

The yeast (*Saccharomyces cerevisiae*) reduced potassium dependency 3 (Rpd3p) is homologous to class I HDACs, while histone deacetylase 1 (Hda1p) is homologous to

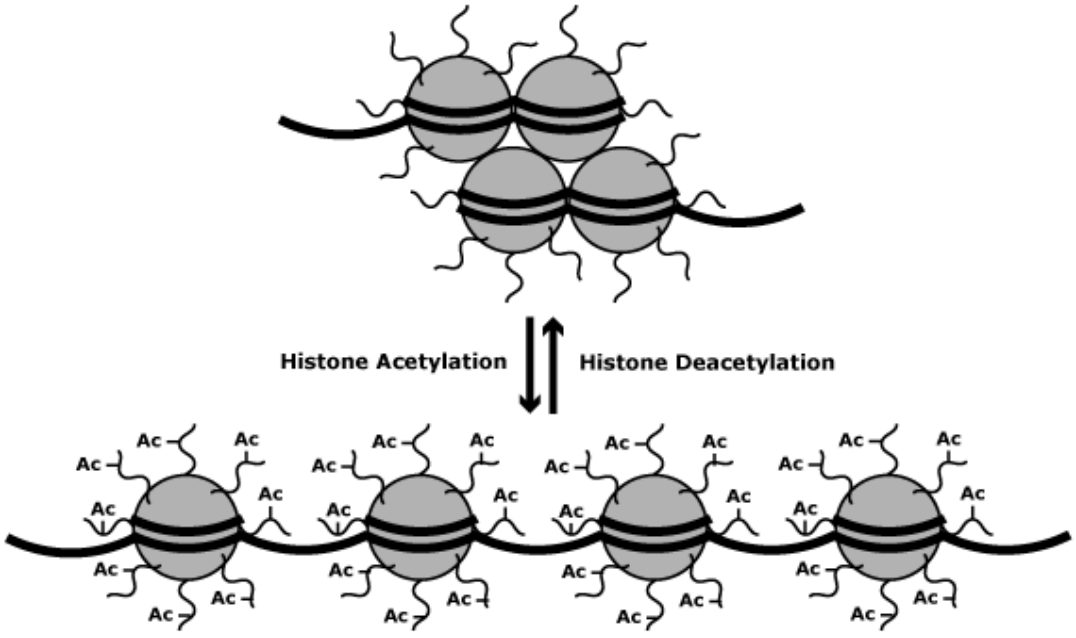

Figure 1.4 Schematic illustration of histone acetylation and deacetylation

(http://missinglink.ucsf.edu/lm/genes_and_genomes/acetylation.html)

class II HDACs. In addition, silent information regulator 2 (Sir2p) is homologous to class III HDACs (Bjerling *et al*., 2002; Sengupta *et al*., 2004).

1.2.3 Histone Methylation

Methylation of histone proteins occurs on lysine and arginine residues on the histone tails of H3 and H4 and is associated with both transcriptional activation and repression.

Histone methyltransferases (HMTs) are the enzymes responsible for this modification of either lysine or arginine residues on histone tails. Based on their specificity, HMTs can be grouped into two families. The methyltransferases that methylate lysine residues are called histone lysine methyltransferases (HKMTs) and methyltransferases that methylate arginine residues are called protein arginine methyltransferases (PRMTs).

Methylation of lysine residues is known to occur on histone H3 Lys 4, Lys 9, Lys1 4, Lys 27, Lys 36 and Lys 79 and histone H4 Lys 20. Histone H3 Lys 4 methylation is a mark for transcriptionally active genes (Noma *et al*., 2001). Methylation of H3 lysine can occur at three stages: mono, di and tri-methylated. The mono and di-methylated states are associated with both transcriptionally active and inactive genes. The tri-methylated state occurs exclusively at transcriptionally active genes (Santos-Rosa *et al*., 2002).

The HMTs is responsible for methylation of arginine residues containing a conserved catalytic domain and an S-adenosyl methionine-binding region. These enzymes can attach one or

two methyl groups to arginine residues. This allows for variation in the symmetry of these groups. Lysine HMTs contain a set of domains, although not all of these domains have HMT activity (O'Carroll D, *et al*. 2000; Yang L, *et al*. 2002).

1.2.4 Histone Code Hypothesis

The "Histone Code Hypothesis" has been proposed in recent years. It suggests that histone tail modifications constitute an epigenetic code that can be read by other proteins. The proteins are able to recognize/read distinct tail modifications, which either occurs sequentially or in combination just like a language or a code. Consequently, this triggers downstream events resulting in a unique and specific biological outcome, such as gene expression or silencing, heterochromatin formation, DNA replication and chromosome segregation.

Proteins such as bromo domain and chromo domain can catalyze or recognize histone modifications. These proteins bind specifically to different lysine modifications and can thus act as starting transmission points of appropriate regulatory signals. Specifically, the bromo domain interacts selectively with acetylated lysines and is in general linked to transcriptional activation, whereas the chromo domain may recognize the methylated marks and is typically associated with gene silencing and assembly of heterochromatic domains (Rice *et al*., 2001; Quana *et al*., 2006; Margueron *et al*., 2005).

In general, methylation marks are known to be correlated with gene silencing and acetylation marks are correlated with transcriptional activation. However, some exceptions do

exist. For example; histone H3 Lys 4 tri-methylation has been found to be associated with the promoter and 5'-coding regions of active genes in yeast and higher eukaryotes and histone H3 Lys 4 di-methylation has appeared on active and inactive genes in yeast (Santos-Rosa *et al*., 2002, Margueron *et al*., 2005). Methylation of arginines in histone H3 and H4 synergistically lead to transcriptional activation. Furthermore, acetylation of histone H4 Lys 12 is a mark for the silent chromatin state (Quana *et al*., 2006; Lancher *et al*., 2003).

Histone modifications are interdependent and can favor or repress other modifications. The histone H3 Lys 4 methylation by an HKMT facilitates subsequent H3 and H4 acetylation by p300. The histone H3 Lys 9 methylation, however, inhibits acetylation events (Wang *et al*., 2001). The histone H4 Arg 3 methylation by PRMT1 is severely decreased by H4 acetylation, whereas histone H4 Lys 8 and histone H4 Lys 12 acetylation is elevated after methylation of Arg 3 (Wang *et al*., 2001). Furthermore, Lys 20 methylation and histone H4 Lys 16 acetylation were found to be inhibit each other [Nishioka *et al*., 2002]. Phosphorylation of Ser 10 facilitates the sequential acetylation of histone H3 Lys 9 and acetylation of Lys 14, whereas histone H3 Lys 9 methylation impairs subsequent Ser 10 phosphorylation (Rea *et al*., 2000). Recently, this view has been challenged by data that shows the coexistence of histone H3 Lys 9 methylation and Ser 10 phosphorylation (Mateescu *et al*., 2004). In yeast**,** Rad6-mediated histone H2B Lys 123 ubiquitination is required for subsequent histone H3 Lys 4 and histone H3 Lys 79 methylation (Margueron *et al*., 2005; Ng *et al*., 2002).

1.3 Chromatin remodelers

Chromatin remodeling complexes are involved in changing chromatin structure. ATP-dependent chromatin remodeling complexes utilize the energy derived from ATP hydrolysis to change the contacts between histone and DNA (Tsukiyama *et al*., 1999) by several mechanisms such as nucleosome sliding, remodeled nucleosome, nucleosome displacement or nucleosome replacement (Mohrmann *et al*., 2005) (Figure 1.5).

Many ATP dependent remodeling complexes have been discovered in yeast. They are categorized into four families – the SWI/SNF (Switching Deficient/ Sucrose Non Fermenting) and RSC (Remodels the Structure of Chromatin) family, the ISWI (Imitation SWItch) family, the CHD (Chromatin – Helicase DNA binding protein) family, and the INO80 and SWR1 family. All four families share an evolutionarily conserved Snf2-like ATPase domain (Figure 1.6). The catalytic subunit of the SWI/SNF family contains a bromodomain at the C-terminus that binds to acetylated lysines. The INO80/SWR1 family is distinct from the other three families by having a split ATPas domain. The ATPase subunit of the ISWI family of remodelers harbors a SANT domain (SWI3,ADA2, N-CoP and TFIIIB domain) and SLIDE domain (SANT like ISWI domain) at the C-terminus, which are thought to bind histone tails and linker DNA, respectively. The CHD family contains an N-terminal chromo domain, which binds methylated lysines, and a C-terminal DNA-binding domain (Venters *et al*., 2009; Tsukiyama *et al*., 2002).

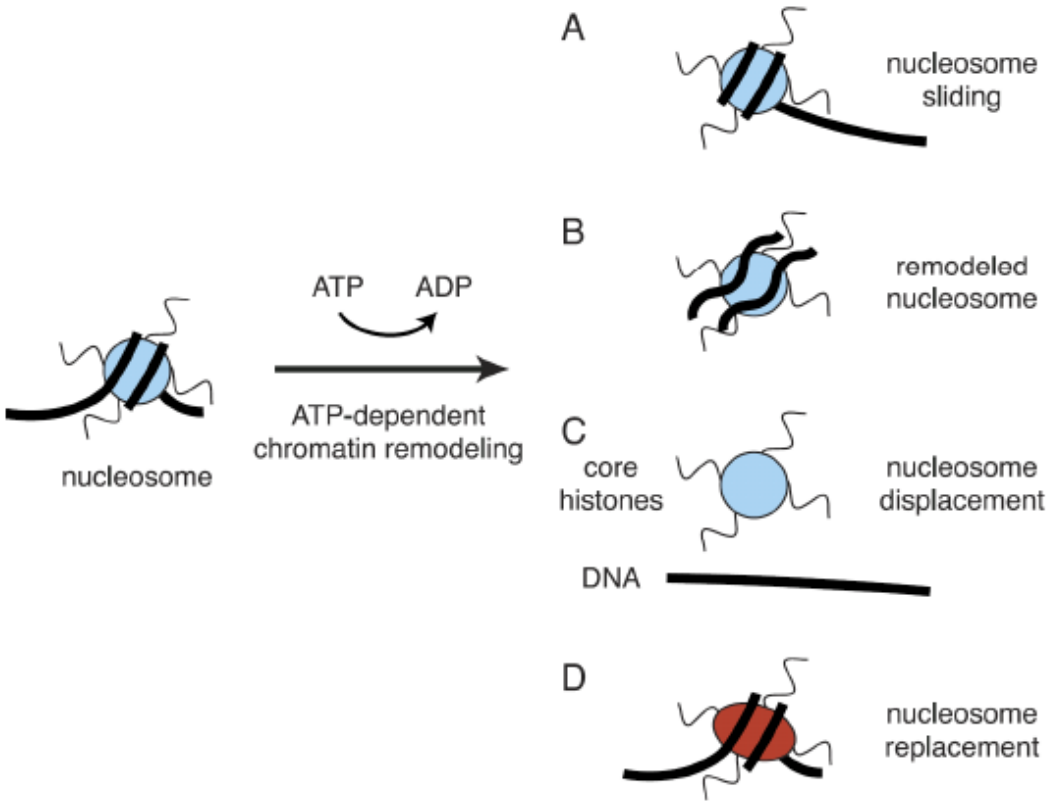

Figure 1.5 Mechanisms of ATP dependent chromatin remodeling complexes (Mohrmann *al el*., 2005). ATP-dependent chromatin remodeling complexes use the energy derived from ATP hydrolysis to alter histone-DNA contacts in such a way that (A) nucleosomes slide to another position, (B) a remodeled state is created in which the DNA becomes more accessible but histones remain bound, (C) DNA and histones dissociate completely, or (D) nucleosome replacement

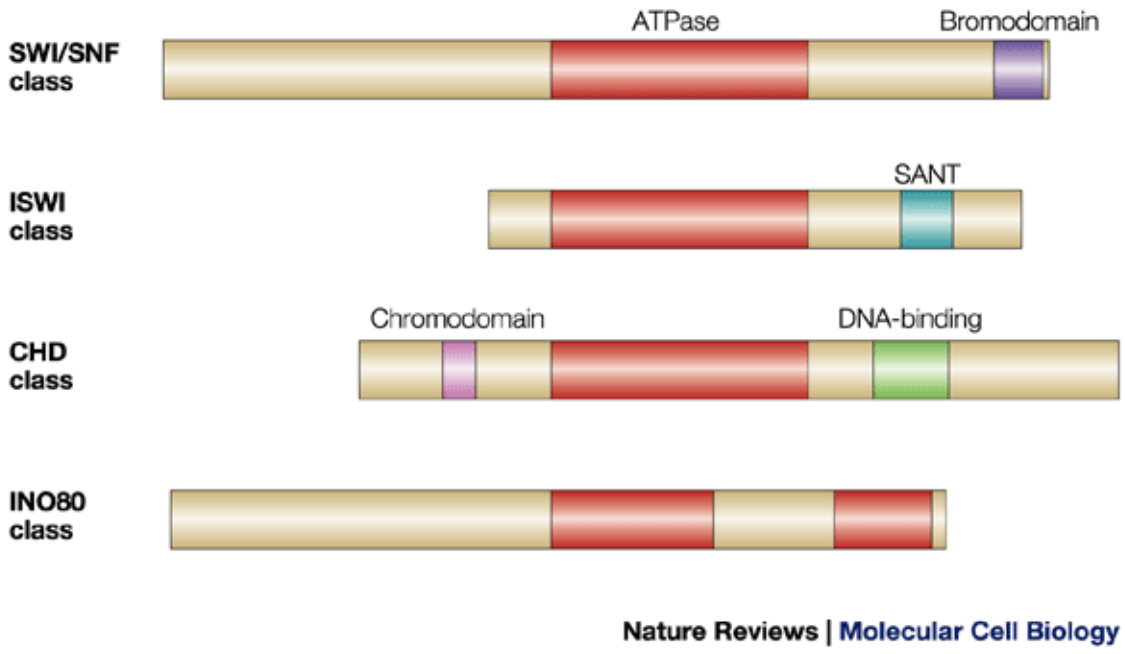

Figure 1.6 Structure of ATPase domains in four main ATP dependent chromatin remodeler families (Tsukiyama *et al*., 2002). ATPase domains are shown in red. Signature motifs in each class- the bromodomain (purple), the SANT domain (light blue), the chromodomain (pink) and a putative DNA-binding domain (green) are shown.

1.3.1. SWI/SNF (Switching Deficient/ Sucrose Non Fermenting) and RSC (Remodels the Structure of Chromatin) Family

The first and the best characterized ATP-dependent remodeling complex group is the SWI/SNF complex identified in *Saccharomyces cerevisiae*. Many subunits of the SWI/SNF complex were isolated in genetic screens that had looked for the factors that were required for mating- type switching, as well as those that were required to use sucrose as a carbon source. The isolated genes were therefore named SWI (for switching) and SNF (for sucrose non-fermenting) (Muchardt *et al.*, 1999; Elfring *et al*., 1994).

SWI/SNF is very well conserved through evolution from yeast to human. The SWI/SNF group of remodelers can be further subdivided into ySWI/SNF and RSC in yeast, BAP and PBAP (Polybromo and Brahma associated proteins) in flies, and BAF (BRG1 or h
brm associate factor) and PBAF (Polybromo associate BAF)in mammals (Table 1.1).

SWI/SNF is a large complex (2 MDa) consisting of at least 11 subunits (Table 1.2), including the ATPase subunit Swi2/Snf2p (Gangaraju *et al*., 2007). It was originally identified as a regulator of *SUC2* genes. Furthermore, nucleosomes partially unwrap at promoter regions because of SWI/SNF activity. This activity facilitates efficient access of transcription factors (Schwaish *et al*., 2007).

Table 1.1 Functional specificity of SWI/SNF-related chromatin remodeling complexes.

ySWI/SNF	RSC
Non-essential for viability	Essential for viability
Low abundance	High abundance
Facilitates expression of several inducible genes	Targets genes distinct from those of ySWI/SNF
Implicated in transcription activation and repression	Involved in transcription activation and repression
Involved in the exit from mitosis through stimulation of expression of some mitotic genes	Sth1, Sfh1, Rsc3 and Rsc9 are essential for cell cycle progression through G2/M

Table 1.2 SWI/SNF Subfamily and their subunits (Gangaraju *et al.*, 2007)

S. cerevisiae		***D. melanogaster***		***H.sapiens***	
SWI/SNF	**RSC**	**BAP**	**PBAP**	**BAF**	**PBAF**
Swi2/Snf2	Sth1	Brahma		Brg1 or hBrm	BRG1
	Rsc1,Rsc2,Rsc3		Polybromo		Polybromo/BAF 180
	Rsc9		BAP170		
Swi3	Rsc8	Moira	Moira	BAF170&BAF155	BAF170&BAF155
Snf5	Sfh1	Snr1	Snr1	hSNF5/INI1	hSNF5/INI1
Swp82/Yfl049w	Rsc7/NpI6p				
Swp73/Swp12	Rsc6	BAP60	BAP60	BAF60a	BAF60 a or b
Arp7/Swp61	Arp7/Rsc11	BAP55	BAP55	BAF53	BAF53
Arp9/Swp59	Arp9/Rsc12				
		Actin	Actin	Actin	Actin
Snf6					
Swp29/Tfg3/Taf14/ An1c					
Rtt102	Rtt102				
Snf11					
	Rsc5,Rsc10, Rsc13,Rsc14, Rsc15				

Remodels the Structure of Chromatin (RSC) is an abundant complex which consists of 15 subunits. RSC is more abundant in the cell than SWI/SNF because it is essential for cell growth. RSC subunits, Sth1, Sfh1, Rsc3 and Rsc9 are involved in cell cycle progression from G2 to M in the mitotic cycle (Table 1.1). It exists in distinct forms containing either Rsc1p or Rsc2p and either with or without Rsc3p and Rsc30p (Cairns *et al*., 1998). SWI/SNF and RSC have been shown to have distinct, non-overlapping roles. RSC and SWI/SNF share two actin-related proteins known as Arp7p and Arp9p. Arp7p is identical to Swp61p and Rsc11p, and Arp9p is identical to Swp59p and RSc12p in the SWI/SNF and RSC complexes, respectively. Also three of the RSC subunits, Sfh1p, Rsc6p and Rsc8p**,** are homologous to Swi5, Swp73p, and Swi3p in the SWI/SNF complex. The Sth1p subunit is a paralog to the yeast Swi2p/Snf2p ATPase subunit (Du *et al*., 1998; Cairns *et al*., 1998; Cairns *et al*., 1996). Recently, Rtt102p was identified as the newest subunit of both SWI/SNF and RSC by mass spectrometry analysis (Lee *et al*., 2004). RSC also functions at many *Pol I* and *Pol III* promoters (Venters *et al*., 2009). This may be the reason why RSC is essential for viability in yeast whereas SWI/SNF is not.

1.3.2 ISWI (Imitation SWItch) Family

Imitation SWItch (ISWI) is very similar to the Swi2p ATPase subunit from the SNF2 subfamily. It contains a SANT domain which can recognize the covalent modifications in the histones. It is named SANT because of the presence of SWI3, ADA2, N-CoR and TFIIIB (Grune *et al*., 2003). In yeast there are two Imitation Switch genes, *ISW1* and *ISW2*, which are highly related to *D. melanogaster*'s *ISWI*. Isw1p forms a four-subunit complex, which possesses nucleosome-stimulated ATPase activity, nucleosome disruption activity and nucleosome spacing

activity. Isw2p forms a two-subunit complex that does not share any common subunits with ISW1. The Isw2p complex has nucleosome-stimulated ATPase activity and nucleosome spacing activity, but does not show nucleosome disruption activity. Isw2p is associated with Itc1p (Gelbart *et al*., 2001). It has been shown that at least one of the *ISW1*, *ISW2* or *CHD1* genes (*ISWI*-related genes) is necessary for yeast cells to survive in stressful conditions (Tsukiyama *et al*., 1999). These two members are likely to influence the regulation of gene expression, including gene silencing, gene repression, gene activation and transcription termination. Proteins associated with these factors may be the key determinants of these diverse functions. For example, Isw1ap is involved in silencing and gene repression, while Isw1bp is associated with the active state of a gene (Mellor *et al*., 2004). Isw1p is isolated as a monomer in two complexes known as Isw1a and Isw1b. The Isw1a complex exhibits stronger nucleosome spacing and sliding activities than the Isw1b complex *in vitro*. Isw1a contains Ioc3p, while Isw1b contains Ioc2p and Ioc4p, which are mutually dependent for their association with Isw1p in the Isw1b complex (Cuperus *et al*., 2002; Vary *et al*., 2003).

1.3.3 CHD (Chromatin – Helicase DNA binding protein)

The Chromatin-helicase DNA binding protein (CHD) was first isolated from mice (Tsukiyama *et al*., 1997) and is the least understood remodeler complex of the four families. Chd1 was isolated from yeast, and was shown to be an ATP-dependent nucleosome remodeling protein which can reposition nucleosomes, along the DNA. Chd1 may operate in parallel pathways with other chromatin remodelers or is targeted to few genes. Biochemical purification of the SAGA and SLIK complex from yeast led to the identification of Chd1 as one of its

component (Pray-Grant *et al*., 2005). Chd1 contains two chromodomains, which bind to methylated lysines (Pray-Grant *et al*., 2005; Biswas *et al*., 2008).

1.3.4 INO 80 and SWR1 family

Both INO80 and SWR1 are large complexes. INO80 contains 15 subunits and is involved in transcription activation. Yeast strains lacking INO80 show misregulated transcription and are hypersensitive to DNA-damaging agents. This may suggest that INO80 not only regulates transcription but also facilitates DNA repair. Ino80p is the largest subunit of the INO80 complex and contains a conserved ATPase/helicase domain. While the ATPase/helicase domain of the other members of SNF2 superfamily, such as Swi2p/Snf2p and ISWI, are continuous, the ATPase/ helicase domain of Ino80p and Swr1p are split by a large spacer region. Actin (Act1p) and three other actin-related proteins, Arp4p, Arp5p and Arp8p are associated with the complex in addition to Ino80p. The other subunits are Rvb1p and Rbv2p. SWR1 (Swi2/Snf2 related complex) contains 14 subunits and is involved in DNA repair. The catalytic subunit of this complex is Swr1p which has an ATPase domain related to Snf2p. Rbv1p, Rbv2p, Act1p and Arp4p are the common subunits for both the SWR1 and INO80 (Shen *et al*., 2000; M*orrison et al.*, 2004; van Attikum *et al*., 2004).

1.4 The model gene – *CUP1*

1.4.1 *CUP1* gene

CUP1 encodes a copper metallothionein responsible for protecting yeast cells from the toxic effects of copper (Fogel *et al*., 1982; Hottiger et al., 1995). The *CUP1* locus is located at chromosome VIII, 42 centimorgans distal to the centromere (Hawthorne *et al*., 1960). The level of resistance is proportional to the copy number of this locus, which can be found in up to 15 tandemly iterated copies (Fogel *et al*., 1982). At the DNA level it consists of a basic repeat unit, 2kb in length. The basic repeat contains two transcription units. The smaller one encodes copper metallothionein, a low molecular weight, cysteine rich, and copper binding protein. The other transcription unit contains an open reading frame for a yet unidentified protein. *CUP1* was chosen as a model gene because its regulation is well understood and it is relatively simple, increasing the likelihood that its activity can be reconstituted *in vitro* (Karin *et al.*, 1983). Furthermore, studies have shown that the yeast *CUP1* gene is used as a selectable marker in transformation (Zhang *et al*., 2011, Wang *et al*., 2008) since it has a strong, inducible promoter and its activity can be controlled and studied easily.

1.4.2 The function and significance of metallothionein proteins

Trace concentrations of copper ion is important for cell survival since it is an essential cofactor for many enzymes, while higher concentrations of copper ion is toxic to the cell. Therefore, copper ion homeostasis is very important. Copper metallothionein (MT) protein protects cells

against copper toxicity through its ability to sequester copper (Butt *et al.,* 1984, Jensen *et al.,* 1996). Yeast copper metallothionein shares common features with higher eukaryotic metallothionein, yet there are striking differences. The molecular weight of yeast MT is 6573 daltons, while the vertebrates MT are around 5900 daltons. The presence of cysteine in yeast copper MT is a typical feature of a metal binding protein. Yeast copper MT contains 20% cysteine as compared to the 32% in the human and mouse MT, while lysine and serine are present at approximately similar amounts. The eukaryotes MT doesn't contain any aromatic amino acids, but yeast MT has two phenylalanine residues (Table 1.3). Mammals MT are dividing in to four subfamilies designated MT1 trough MT4. The electrophoretic mobility of the yeast copper MT mRNA is identical to the human MT mRNA. This may suggest that metal regulating genes are conserved throughout eukaryotes (Butt *et al*., 1984). This conservation makes *Saccharomyces cerevisiae* as an excellent model organism to study about mammalian copper metabolism.

MT acts as a scavenger for free radicals. MT's great antioxidant activity was proven *in vivo* and *in vitro* towards the free hydroxyl and superoxide radicals (Sato *et al.,* 1993). Studies have shown that copper (II) acts as the oxidant of Zn-MT3 molecules which incorporate copper (I). This protects the brain from the toxic effect of the free copper (II) (Meloni *et al.,* 2008; Meloni *et al.,* 2007). MT was primarily known as a protein that was involved in the detoxification of excess heavy metals in the organisms. MT had showed the heavy metal homeostasis and toxicity prevention in the *Drosophila melanogaster* (Egli *et al.,* 2006). Furthermore the role of detoxification of heavy metals such as Cd and Cu by MT was shown in marine invertebrates (Viarengo *et al*., 1989; Viarengo *et al*.,1993). It is considered that Cd, Cu,

and Hg are good inducers of MT biosynthesis. The studies about metal pollution in the marine ecosystems using marine molluscs led MT to be considered as an aquatic bio marker (Amiard *et al.*, 2006).

A higher level of MT was determined in various tumors such as gastric tumors and melanoma (Galiza et al., 2006; Petrlova *et al*., 2006; Weinlich *et al*., 2006; Weinlich *et al*., 2009). Further studies discovered that the level of MT in tumors was three times higher than the controlled samples. The clinical stage of the disease was detected based on the MT levels in the peripheral blood and serum of the cancer patients. Therefore MT can be considered as a new indicator for censer diagnosis (Krizkova *et al*., 2009; Adam *et al*., 2007).

Table 1.3 Comparison of amino acid composition of yeast and human MT

(Butt *et al*., 1984)

Amino Acid	Percentage	
	Yeast	Human
Alanine	0	11.5
Cysteine	20.0	32.8
Aspartic acid	3.3	3.3
Glutamic acid	10.0	1.6
Phenylalanine	3.3	0
Glycine	8.3	8.2
Histidine	1.6	0
Isoleusine	1.6	0
Lysine	11.6	11.5
Leucine	1.6	1.3
Methionine	1.6	1.6
Asparagine	10.0	1.6
Proline	3.3	1.6
Glutamine	8.3	1.6
Arginine	0	0
Serine	13.3	13.1
Threonine	3.3	4.9
Valine	0	4.9
Tryptophan	0	0
Tyrosine	0	0

1.4.3 *CUP1* promoter and gene activation

The *ACE1* gene encodes a copper regulated DNA binding protein. It is also known as Cup2p; transcription activator. This Ace1p contains a cysteine rich domain. When copper ions enter the cell, they bind to the cysteine residues at the N-terminal domain of Ace1p, which folds and binds specifically to the Upstream Activation Sequence (UASs) in the *CUP1* promoter (Buchman *et al*., 1989; Szczypka *et al*., 1989; Thiele *et al*., 1988; Furts *et al*., 1989). Ace1p then activates transcription through its C-terminal acidic activation domain (Figure 1.7). There are two UASs. The distal UAS is located from -183 to -143, while the proximal UAS is located from -137 to -107 relative to the transcription starting site. Both UASs have binding sites for Ace1p and HSF (Heat Shock Factor). *CUP1* is also induced relatively weakly by heat shock factor at heat shock. The *CUP1* promoter has two TATA boxes. The distal TATA box starts at -76 and the proximal TATA box starts at -32. It has been shown that a distal TATA mutation is more severe than a proximal TATA mutation. When enough metallothionein is produced, it will bind to Ace1p and will lead to the release of Ace1p from the UAS, which will then lead to the shut off of *CUP1* transcription (Shen *et al*., 2002).

Previous studies have shown that *CUP1* induction is accompanied by nucleosome repositioning over the entire *CUP1* gene and flanking sequences. Furthermore, nucleosome repositioning requires the transcriptional activator but not the TATA boxes, suggesting an activator-dependent chromatin remodeling activity (Shen *et al*., 2001). The only other transcription factor that influences *CUP1* expression directly is the heat shock factor. It has also been shown that there is targeted acetylation of both H3 and H4 at the *CUP1* promoter under

inducing conditions. This targeted acetylation requires the presence of the activator and TATA boxes, suggesting a late event of histone acetylation in *CUP1* induction. Furthermore, the *SPT10* gene is required for the targeted acetylation of both H3 and H4 at the *CUP1* promoter. The Spt10p contains a domain homologous to the HAT domain of Gcn5p. Based on these findings, a working model of *CUP1* gene activation has been proposed (Shen *et al*., 2002).

However, it is still not clear which chromatin remodeler(s) is/are involved in *CUP1* activation. Therefore, it is essential to find out which remodeler(s) play(s) an important role in *CUP1* induction so that we can further understand the mechanism of gene activation.

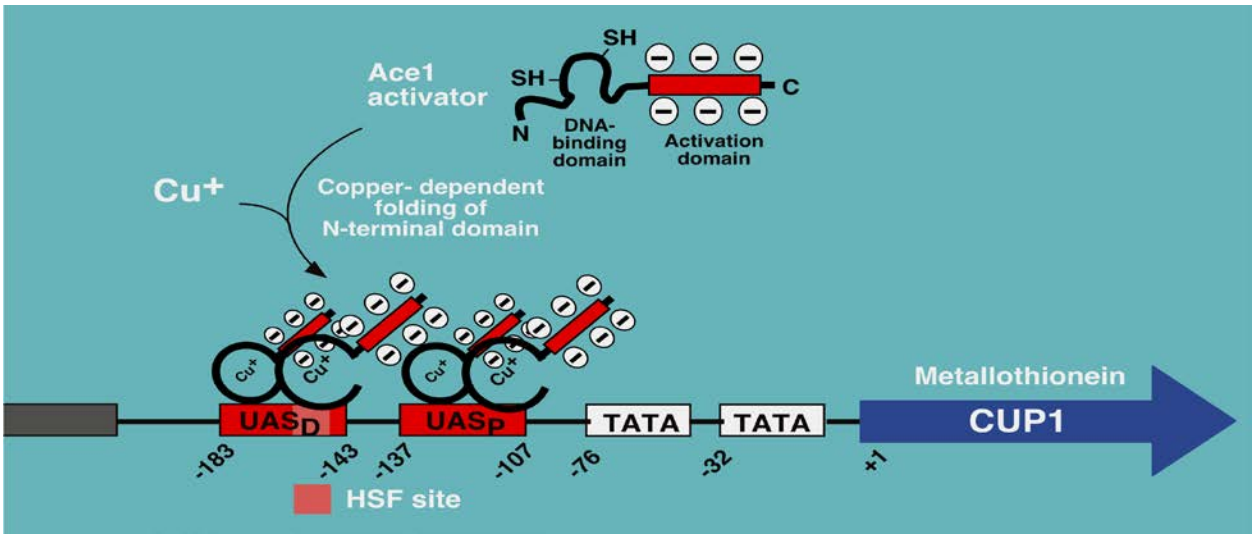

Figure 1.7 *CUP1* gene activation. Red boxes: UAS_D represents the Distal Upstream Activating Sequence which is positioned between -183 and -143, UAS_P represents the Proximal Upstream Activating Sequence which is positioned between -137 and -107. Distal TATA box starts at -76 and Proximal TATA box starts at -32. Blue arrow represents the *CUP1 ORF* region starting from +1. Ace1: Transcriptional Activator which has a negative C terminal.

CHAPTER 2

2 Materials and Methods

2.1 Media

SC (Synthetic complete media) - 2% Dextrose (w/v) (Fisher Scientific), 0.67% YNB (yeast nitrogen base) with ammonium sulfate (w/v) (MP Biomedicals, Cat: 114027522), 0.079% CSM (complete supplement mixture) (w/v) (MP Biomedicals, Cat: 4500 022)

SC-Cu - 2% Dextrose (w/v), 0.67% YNB without copper, dextrose and amino acid (w/v) (BIO 101 systems, Cat: 4029912), 0.079% CSM (w/v)

SC-Cu-Trp - 2% Dextrose (w/v), 0.67% YNB without copper, dextrose and amino acid (w/v), 0.074% CSM without tryptophan (w/v) (MP Biomedicals, Cat: 4511022)

SC-Cu-Ura - 2% Dextrose (w/v), 0.67% YNB without copper, dextrose and amino acid (w/v), 0.77% CSM without uracil (w/v) (MP Biomedicals, Cat: 4511222)

SC-Cu-Ade - 2% Dextrose (w/v), 0.67% YNB without copper, dextrose and amino acid (w/v), 0.079% CSM without adenine (w/v) (MP Biomedicals, Cat: 4510022).

SM (Spheroplast Medium) – 2% Dextrose (w/v) (Fisher Scientific), 0.67% YNB (yeast nitrogen base) with ammonium sulfate (w/v) (MP Biomedicals, Cat: 114027522), 0.079%

CSM (complete supplement mixture) (w/v) (MP Biomedicals, Cat: 4500 022), 18.22% D-sorbitol (w/v), 50mM Tris HCl (pH 8).

LB broth – Luria-Bertai medium was prepared by dissolving 10g of bacto-tryptone (Difco, Cat: 211705), 5g bacto yeast extract (Difco, Cat: 212750) and 10g NaCl in 1L distilled water and autoclaved

LB/ Amp Agar – 1.5g of Bacto agar was added to 100ml LB medium and autoclaved Ampicillin was added to 0.1mg/ml immediately before pouring plates.

\

2.2 Reagents and Solutions

Ammonium acetate – 5M ammonium acetate (pH 7.5)

Antibodies- Anti-acetyl-histone H3 rabbit polyclonal antibody (Millipore, Cat:06-599), Anti-acetyl-histone H4 rabbit polyclonal antibody (Millipore, Cat:06-866), Anti-RNA polymerase II mouse monoclonal antibody(Millipore, Cat:05-623), Isw1p (Y-90) rabbit polyclonal antibody (Santa Cruz Biotechnology, Cat: sc-98831), Arp8 rabbit polyclonal antibody (abcam, Cat:12098), Anti-Snf2 (yeast specific) rabbit polyclonal antibody (upstate, Cat:07-319), Anti-histone H4 rabbit polyclonal antibody (abcam, Cat:ab10158), Anti-histone H3 rabbit polyclonal antibody (abcam, Cat:ab1791)

Chloroform – 99.8% (Acros, Cat:61003-0040)

ChIP Dilution Buffer – 0.01% SDS, 1.1% Triton X-100, 1.2mM EDTA, 16.7mM Tris HCl (pH 8.1), 167mM NaCl.

$CuSO_4$ – 0.2M solution was prepared by dissolving 3.192g $CuSO_4$ (Acros organics, Cat: 197711000) in 100ml distilled water and sterilized by filtering.

DEPC treated water – 0.1% of diethyl pyrocarbonate (Sigma) was added to distilled water and autoclaved after 12 hours.

DNase 1– RNase free DNase (Qiagen, Cat: 79254) 1500 kunitz units

dNTPs *(*deoxynucleotriphosphate) – 2mM concentration solution of dNTPs were made from adding 2 µl of 100 mM of each of dGTP (Promega, Cat:U121A), dTTP (Promega, Cat:U123A **),** dATP (Promega, Cat:U120A), dCTP (Promega, Cat:U122A) into 92 µl of autoclaved H_2O. Stored at -20^oC.

EDTA – 0.5M solution contains disodium EDTA $2H_2O$ 186.12 g/L (DNase RNase and proteases free (Quality Biological, Cat: 351 027 100)); pH 8.80 was adjusted using NaOH. Store at: 15-30°C.

Elution buffer –buffer was prepared by adding 1% SDS and 100mM $NaHCO_3$.

EtBr (Ethidium Bromide) – Concentration was 10mg/ ml. (Invitrogen, Cat: 15585-011). Stored in a light-proof bottle at room temperature.

Formaldehyde solution – 37% concentration solution (w/w) (Fisher Scientific, Cat:F79-1)

G2 buffer – Buffer contains 800 mM GU-HCl, 30 mM Tris-HCl pH 8.0, 30 mM EDTA pH 8.0, 5% Tween-20 and 5% Triton-X100 (Qiagen, Cat:1014636).

Glycerol – 99.5% UltraPure™ Glycerol (Invitrogen, Cat: 15514-029)

Glycine – 2.5M solution was prepared by dissolving 187.675g (Fisher Chemicals, Cat: G46-1) in 1L and autoclaved.

High salt wash buffer – 50 ml buffer contains 0.1% SDS, 1% Tritone X-100, 2mM EDTA, 20mM Tris HCl (pH 8.1) and 500mM NaCl.

LB Agar – 1.5g of bacto agar (Difco, Cat: 214010) was added to 100ml LB medium and autoclaved

LB/ Amp Agar – 1.5g of Bacto agar was added to 100ml LB medium and autoclaved. Ampicillin was added to 0.1mg/ml immediately before pouring plates.

LiCl (lithium chloride) wash buffer – 50ml buffer contains 50mM Hepes KOH (pH 7.5), 0.14M NaCl, 1mM EDTA, 1% Triton X100, 0.1% Sodium deoxycholate.

Low salt wash buffer – 50ml buffer contains 0.1% SDS, 1% Triton X-100, 2mM EDTA, 20mM Tris HCl (pH 8.1) and 150mM NaCl.

Lysis buffer – Buffer contains 50mM Hepes-KOH pH 7.5, 0.14M NaCl, 1mM EDTA, 1% Triton X100, 0.1% Nadeoxycholate

Lyticase enzyme – 20mg/ml enzyme solution was prepared using powder lyticase from arthrobacter leuteus, crude (Sigma, Cat: L4025). Stored at -20^{o}C.

Magnesium chloride– 1M solution was prepared by dissolving 10.16g $MgCl_2$ (Fisher Chemicals, Cat: BP214-500) in 50 ml distilled water.

Phenol saturated - pH 6.6 (Fisher Scientific, Cat: BP1750-400). Stored at 4°C.

Phenol buffer saturated - pH 4.3 (Shelton Scientific, Cat: IB05184). Stored at 4°C.

P1 buffer – Re-suspension buffer contains 50 mM Tris-HCl pH 8.0 and 10 mM EDTA. RNase A not included. (Qiagen, Cat: 19051). After 100µg/ml RNaseA addition, the buffer was stored at 2–8°C.

P2 buffer – Lysis buffer contains 200 mM NaOH and 1% SDS EDTA (w/v) (Qiagen, Cat: 19052). Stored at room temperature.

P3 buffers –3.0 M potassium acetate pH 5.5 (Qiagen, Cat: 19053). Stored at 4°C.

PMSF (phenylmethylsulfonyl fluoride) – 0.034g PMSF (Sigma) is dissolving in 1ml 100% ethanol.

Protein A agarose/Salmon Sperm DNA – stored at 2°C-8°C. (Millipore, Cat: 16-157)

Proteinase K from tritirachium album – Stock solution was 20mg/ml (Sigma-Aldrich, Cat: P2038-100MG)

Proteinase inhibitor cocktail –100X cocktail contains 104mM 4-(2-aminoethyl) benzenesulfonyl fluoride hydrochloride, 80uM Aprotinin, 4mM Bestatin and 1.4 mM trans-epoxysuccinyl-L-leucylamido-(4-guanidino)butane(E64) in dimethylsulfoxide (DMSO) (Sigma- Aldrich, Cat: P8340-5ML).

RNA sample buffer – 2mM EDTA, 10mM Tris HCl (pH 8), 1% β-mercaptoethanol, 1% SDS and 10% glycerol.

RNase A – Concentration was 100mg/ ml. Stored at 4^{o}C. (Qiagen, Cat: 1007885)

RNase-free Buffer – 10X buffer is prepared by adding 200mM Tris HCl (pH 8.0) and 20mM $MgCl_2$

SDS – 20% solution was prepared by dissolving 200g sodium dodecyl sulphate (Sigma) in 1L distilled water.

Sodium acetate – 3M solution prepared by dissolving 408.1g sodium acetate in 1L distilled water. Adjusted the 5.3 pH using HCl. Stored at room temperature.

Sodium bicarbonate – 1M solution prepared by dissolving 4.2g $NaHCO_3$ in 50ml distilled water and filter sterilized.

Sodium chloride – 5M solution was prepared by dissolving 29.22g NaCl in 100 ml distilled autoclaved water.

Sorbitol – 1M solution prepared by dissolving 9.10g of D-sorbitol (Acros organics, Cat: 132730010) in 50 ml distilled water. Sterilized by filtering or autoclaving.

Sucrose solution - 50% sucrose solution prepared by dissolving 50g sucrose in 100ml distilled water and sterilized by autoclaving.

SYBER® GreenER™ Two-Step qRT-PCR Kit Universal – This kit (Invitrogen, Cat No: 11765-100) consist of two kits,

- SuperScript™ III First-Strand Synthesis SuperMix for qRT-PCR kit (RT enzyme mix: RNaseOUT™ recombinant ribonuclease inhibitor and SuperScript™ III reverse transcriptase, 2X RT reaction mix: 2.5μM oligo $(dT)_{20,}$ 2.5ng/μl random hexamers, 10mM MgCl2 and dNTPs, and *E.coli* RNase H). Stored at -20^{o}C.
- SYBR® GreenER™ qPCR SuperMix Universal kit (2X SYBR® GreenER™ qPCR SuperMix Universal:*Taq* DNA polymerase, SYBR® GreenER™ fluorescent dye, $MgCl_2$ dNTPs with dUTP instead of dTTP, UDG and ROX reference dye). Stored at 4^{o}C.

Taq DNApolymerase – 5000 u/ml (BioLab, Cat: M02675). Stored at -20^{o}C.

Taq DNApolymerase – 5000 u/ml (Fisher scientific, Cat: FB 600050). Stored at -20^{o}C.

Taq Man Gene Expression Master Mix – (Applied Biosystems, Cat: 4369016) Supplied at 2X concentration. The mix is optimized for real-time PCR quantitative analysis and contains AmpliTaq Gold® DNA Polymerase, UP (Ultra Pure), Uracil-DNA Glycosylase (UDG) and dTNPs with dUTP.

TBE (Tris-Borate-EDTA) buffer – 10X solution was prepared by adding 108g of TrisBase, 55g boric acid and 7.4g EDTA in 1L distilled water. The solution was autoclaved.

TBS – 20mM Tris HCl (pH 7.5) and 150mM NaCl

TE – 50X solutions was prepared by adding 10mM Tris and 0.1mM EDTA. Sterilized by filtering.

ThermoPol 10X buffer – (BioRad, Cat:B90045) Diluted the 10X stock with dH_2O to a final concentration of 1X. 1X buffer contained 10mM KCl, 10mM $(NH_4)2SO_4$, 20mM Tris-HCl, 2mM $MgSO_4$ and 0.1% Triton-X-100. Stored at -20^{o}C.

TES (Tris-EDTA-SDS) buffer – Solution was prepared by adding 10 mM Tris HCl pH 7.5, 10 mM EDTA and 0.5% SDS. Sterilized by autoclaving.

Trichostatin A- 10mM solution was prepared by dissolving 1mg trichostatin A in 330ul 100% ethanol (Wako, Cat: 203-17561)

Tris HCl – 1M solution was prepared by dissolving 78.82g Tris HCl in 500ml distilled autoclaved water. 8 pH was adjusted using NaOH.

Triton X-100 – (Sigma, Cat: T8532-500ML).

2.3 Transformation

2µl competent cells and 20µl plasmid were added together and incubated on ice for 30 minutes. The cells were then subjected to heat-shock at 42^{o}C for 45 seconds, chilled on ice for 2 minutes, followed by adding160µl LB. Then, the cells were incubated at 37^{o}C for 45 minutes. 40µl and 120µl aliquots of transformed cells were spread onto LB agar plates containing 100µg/ml ampicillin. The plates were incubated at 37^{o}C for over night.

2.4 Mini-Preparation of Plasmid DNA

Plasmids were streaked into the LB plates using glycerol stocks and grew at 37^{o}C for overnight. Single colonies were inoculated into 6ml LB media tubes and grew at 37^{o}C overnight. Cells were pelleted at 13000rpm for 1 minute. The cell pellet was re-suspended in 300µl P1 buffer and incubated on ice for 5 minutes. 300µl P2 buffer was added and incubated at room temperature for 5 minutes. 300µl ice-cold P3 buffer was added to the tubes and incubated on ice for 5 minutes. Precipitate was pelleted at 13000rpm for 10 minutes. Supernatant was transferred to new tubes and DNA was recovered by performing phenol chloroform extraction followed by ethanol precipitation. The pellet was re-suspended in 20 µl of TE.

2.5 Amplification of DNA fragments by polymerase chain reaction (PCR)

PCR amplification of DNA was achieved by repeated cycles of three temperature dependent steps, which were denaturing, annealing and extension. The double-stranded DNA (dsDNA) template was denatured at 92-95^{o}C. The two oligonucleotide primers defined as forward and reverse were annealed to the single-stranded DNA (ssDNA) template (one primer was designed to anneal to a specific region on the left side of one of the strands of DNA and the other primer was designed to anneal to a specific region on the right side of the complementary strand of DNA). The annealing temperature (T_{ann}) can be varied based on the melting temperature (T_m) of the primer-template hybrid. It was calculated using following formula.

$$T_{ann} = 61.2 + 0.41(GC\%) - 500/L$$

Where %GC was the absolute value of the percentage of Guanine (G) + Cytosine (C) bases in the primer and L was the total number of bases in the primer. Annealing temperatures typically range around 45-55^{o}C. Taq DNA polymerase enzyme extended each primer in the 5' to 3' direction, duplicating the DNA fragment between the primers. The optimal temperature for *Taq* polymerase was about 75-80^{o}C. With each cycle of denaturing, annealing, and synthesis the specific DNA fragment was amplified exponentially. The basic idea was shown in Figure 2.1.

The general PCR cocktail mixture contained 5µl DNA template, 1µM of the appropriate forward and reverse primers, 0.005u/µl Taq DNA polymerase, 200µM deoxyribonucleotide triphosphate (dNTPs), 2mM $MgCl_2$, 1X buffer and volume up to 25µl using autoclaved distilled

water. The general PCR program was as followed. Initial denaturing was done at 95^{o}C for 4 minutes. 30 cycles of denaturing at 95^{o}C for 30 second, annealing at 62^{o}C for 30 seconds and extension at 72^{o}C for 1.20 minutes was done. Final extension was done for 3 minutes at 72^{o}C and subsequently, it was held at 7^{o}C.

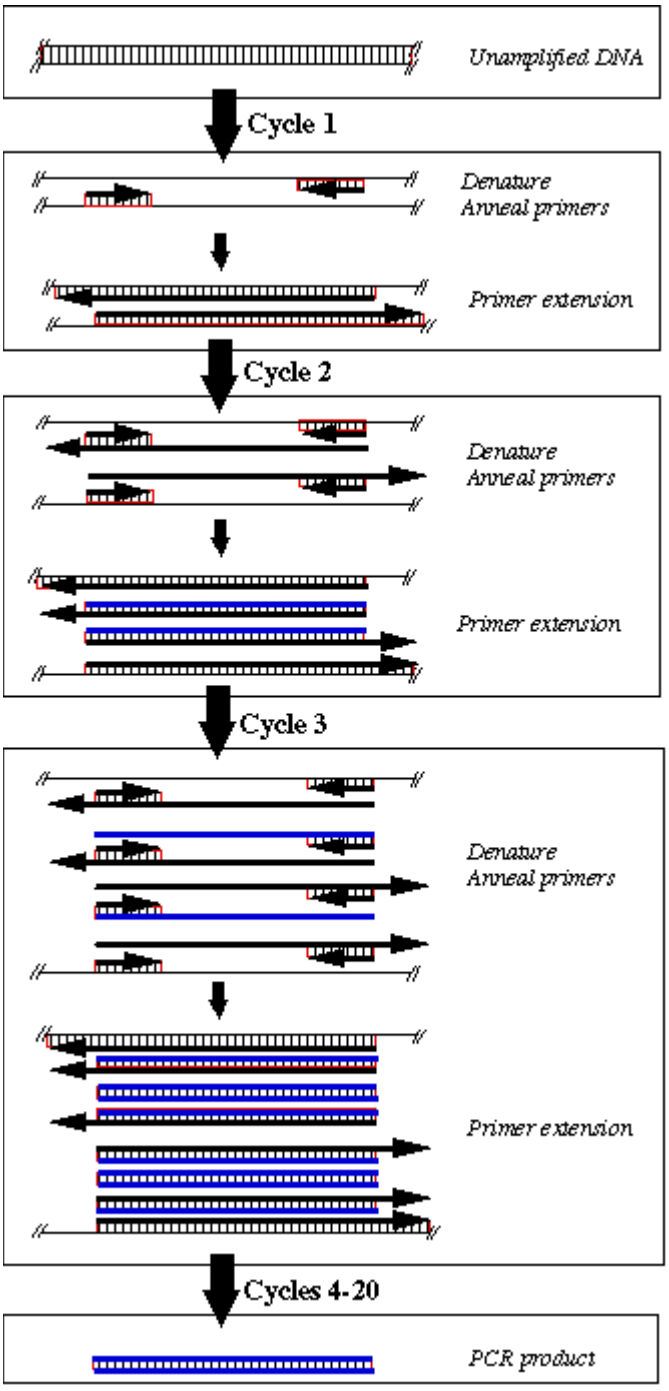

Figure 2.1 Polymerase chain reaction (PCR). DNA strands can amplify by repeated cycles of three temperature based steps which were denaturing, annealing and extension.

http://www.sci.sdsu.edu/~smaloy/MicrobialGenetics/topics/in-vitro-genetics/PCR.html

2.6 Electroporation

PCR product was transformed into WT competent cells using electroporation. To conduct this electroporation, WT cells were grown from single colonies and harvested when the optical density (OD) reached around 0.8 (mid logarithmic phase). The cells were washed with ice-cold 1M sorbitol and re-suspend in a final volume of about 200µl 1M sorbitol. 5µl (0.2µg for autonomously replicating plasmids) of transforming DNA (plasmid) was added to the cells and the mixture was left on ice for 5min. Cells /DNA were pipette into an electroporation cuvette (Bio Rad 0.2cm electrode gap). The cells were then subjected to electroporation at 1.5kV using a Bio Rad MicroPulser (one pulse), which was then followed by the addition of 450µl of 1M sorbitol to the cuvette. A selective medium was then used to select for recombinant cells. 50µl, 100µl and 300µl were plated on appropriate selection plates. Plates were incubated at 30^{o}C to get transformed cells.

2.7 Yeast Genomic DNA Preparation

A single colony was picked and re-inoculated in the media (broth). It was then grown at 30^{o}C in 300rpm till it reached to mid logarithmic phase (0.8 OD). The cells were then spun down at 3400 rpm (rounds per minute) for 15 minutes at 4^{o}C. The pellet was re-suspended in 600µl of spheroplast medium (SM). The growth medium was used to avoid starvation of the cells during the spheroplasting process. Sorbitol in the SM acted as an osmotic stabilizer. Cells were incubated in 30^{o}C for 2-3 minutes and 100µl of lyticase enzyme (20mg/ml) was added. The incubation was continued at 30^{o}C for 1 hour with occasional swirling to prevent settling. The spheroplast was then spun down and re-suspended in 960µl Qiagen G2 buffer, 10µl RNase A and 30µl Protinase K. It was incubated at 50^{o}C for 2 hours and insoluble materials were spun out in 13K for 4 minutes. Phenol chloroform extraction was done to elute genomic DNA. The pellet was dissolved in 20µl TE.

2.8 Phenol-Chloroform extraction

400µl of phenol (pH 6.6) was added to the supernatant, vortexed vigorously for few seconds and spun down at 13000 rpm for 5 minutes. The top aqueous layer was transferred to a new tube and 400µl of chloroform was added. Each tube was vortexed vigorously for few seconds and spun down at 13000 rpm for 5 minutes. 360µl of the top aqueous phase was transferred to a new tube, and subsequently 40µl of 3M sodium acetate (NaOAC) (pH 5.3) and 1mL of 100% ethanol was added to each sample. The tubes were then incubated in dry-ice for 20-25 minutes or at -80^{o}C for an hour or at -20^{o}C overnight. Samples were then spun down at 13000 rpm for 15 minutes and the supernatant was removed. Each sample was then washed with 1ml ice-cold 70% ethanol and again the supernatant was removed. In order to dry out all of the ethanol, a speed-vacuum machine was utilized. At the end of the ethanol precipitation, the pellet was re-suspended in 20µl TE buffer. Short term storage was conducted at -20^{o}C and long term storage was conducted at -80^{o}C.

2.9 Agarose Gel Electrophoresis

SeaKem agarose (fragment ≥ 1kb) was boiled and dissolved at the desired percentage (for 1% gel- 0.6g) in 60ml of 1X TBE containing 0.5µg/ml of EtBr. The gel was cast with an appropriate comb insert and allowed to solidify. DNA samples were dissolved in 1X TBE loading buffer (5X stock solution: 40% sucrose, 5% glycerol, 4mM EDTA, 0.05% bromophenol blue). The gel was run at 75 V in 1X TBE buffer containing 0.5µg/ml of EtBr until the desired resolution was achieved. DNA was detected on an UV transilluminator.

2.10 Determination of DNA and RNA concentrations

DNA and RNA absorbed ultraviolet light at 260nm wavelength. The photo-detector inside the spectrophotometer measured the light pass through the samples. The more light absorbed by the sample, the higher the nucleic acid concentration in the sample. It was possible to relate the amount of light absorbed to the concentration of the absorbed molecule using the Beer- Lambert Law. DNA concentration was achieved by spectroscopy at 260nm wavelength taking 1 optical density (OD) unit as equivalent to 50ug/ml of double–stranded DNA, 20 μg/ml of single–stranded oligonucleotide and 40ug/ml of single-stranded DNA or RNA (Sambrook *et al.,* 1989). If the OD_{260}/OD_{280} was significantly less than 1.8, then it was necessary to further purify the DNA by phenol chloroform extraction followed by ethanol precipitation.

Concentration of double stranded DNA = absorbance at 260nm * 50 * dilution factor

Concentration of double stranded RNA = absorbance at 260nm * 40 * dilution factor

2.11 Total RNA Preparation

2.11.1. Cell preparation

Cells were grown from a single colony and collected in induced and uninduced conditions. The cell pellets were re-suspended in 400µl ice-cold autoclaved water and were spun down at 13000 rpm for 15 seconds at 4^{o}C. The supernatants were discarded and the pellet was completely rinsed in 400µl TES buffer. The phenol chloroform extraction was then performed using an acid phenol (pH 4.3) followed by the ethanol precipitation.

2.11.2. Phenol (acid)-Chloroform extraction

400µl of acid phenol (pH 4.3) was added into the dissolved pellet and was incubated at 65^{o}C for an hour. The tube was then kept in ice for 5 minutes. It was subsequently spun down at 13000 rpm for 5 minutes at 4^{o}C in order to separate the aqueous layer. 400µl of acid phenol (pH 4.3) was the added to the aqueous layer. The sample was then vortexed vigorously for 10 seconds and placed on ice for 5 minutes. It was then spun down at 13000 rpm for 5 minutes at 4^{o}C to separate the aqueous layer, which then had 400µl of chloroform added to it. The tube was then vortexed vigorously and spun down at 13000 rpm for 5 minutes at 4^{o}C. 360µl of the aqueous phase was transferred to a new tube, followed by the addition of 40µl of 3M sodium acetate (NaOAC) (pH 5.3) and 1ml of ice-cold 100% ethanol. The sample was then incubated in dry-ice for 20-25 minutes or at -80^{o}C for an hour or at -20^{o}C overnight. Next, it was spun down at 13000 rpm for 5 minutes at 4^{o}C and the supernatant was removed. Then, it was washed with

1ml ice-cold 70% ethanol and the supernatant was removed. A speed-vacuum machine was then used to dry out all the ethanol. At the end of the ethanol precipitation the pellet was re-suspended in 200µl RNA sample buffer. Short term storage was conducted at -20^{o}C and long term storage was conducted at -80^{o}C.

2.11.3. DNase Treatment

According to the RNA quantifications, 10µg of RNA sample was added to 5µl of 10X Buffer and 3.5µl DNase-1 in a micro-centrifuge tube. Total volume was then increased to 50ul by adding DPEC treated water. The sample was incubated at 37^{o}C for an hour. Then the phenol chloroform extraction was performed, followed by ethanol precipitation. Phenol (pH 6.6): Chloroform ratio should be 3:1. At last, the pellet was re-suspended in 20µl DEPC treated water or TE made up of DPEC treated water.

2.11.4 Real-time quantitative RT-PCR (qRT-PCR)

The SYBER Green ER Two-Step qRT-PCR kit was used (Invitrogen, Cat No: 11765-100) to did the real time PCR. There were two steps (Figure 2.2).

1. Reverse transcriptase polymerase chain reaction (RT-PCR)

In the first step, c-DNA was made from mRNA using SuperScript™ III First-Strand Synthesis SuperMix for qRT-PCR kit. Each reaction contained approximately 1 ug of mRNA, 10µl 2X RT reaction mix and 2µl RT enzyme mix. A total volume of 20µl was achieved using DPEC treated water. Tubes were gently mixed and incubated at 25^{o}C for 10 minutes followed by

incubation at 50^{o}C for 30 minutes. The reaction was terminated at 85^{o}C for 5 minutes, and then chilled on ice. 1µl of *E.coli* RNase H was added and the tube was incubated at 37^{o}C for 20 minutes. The reactions could be stored at -20^{o}C until use.

2. Quantitative polymerase chain reaction (qPCR)

In the second step we did qPCR (used SYBR Green method) to quantitate the amount of cDNA templates using SYBR® GreenER™ qPCR SuperMix Universal kit. For each reaction added 7.8µl SYBR® GreenER™ qPCR SuperMix Universal, 0.4µl forward primer, 0.4µl reverse primer, 0.4µl ROX reference dye, and 2µl cDNA template (from the first step). The total volume was brought up to 25µl using autoclaved distilled water. The PCR plate was sealed and it was made sure that all of the components were at the bottom by mixing and brief centrifuging. The reactions were placed in a preheated thermal cycler programmed as described bellow. The real time instrument used was the 7500 real time PCR system (Applied Biosystems).

- 50 ^{o}C for 2 minutes hold
- 95 ^{o}C for 10 minutes hold
- 45 cycles of:
    - 95 ^{o}C for 15 seconds
    - 60 ^{o}C for 60 seconds

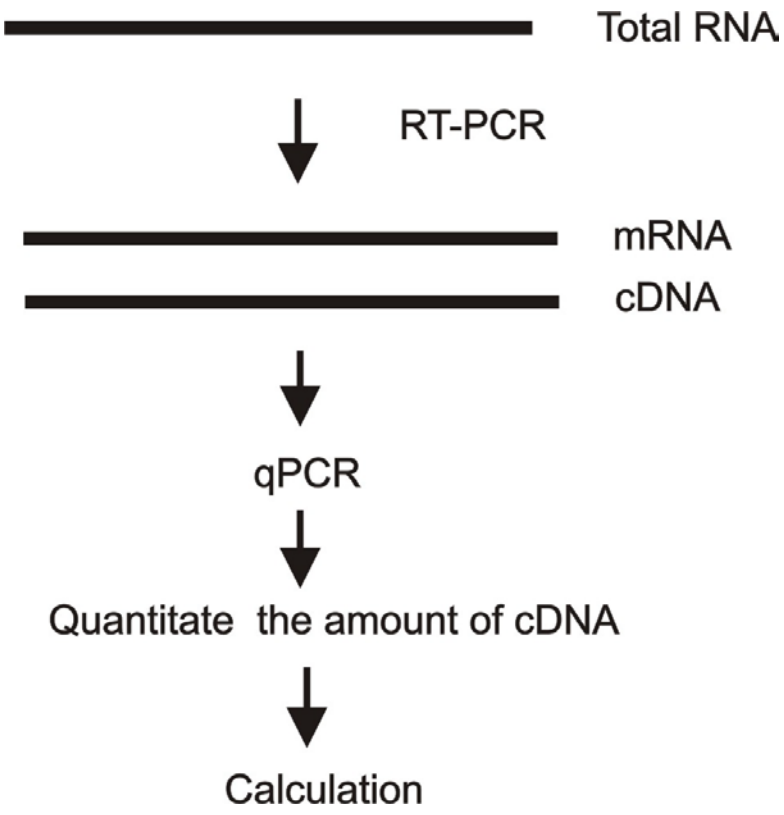

Figure 2.2 RNA analysis, Real-time qRT-PCR consist of two steps, In the 1st step produce cDNA from mRNA by RT-PCR and in the 2nd step quantitate the amount of cDNA using qPCR

2.12 Chromatin Immunoprecipitation (ChIP)

2.12.1. Cross Linking

Yeast cells were grown from a single colony and allowed to grow at 30^{o}C, 300rpm overnight. Each of the 6 ml culture tubes were then transferred to a 244 ml media flask and the optical density at 600 nm was measured until it reached around 0.8 (mid logarithmic phase). The cells were then induced in one flask with 2mM $CuSO_4$ and both induced and uninduced flasks were incubated for another hour. The cells were then cross-linked (Figure 2.3) by adding 6.92ml of 37.2% formaldehyde and incubated at room temperature (25^{o}C) for 25 minutes at 120rpm. The cells were subsequently quenched by adding 42ml of 2.5M Glycine for 5 minutes at room temperature at 90rpm. Lastly the cells were spun down and washed twice at 3400rpm for 10min.

2.12.2. Lysate Preparation

The cells were re-suspended in 0.4ml positive lysis buffer [positive lysis buffer contained 1ml lysis buffer, 1µl TSA, 1µl Protease inhibitor and 1µl PMSF]. Cell suspension was added to the micro-centrifuge tubes, which had equal volumes of glass beads (0.5g beads of 0.5mm diameter Sigma, Cat: G8772-500G). The sample was then vortexed for 25 minutes at 4^{o}C in order to break 90% of the cells. The cells were then spun down at 2000rpm for 5 seconds and the supernatant was collected and again spun down at 13000rpm for 15 minutes at 4^{o}C. The supernatant was removed and each of the pellets were re-suspended in 1ml ice cold negative lysis buffer (negative lysis buffer contained 1ml lysis buffer, 1µl TSA and 1µl Protease

inhibitor). The cells were then sonicated to break the genomic DNA into small uniform fragments (900bp-1000bp).Cells were then spun down at 4000rpm for 20 minutes to collect the supernatant. Stored at -20^{o}C.

2.12.3. Input sample preparation

390µl elution buffer (1% SDS + 0.1 M $NaHCO_3$) and 16µl of 5M NaCl were added to the 10µl of lysate, and incubated the tubes at 65^{o}C for 4 hrs. Then, 8µl 0.5M EDTA, 16µl 1M Tris HCl pH 6.5 and 1µl Protinase K were added to the tubes and incubated again at 45^{o}C for 1hr. Phenol chloroform extraction was then conducted and followed by the ethanol precipitation. There was no need to add NaOAc during the phenol chloroform extraction since Na was added by adding 5M NaCl, in the previous step. DNA quantification was done using spectrophotometer.

2.12.4. Immunoprecipitation

Sonicated cell lysate (5.5µg) was diluted in 10 fold ChIP dilution buffer and 1 µl of TSA and 1ul of protease inhibitor were added to a centrifuge tube. 40µl of salmon sperm DNA/Protein A agarose was added to the same tube and incubated at 4^{o}C for one hour with rotation to reduce nonspecific background. This step removed the proteins, which interact nonspecifically with the agarose.

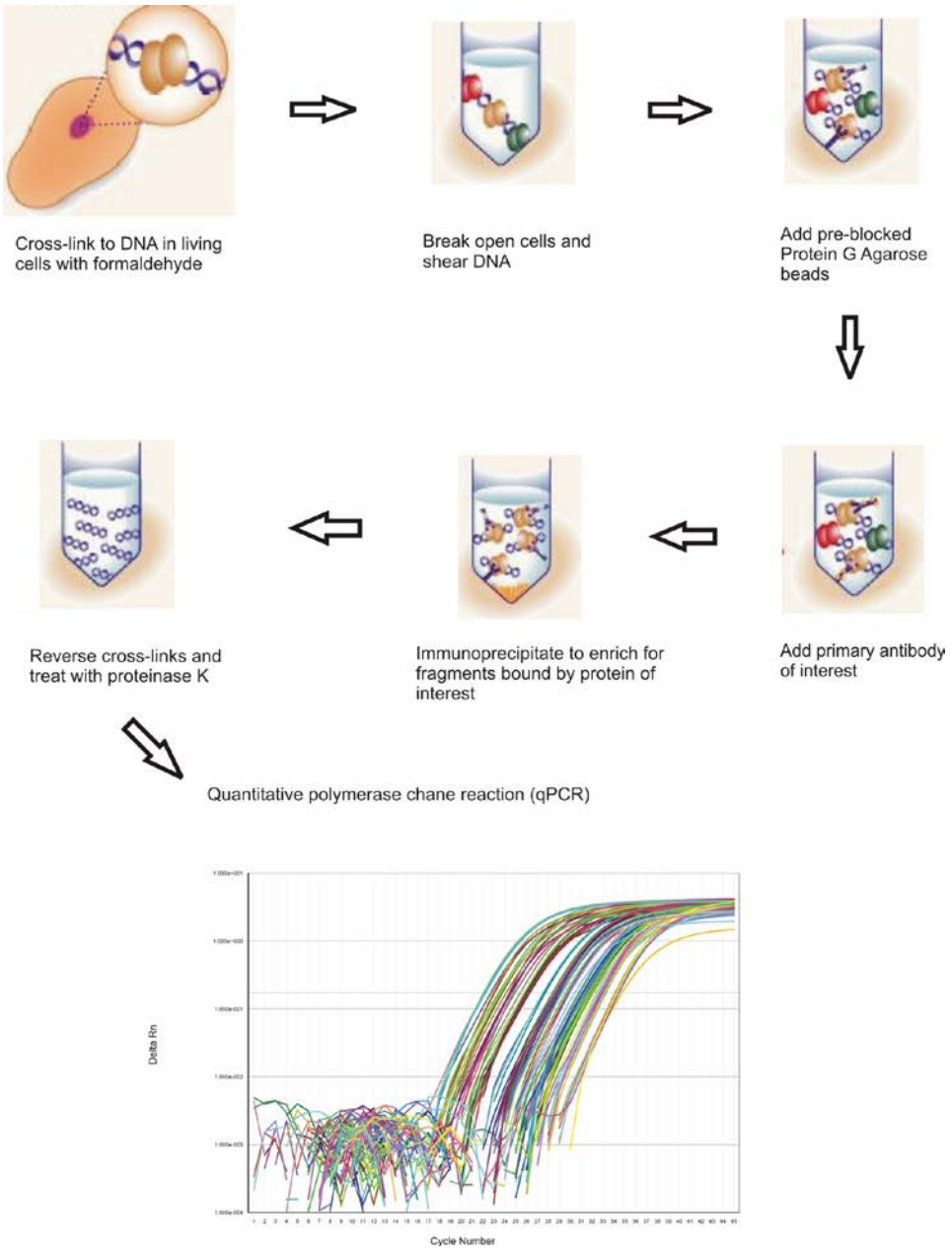

Figure 2.3 Chromatin immunoprecipitation: Protein and DNA cross-linked with formaldehyde, shear the DNA by sonication, immunoprecipitate, capture with protein A agarose beads, reverse cross-linked, DNA was purified and quantified.

Agarose was pelleted (at 2000rpm for 5 seconds) by brief centrifugation and the supernatant fraction was collected. Antibodies were added directly against Snf2p, Ino80p, PolIIp, H3p, H4p, acH3p and acH4p separately. The tubes were incubated overnight at 4^{o}C with rotation. Then, 60µl salmon sperm DNA/ protein A agarose were added and incubated for one hour at 4^{o}C with rotation to collect the antibody histone complex. The negative controller performed a non-antibody immunoprecipitation by incubating the lysate with 60µl of salmon sperm DNA/ protein A agarose for one hour at 4^{o}C with the rotation. Agarose was then pelleted by centrifugation at 2000rpm for 5 seconds. The supernatant, which contained unbound, non–specific DNA was removed. The pellet was washed with low salt, high salt, LiCl and twice with 1X TE respectively. The histone complex was eluted from the antibody by adding 200µl of freshly prepared elution buffer. 5M NaCl was added and reverse cross-linked by heating at 65^{o}C for 4 hours. Then, 8ul of 0.5 M EDTA, 16ul of 1M Tris-HCl, pH6.5 and 1µl of Protinase K was added and incubated for one hour at 45^{o}C. The DNA was then recovered by phenol/chloroform extraction and ethanol precipitation. Finally, the pellet was re-suspended in 20µl of TE.

2.12.5. Quantitative PCR (qPCR)

The PCR was used to determine the abundance of DNA fragments that were bound by the protein of interest. Probe-based real-time PCR (7500 real-time PCR system) was used during this experiment. The qPCR required a pair of PCR primers and an additional fluorogenic probe. Primers and probes were designed using primer express software 3.0. TaqMan Gene Expression Master Mix was used to setup the reactions.

Each reaction contained 12.5µl TaqMan mix, 2.5µl forward primer, 2.5µl reverse primer, 2.5µl probe and1µl of DNA. The total volume was increased up to 25µl by adding distilled autoclaved water.

2.13. Cell growth

2.13.1. Cell culture

Yeast strain was grown from a single colony in appropriate media. These cultures were grown at 30^{o}C and 300rpm. All these strains were subjected to inducing (adding $CuSO_4$) and un-inducing conditions. The optical density was measured at 600 nm using Lambda 35 UV/VIS spectrometer (Perkin Elmer). The critical parameters in performing these experiments were copper concentration, temperature and the rotation speed.

2.13.2 Glycerol stock preparation

50% glycerol was prepared by mixing 100% glycerol and appropriate media in 1:1 ratio. Overnight culture of particular yeast strain was mixed with 50% glycerol in a 1: 1 ratio followed by immediate freezing in dry ice. Glycerol stocks were stored in -80^{o}C.

CHAPTER 3

3 Both Ino80p and Snf2p are required for *CUP1* expression

3.1. Aims of this chapter

Many yeast chromatin remodelers have been characterized recently, including SWI/SNF, RSC, INO80 and IWSI (Cairns *et al*., 1998; Muchardt *et al*., 1999; Ebbert *et al*., 1999; Mellor *et al*., 2004). They are mainly responsible for the reconfiguration of chromatin structure during gene activation. For example, it has been shown that SWI/SNF is responsible for the nucleosome mobilization over the entire *HIS3* gene (Kim *et al*., 2006). It has also been shown that SWI/SNF and INO80 remodelers are involved in nucleosome disruption at the promoter of *INO1* (Ford *et al*., 2007). As such, different remodelers may be required for the activation of different genes. We have chosen *CUP1* as the model to understand the mechanism of gene expression. To this end, it is important to identify which transcriptional co-activators work on the *CUP1* promoter and their functional interdependence in induction. To date, it is still unclear precisely which remodelers are involved in *CUP1* activation. Therefore, my first aim is to identify which remodelers are required for *CUP1* induction as the first step to understand the mechanism of *CUP1* expression.

In our first aim we have conducted the growth analysis using knockout mutants to determine which one is lethal in the presence of copper. Further we have conducted RNA analysis to identify whether this metallothionein deficiency is controlled at transcriptional or translational level.

3.2. Materials and Methods

3.2.1 Generation of yeast *rsc3*Δ strain

The *RSC3* deletion strain was created through a homologous recombination technique by using the pRS416 vector. The schematic procedure is shown in Figure 3.1 and the detail is described in section 3.3.1. First, the PCR was used to produce a 1239-bp DNA fragment that included the *URA3* sequence with the *RSC3* flanking sequence. Electroporation was performed to introduce this PCR product into the WT cells (Table 3.1). A recombinant phenotype was identified through the auxotroph mutant and the recombinant genotype was confirmed by PCR. PCR was performed as shown below: 95^{o}C for 2 minutes followed by 30 consecutive cycles of 95^{o}C for 30 second, 55^{o}C for 30 seconds and 72^{o}C for 2 min. under the presence of 200μM of each dNTPs, 2mM $MgCl_2$, 1X buffer, 1μM forward primer, 1μM reverse primer, 5μl of genomic DNA, 0.005u/ml Taq polymerase and volume up to 25μl adding autoclaved distilled H_2O.

3.2.2 Growth media for WT (BY4741), s*nf2Δ*, *isw1Δ*, *ino80Δ* and *ura3Δ* strains

Yeast strains used in this experiment are shown in Table 3.1. WT and s*nf2Δ* strains were grown in SC-Cu media (synthetic complete medium lacking copper). The *ino80Δ*, *rsc3Δ*, and *isw1Δ* yeast strains were grown in SC-trp-Cu (SC medium lacking both tryptophan and copper), SC-ura-Cu (SC medium lacking both uracil and copper) and SC-ade-Cu (SC medium lacking both adenine and copper) media, respectively. The definition of each growth medium can be found in Chapter 2. Cells were grown at 30^{o}C. For growth experiments, all strains were grown in

different copper concentrations (1.5, 2, 2.5 and 3mM) and the growth curve was observed over 30 hours.

3.2.3 Total RNA preparation

Cells were grown from a single colony till mid-logarithmic phase (optical density (OD)-0.8-1.2), followed by incubation in the presence (2mM Copper) or in the absence of copper. Samples were collected at different time intervals (0, 15, 30, 45 and 60 minutes). Cells extracts were subject to phenol chloroform extraction using an acid phenol (pH 4.3) followed by ethanol precipitation. RNA quantification was done by reading A_{260}. Subsequently, total RNA was subject to DNase treatment and stored in -20^{o}C until use.

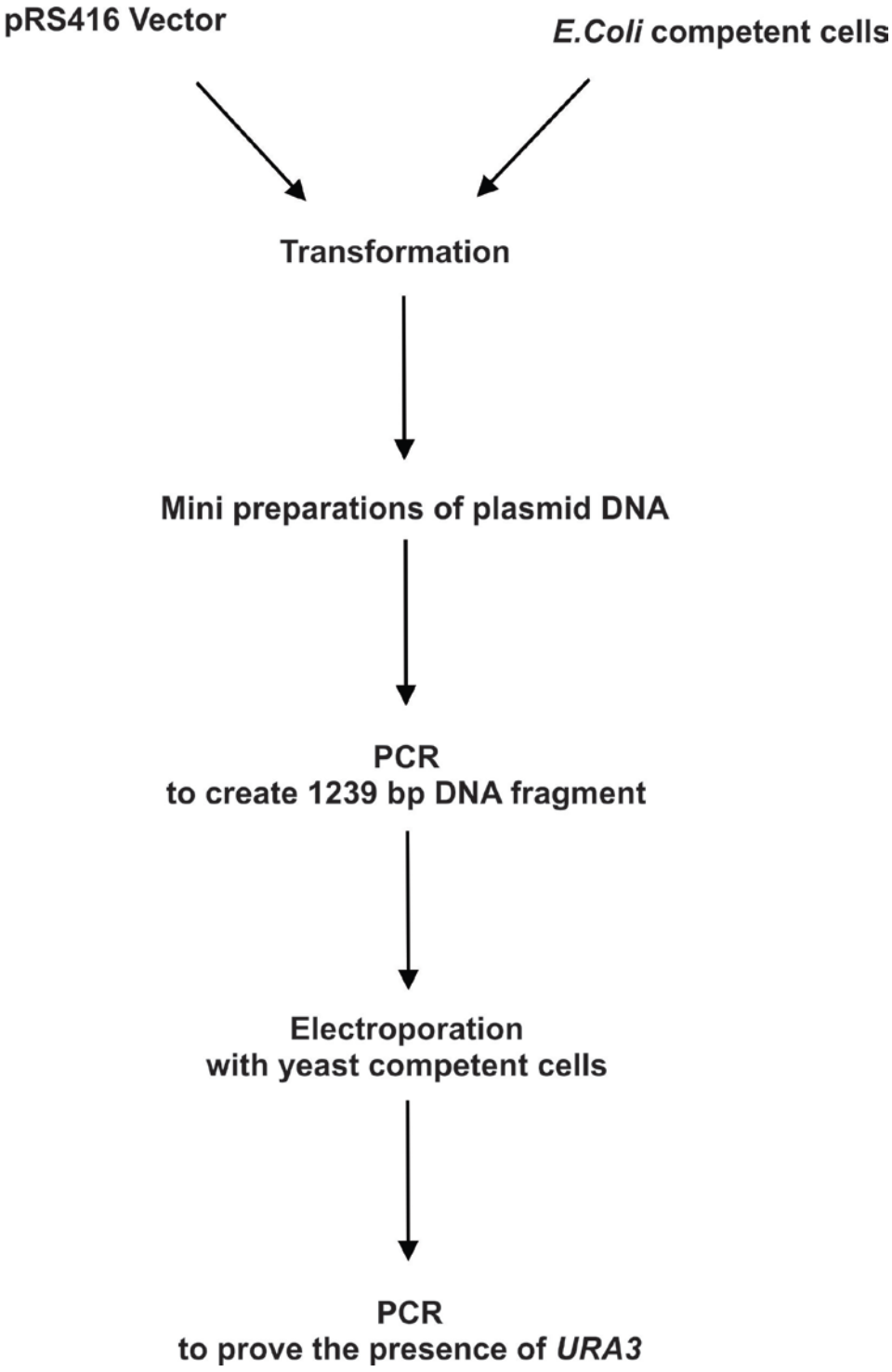

Figure 3.1 Schematic procedure of homologous recombination.

Table 3.1 Yeast Strains used in this study

Strains	Genome type
WT (BY4741)	*MATa his3Δ1 leu2Δ0 met15Δ0 ura3Δ0*
s*nf2Δ*	*MATa his3Δ1 leu2Δ0 met15Δ0 ura3Δ0* s*nf2Δ*
isw1Δ	*MATa ade2-1 cabn1-100 HIS3 leu2-3, 112trp1-1 ura3-1 RAD5+ SWI2-3FLAG-KanMX isw1Δ::ADE2*
ino80Δ	*MATa ino80Δ::trp1 his3Δ200 leu2Δ0 met15Δ0 trp1Δ63 ura3Δ0*
rsc3Δ	*MATa his3Δ1 leu2Δ0 met15Δ0 rsc3Δ*

3.2.4 Quantitative reverse transcription polymerase chain reaction (qRT-PCR)

SYBER Green ER Two-Step qRT-PCR kit (Invitrogen, Cat No: 11765-100) was used to perform RNA analysis. cDNA was made from mRNA in the first step by performing RT-PCR. Approximately 1 μg of mRNA was used in each reaction. In the second step qPCR was performed to examine the amount of cDNA templates. Primers used in the qPCR reaction are shown below.

CUP1 primers,

Forward Primer: 5'-GCAGCCAATGTGGTAGCTGCAAA- 3'

Reverse Primer: 5'-CATTTCCCAGAGCATGA-3'

ACT1 Primers,

Forward Primer: 5'-CCAAGCCGTTTTGTCCTTGT- 3'

Reverse Primer: 5' –ACCGGCCAAATCGATTCTC- 3'

ACE1 Primers,

Forward Primer: 5'-AGCAGCGCATGTCAATGGT- 3'

Reverse Primer: 5'-ACTCGGCAATGTGGTTGTCA- 3'

3.2.5 Analysis of RNA quantity

Each PCR reaction was repeated 3 times. The target RNA quantities were estimated from the threshold amplification cycle number (C_T) using Sequence Detection System software (Applied Biosystem). A ΔC_T value was calculated for each sample by subtracting the C_T value for the specific time point from the C_T value for the starting point (0 minute). Each RNA quantity at each specific time point was then calculated with the formula shown below. To normalize the expression level, each time point was normalized to the *ACT1* mRNA value by taking the ratio of *CUP1* to *ACT1* at the specific time point (*CUP1*/*ACT1*).

Formula:

CUP1 mRNA at X minute after induction = $2^{(a-b)} = 2^e$

Whereas a is the C_T from 0 minute and b is the C_T from X minute

ACT1 mRNA at X minute after induction = $2^{(c-d)} = 2^f$

Whereas c is the C_T from 0 minute and d is the C_T from X minute

$$CUP1/\ ACT1\ = 2^e/2^f$$

3.3. Results

3.3.1. Creation of yeast *rsc3*Δ strain

All the other remodeler mutants are available except RSC, therefore, we have created the rsc3 mutant. A pRS416 vector that carries a *URA3* marker was used for homologous recombination to create an *rsc3*Δ strain (Figure 3.2). A PCR technique using the chimeric primers (as shown below) was used to create a 1239-bp DNA fragment that contains *URA3* and *RSC3* flaking sequences (Figure 3.3).

Forward primer: 5'-TTTCAAACCAAAGTCATTGG *TGCTCTGCTGCAATTGCCCC*

RSC3 *URA3*

AGATTGTACTGAGAGTGCAC-3'

Reverse primer: 5'-*ATTTGGGCGCTTTGGTGGGCTATACTATCG* GTGCCTATAT

RSC3 *URA3*

CTGTGCGGTATTTCACACCG-3'

This PCR product (1239-bp DNA fragment) was introduced into WT cells through electroporation (Figure 3.4) followed by recombinant selection using SC-ura media. The concept of electroporation depends on the relatively weak nature of the phospholipids bilayer's hydrophobic/hydrophilic interactions and its ability to spontaneously reassemble after disturbance. A quick voltage shock disrupted areas of the membrane temporarily, allowing the polar molecules to pass and then, the membrane resealed quickly. The resulting recombinant

cells were *rsc3*Δ cells that carried *URA3*. To confirm the recombinant genotype, yeast genomic DNA was prepared. Subsequently, PCR was used to prove the presence of *URA3* in the *rsc3*Δ strain by using the primers as shown below.

Forward primer: 5'-GGAACGTGCTGCTACTCATC-3'

Reverse primer: 5'-GCTGGCCGCATCTTCTCAAA-3'

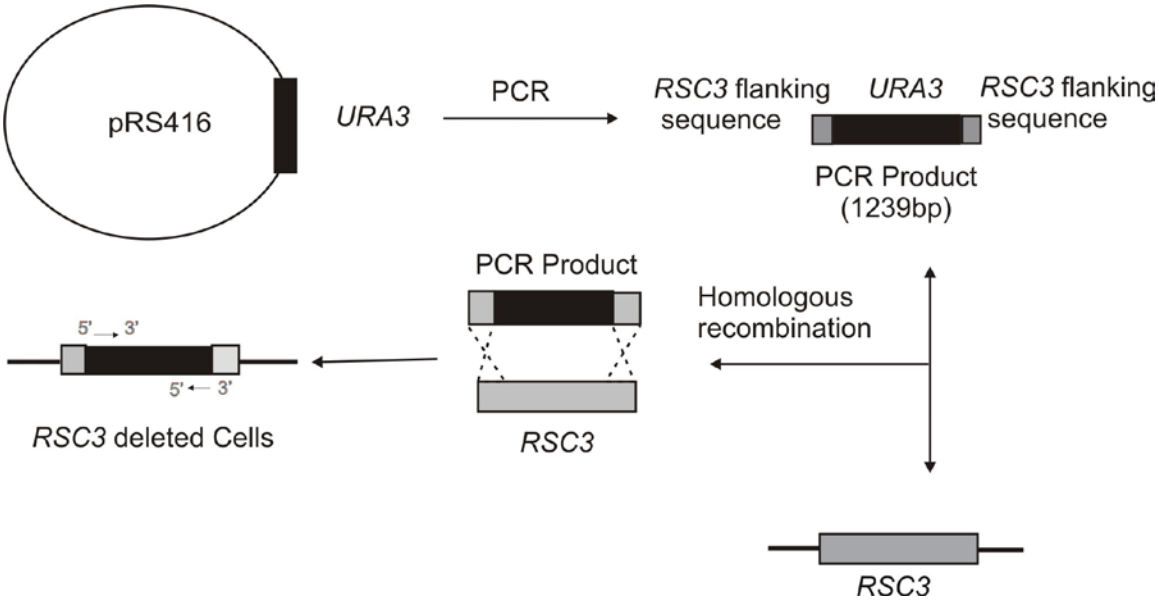

Figure 3.2 Schematic process of the creation of *rsc3Δ* mutant

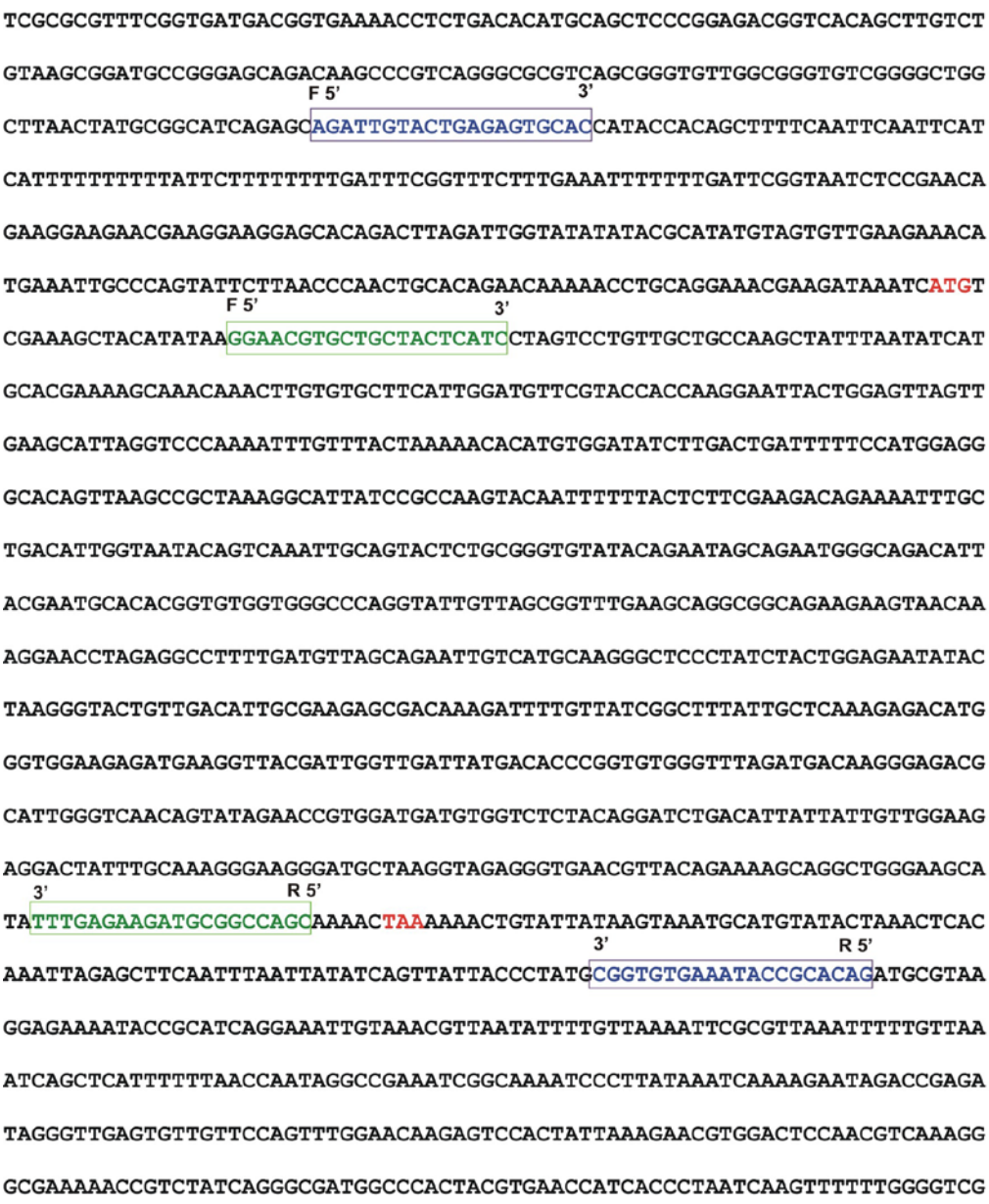

Figure 3.3 The *URA3* region of pRS416 DNA. Blue boxes represent the 20 bp DNA sequences that were used to make forward and reverse chimeric primers for PCR reaction. Red highlighted DNA sequences represent the starting codone (ATG) and the stop codon (TAA) of *URA3*. Green boxes represent the forward and reverse primers used to confirm the presence of *URA3*.

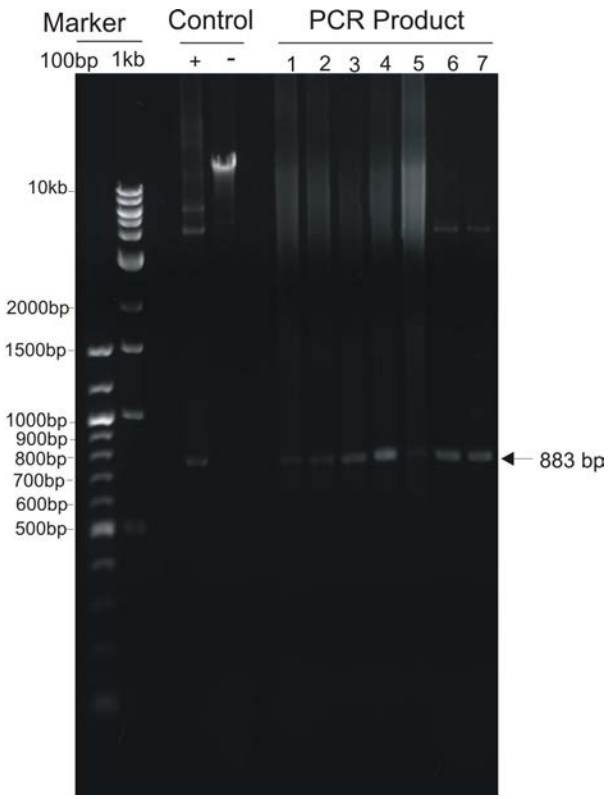

Figure 3.4. A 1% agarose gel analysis of the PCR product. Genomic DNA was extracted from recombinant cells and was used as a template for PCR reaction. A DNA fragment of 883-bp would suggest the presence of *URA3* in the recombinant cells. Lane 1 to 7 represents each recombinant strain obtained from the selective medium. The negative control (-) was the parental strain that was used for recombination and the positive control (+) was pRS416 vector DNA.

A PCR product with 883-bp long DNA fragments would indicate the presence of *URA3* gene in the genome. If the genome doesn't have *URA3,* there will be no any PCR product. Figure 3.3 shows the analysis of the 1% Agarose gel electrophoresis. The DNA obtained from the WT cells were used as a negative control and vector pRS416 DNA as a positive control. Lanes 1 to 7 represent the PCR products obtained using 7 different phenotypic recombinant cells genomic DNA as templates. The result showed that an 883-bp long PCR product appeared in each lane and indicated that these phenotypic recombinant cells all carry *URA3*.

3.3.2. Growth experiment to identify which mutant is sensitive to the presence of copper.

In order to identify which remodeler works on the *CUP1* promoter, growth survival experiments were performed in the presence of copper. Our hypothesis was that if a specific chromatin remodeler was involved in *CUP1* expression the cells would not survive in the absence of that remodeler under the presence of copper. To this end, we grew each of the remodeler knockout mutants in the presence of different copper concentrations ranging from 0 mM to 3 mM. Yeast strains used in this experiment are listed in Table 3.1. If the growth rate of specific mutant decreased significantly upon increasing copper concentrations, it would suggest that the specific remodeling complex is responsible for *CUP1* gene expression. Conversely, if the growth curve is similar to the WT cells, it would suggest that the particular remodeling complex may not be responsible for *CUP1* gene expression.

For the WT, cells grew well in the absence of copper. As the copper concentration increased every 0.5 mM in the medium, the doubling time increased about 20% to 40% longer.

The WT cells were inviable in the presence of 2.5 mM copper (Figure 3.5A). These results suggest that the WT cell is resistant to copper up to 2.5 mM. The effect of copper on cell growth is shown in Table 3.2. Here, the A_{600} value (optical density at 600 nm) at the 24^{th} hour for the presence of 1.5 mM copper was subtracted from the A_{600} value at the 24^{th} hour for the absence of copper and, the value was divided by the original A_{600} value for the absence of copper. This can help us to identify the effect of copper on cell growth. Also we calculated the relative cell doubling time (in folds) in order to reveal the sensitivity of each strain to copper concentration. For WT cells, the decrease of growth rate was about 55%, indicating that in the presence of 1.5 mM copper the increase of doubling time was 2.22 folds for the WT cells (Figure 3.6A).

The *isw*1Δ and *rsc3*Δ cells showed a very similar pattern as the WT cells in both the absence and presence of copper (Figure 3.5D and 3.5E). Their cell doubling time was very similar to WT cells, which were 1.25 and 1.57 for *isw*1Δ cells and *rsc3*Δ cells, respectively (Figure 3.6.A). Also they had lower reduced growth rate values, which was 20.28% for *isw*1Δ cells and 36.3% for *rsc3*Δ cells (Figure 3.6B) when compared to WT cells (Table 3.2). These results suggested that the deletion of *ISW1* or *RSC3* has no negative impact on *CUP1* expression. Therefore, they are not likely to function positively on *CUP1* expression.

For both *ino80*Δ cells and *snf2*Δ cells, they grew well in the absence of copper, but were inviable in the presence of copper (Figure 3.5B and 3.5C). Both *ino80*Δ cells and *snf2*Δ cells had the highest reduced growth rate values, which were 70.49% and 80.78% for *ino80*Δ cells and *snf2*Δ cells respectively (Figure 3.6. B; Table 3.2). Furthermore, both *ino80*Δ and *snf2*Δ cells showed a longer cell doubling in the presence 0f 1.5mM [Cu] time compared to WT cells. Their

doubling time increased 3.41 folds and 5.2 folds for both *ino80*Δ and *snf2*Δ cells, respectively. This indicated that both *INO80* and *SNF2* knockout mutants cannot survive in the presence of copper, suggesting that the *CUP1* expression has been repressed. Therefore, the cells were sensitive to copper when either *INO80* or *SNF2* was deleted, indicating that *INO80* and *SNF2* have a positive effect on the *CUP1* gene activation**.** Cells were not sensitive to copper when either *ISW1* or *RSC3* was deleted, which showed that *ISW1* and *RSC3* may not be positively involved in *CUP1* gene activation.

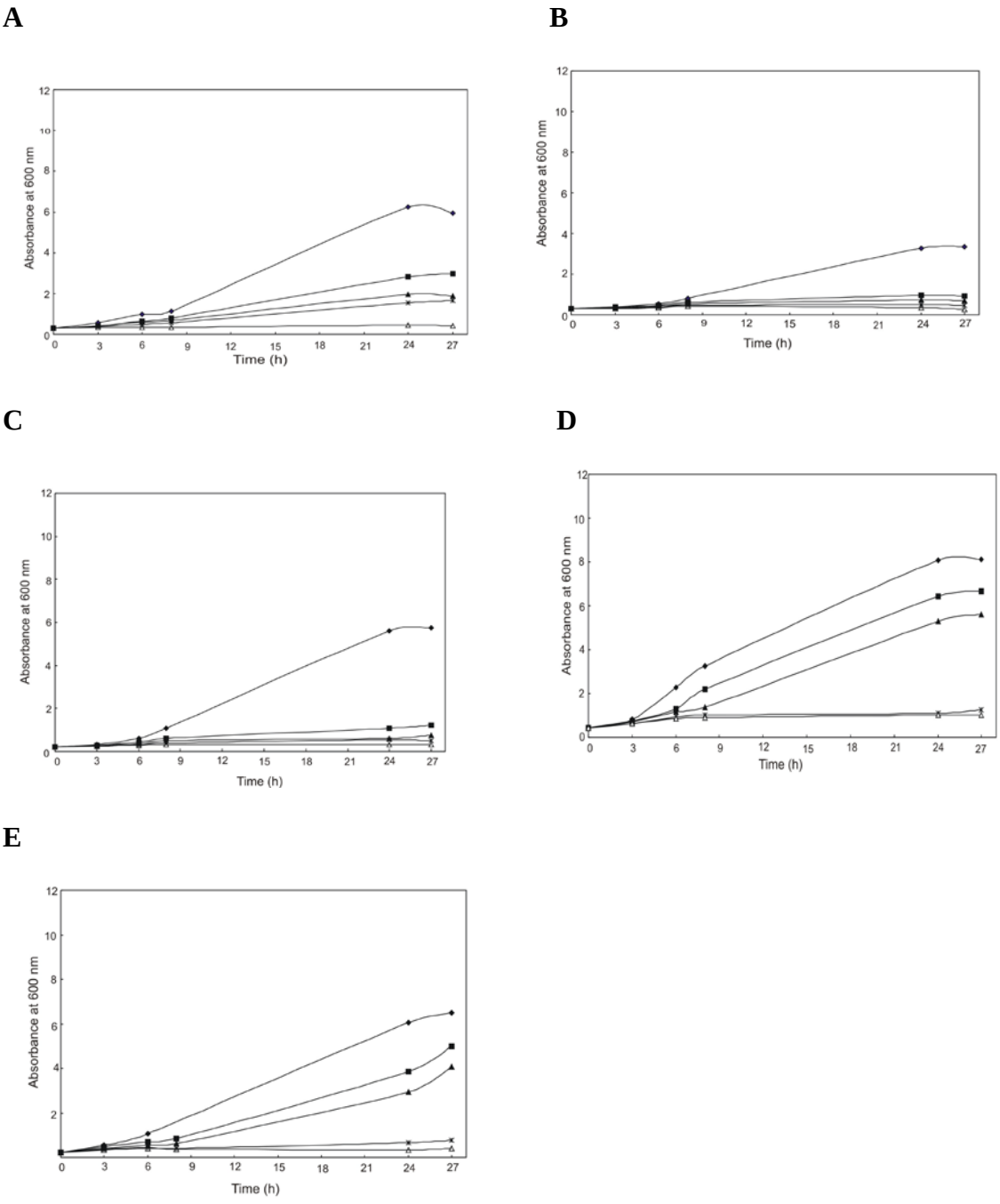

Figure 3.5 Growth curves demonstrate the sensitivity of remodeler knockout cells at the different copper concentrations[(◆)0 mM, (■) 1.5mM, (▲) 2mM, (∗)2.5mM, (△) 3mM], (A)WT cells , (B)*ino80*Δ cells, (C)*snf2*Δ cells, (D)*isw*1Δ cells, (E)*rsc3*Δ cells.

Table 3.2 Decrease of growth rate percentage at the 24th hour

Cell Type	O.D. at 0 mM[Cu]	O.D. at 1.5 mM[Cu]	Changes of cell doubling time (Folds)	Decrease of growth rate %
WT	6.25	2.8	2.22	55.14
*isw*1Δ	8.08	6.44	1.25	20.28
*snf2*Δ	5.62	1.08	5.2	80.78
*ino80*Δ	3.27	0.96	3.41	70.49
*rsc3*Δ	6.06	3.86	1.57	36.3

A.

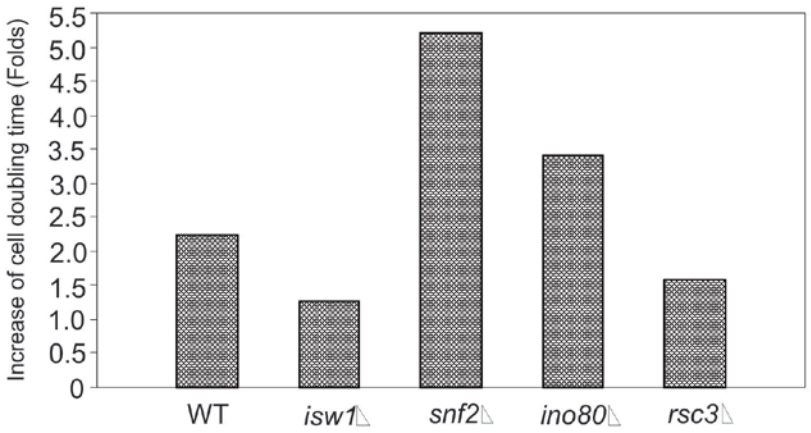

B.

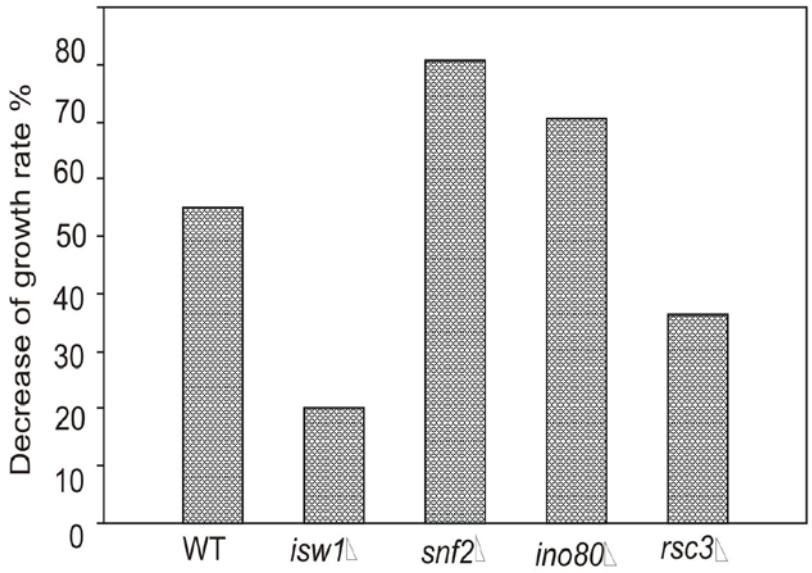

Figure 3.6 The toxic effect of copper on yeast cell growth. Growth curve data from WT, *isw*1Δ, *snf2*Δ, *ino80*Δ and *rsc3*Δ cells arranged in to bar chats. (A) Bar chart showing the increase of cell doubling time at 24th hour. (B) Bar chart showing the decrease of the growth rate percentage.

3.3.3 The analysis of *CUP1* mRNA

The growth survival results showed that both *snf2Δ* and *ino80Δ* cells were sensitive to the toxic levels of copper, suggesting a lack of metallothionein (MT) in these two strains in the presence of copper. The lack of MT could be the result of a defect of *CUP1* gene expression at the transcriptional level or translational level. To further confirm transcriptional control, qRT-PCR was used in this study. WT, *snf2Δ, isw1Δ and ino80Δ* cells were grown to an optical density at 600nm of about 1.0, and then copper was added to a concentration of 2 mM. The total RNA was prepared at various time intervals after induction. The total RNA was prepared and treated with DNase to remove DNA, followed by phenol chloroform extraction. The SYBER Green Two-Step qRT-PCR kit was used to prepare cDNA and to quantitate the amount of cDNA. The quantitative PCR method was used to determine the copy number of DNA templates in a PCR reaction. There are two types of real time PCR; probe-based method and SYBR Green method. Both methods required a special thermocycler equipped with a sensitive camera that monitored the fluorescence in each well of the 96-well plate at frequent intervals during the PCR reaction. The cDNA was prepared from mRNA in the first step, using RT-PCR. In the second step, we did qPCR to quantitate the amount of templates. Figure 3.7 shows the location of primers we used in the qPCR reaction.

In the WT cells, *CUP1* mRNA was induced by copper (2mM) as soon as 15 minutes after induction. This *CUP1* mRNA level accumulated steadily, and reached a maximum level at 60 minutes after induction.

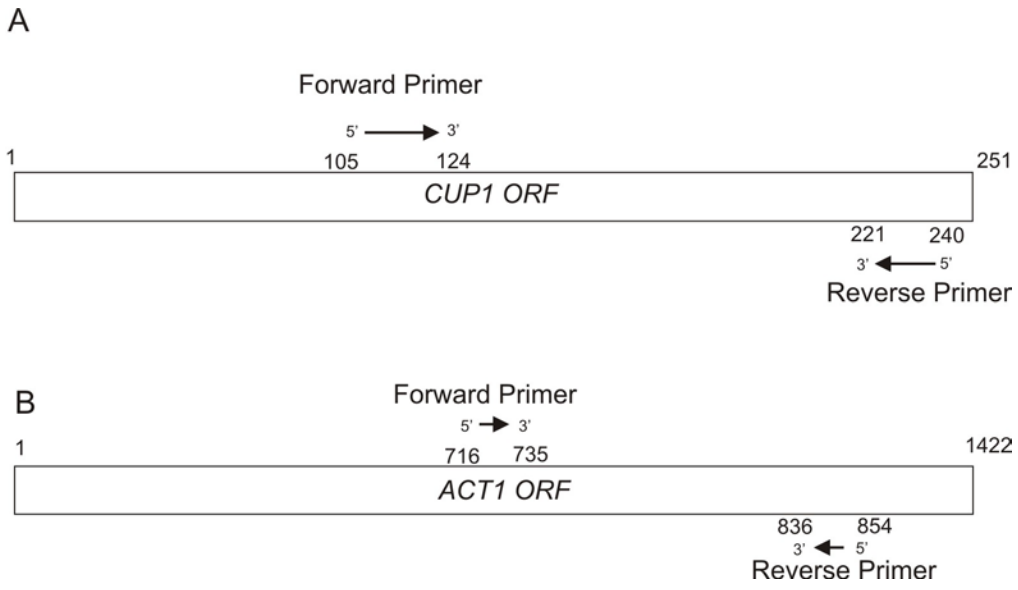

Figure 3.7 Two sets of primers used in the qPCR. (A) The location of the *CUP1* forward and reverse primers on the *CUP1 ORF* region. **(B)** The location of the *ACT1* forward and reverse primers on the *ACT1 ORF* region.

The maximum level of induction was about 40 folds compared to un-induced cells (Figure 3.8A). For both *isw1*Δ and *rsc3*Δ cells, they also showed similar amount of *CUP1* mRNA induction, although to a lesser extent (Figure 3.8D and E). In *isw1*Δ and *rsc3*Δ cells, the maximum level of induction was about 16 folds and 23 folds compared to un-induced cells respectively. These maximum levels of *CUP1* mRNA was about half of what is in WT cells. There were no difference in the level of *CUP1* mRNA between un-induced and induced conditions in both *snf2*Δ and *ino80*Δ cells (Figure 3.8B and C).

To compare these mRNA levels more closely, normalized mRNA levels after 30 minutes copper induction were calculated and plotted in Figure 3.9. The mRNA levels of both *snf2*Δ and *ino80*Δ cells were significantly lower than the WT cells mRNA levels, suggesting a transcriptional control of *CUP1* by both Snf2p and Ino80p (Figure. 3.9). The mRNA levels of both *isw1*Δ and *rsc3*Δ cells were insignificant from the WT cells mRNA levels, indicating that both Isw1p and Rsc3p are not required for *CUP1* transcription (Figure. 3.9). These results suggested that *SNF2* and *INO80* are required for *CUP1* gene expression at the transcriptional level. The loss of either one was lethal at high copper concentrations, presumably because insufficient *CUP1* mRNA was made in order to direct the synthesis of enough metallothionein to chelate all the copper ions entering to the cell.

To rule out the effect of *ACE1* quantity in each mutant, *ACE1* mRNA levels were also examined for all strains used in the experiment (Figure 3.10). The ratios of *ACE1/ACT1* were observed 0.4 and 0.79 for repressive and induced conditions of the WT.

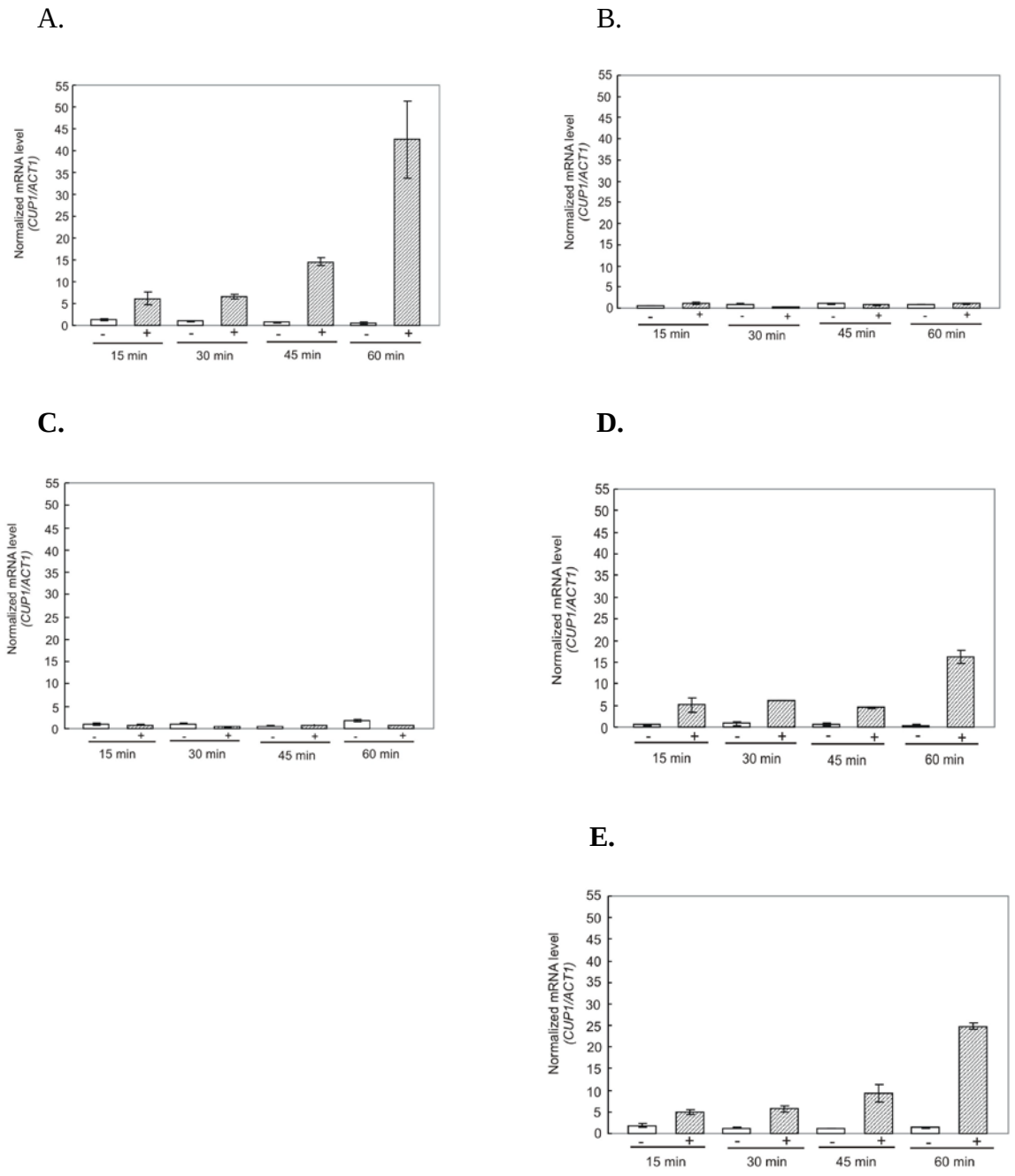

Figure 3.8 Induction of *CUP1*. (A)WT cells, (B)*ino80*Δ cells, (C)*snf2*Δ cells, (D)*isw*1Δ cells, (E)*rsc3*Δ cells. Cells were prepared from induced conditions (▨) adding 2mM CuSO4 or un-induced conditions (□) at different time intervals (15, 30, 45 and 60 minutes) after addition of copper.

cells. The ratios of *ACE1/ACT1* were observed 0.68, 0.93, 1.0 and 0.61 in *isw1*Δ, *ino80*Δ, *snf2*Δ and *rsc3*Δ cells respectively for repressive condition. Further the ratios of *ACE1/ACT1* in induced condition were 0.75, 0.53, 0.72 and 0.84 in *isw1*Δ, *ino80*Δ, *snf2*Δ and *rsc3*Δ cells respectively. There was no significant difference observed in *ACE1* mRNA levels between WT and mutant strains in both repressive and induced conditions. Our results showed that there was no significant difference between all mutant strains and the WT cells. These results suggested that Ace1p expression was not influenced by the deletion of the remodelers. The *ACE1* mRNA remained constant in all yeast strains tested. Therefore, the mRNA levels among *snf2*Δ and *ino80*Δ cells and WT cells were not due to the amount of Ace1p but instead were due to the deletion of *SNF2* and *INO80*.

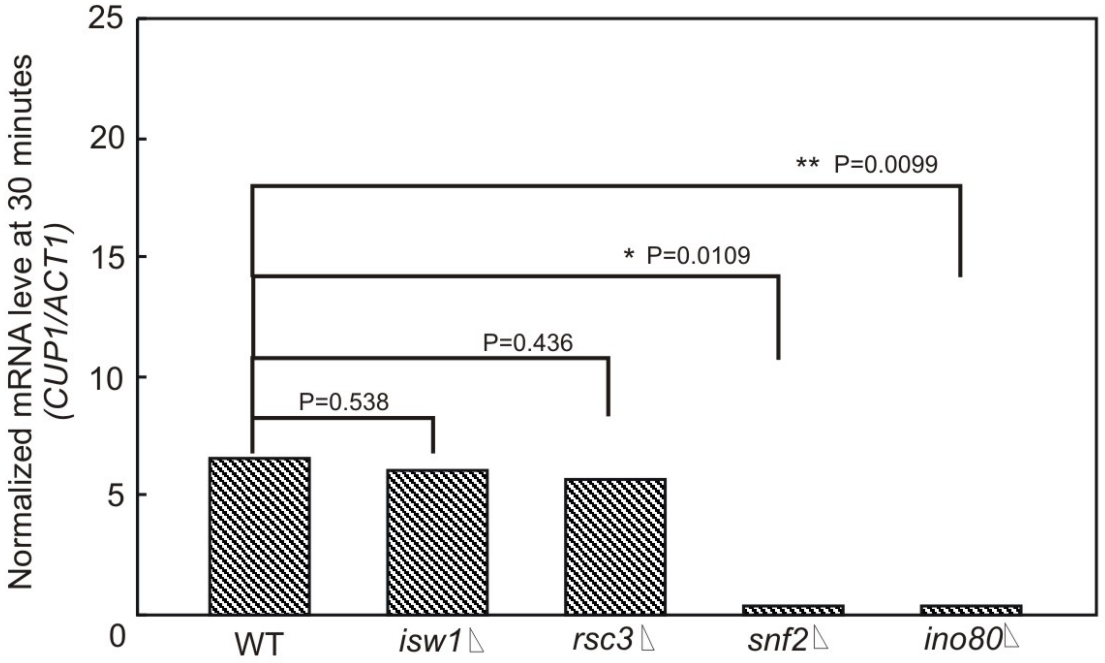

Figure 3.9 The qRT-PCR analysis of *CUP1* mRNA levels of WT, *isw*1Δ, *rsc3*Δ, *snf2*Δ and *ino80*Δ cells after 30 minute 2mM CuSO4 induction. (**: p < 1%; *: p < 5%)

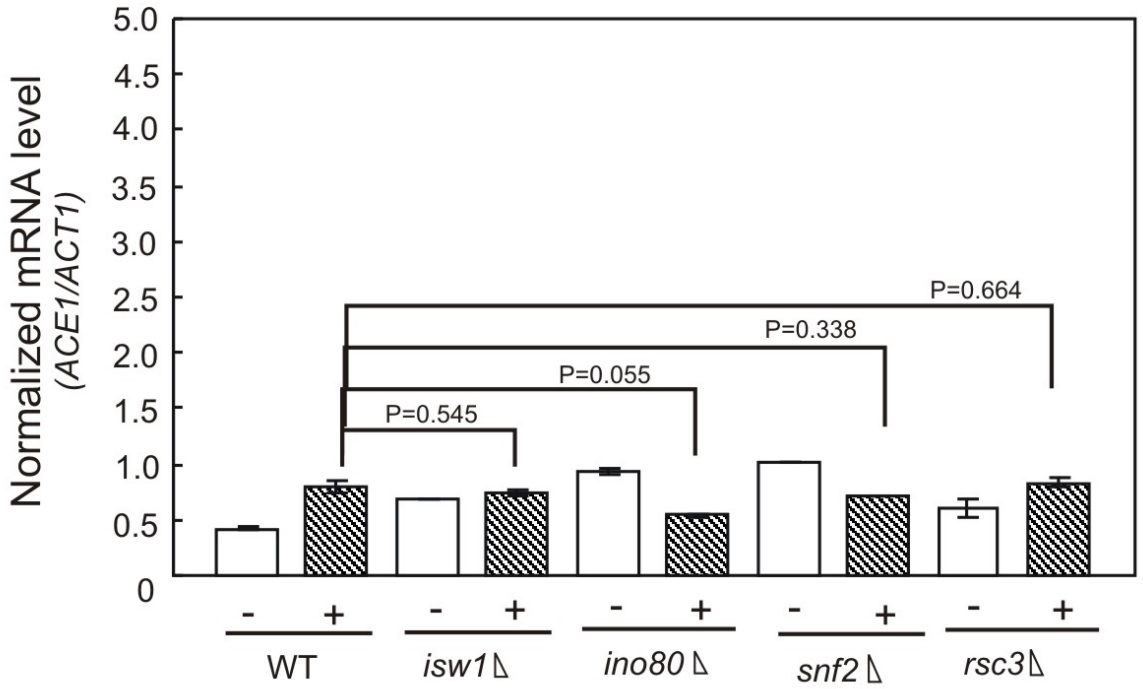

Figure 3.10 Normalized mRNA levels of *ACE1/ACT1*. The analysis of *ace1* mRNA levels using qRT-PCR for WT cells, *ino80*Δ cells, *snf2*Δ cells, isw1Δ cells and *rsc3*Δ cells. Cells were prepared from induced conditions (▨) adding 2mM CuSO4 or un-induced conditions (□).

3.4. Summary

To address our aim and identify which chromatin remodelers are responsible for *CUP1* expression, both growth survival experiments and *CUP1* mRNA analysis were performed. The yeast strains used in these experiments included WT, s*nf2*Δ, *isw1*Δ, *ino80*Δ and *rsc3*Δ strains. We first created an *rsc3*Δ strain since it was not commercially available. From the growth experiments, we showed that both s*nf2*Δ and *ino80*Δ strains were highly sensitive to copper. Both *isw1Δ* and *rsc3Δ* strains displayed similar growth patterns as WT cells in the presence of copper. Our findings suggest that ISW1 and RSC3 remodeling complexes have no positive effect in *CUP1* activation or that it may have a negative effect in *CUP1* activation. On the other hand, the deletion of *SNF2* and *INO80* resulted in the death of cells in the presence of copper, indicating that both Snf2p and Ino80p might be responsible for *CUP1* expression.

RNA analysis was performed to further examine whether the effect of Snf2p and Ino80p deletion were at the transcriptional level. Both the s*nf2*Δ strain and *ino80*Δ strain showed very low mRNA levels compared to the WT mRNA levels after induction. However, both the *isw1*Δ strain and *rsc3*Δ strain showed increasing amount of mRNA after induction, although it was at a lesser extent compared to WT cells. From these experiments we conclude that both SNF2 and INO80 remodeling complexes are involved in *CUP1* gene expression at the transcriptional stage. Both ISW1 and RSC3 remodeling complexes, however, may not be positively involved in *CUP1* gene expression. Furthermore, ISW1 and RSC3 remodeling complexes may have negative effect on *CUP1* gene expression.

CHAPTER 4

4 Determine the presence of that specific remodeler at the promoter

4.1 Aims of this chapter

We have identified that both Snf2p and Ino80p are important to *CUP1* expression during transcriptional regulation. To further confirm that they are directly involved in *CUP1* transcriptional activation, it is necessary to demonstrate their presence at the *CUP1* promoter during activation. To this end, chromatin immunoprecipitation (ChIP) coupled with the real-time PCR method was performed. The ChIP assay is a powerful tool to identify the interaction between a particular protein and a specific region of DNA. Real-time PCR is a quantitative PCR method to determine the copy number of DNA templates in a sample. There are two types of real time PCR: the probe-based method and the SYBR Green method. Both methods require a special thermocycler equipped with a sensitive camera that monitors the fluorescence in each well of the 96- well plate at frequent intervals during the PCR reaction. In this aim, we used the probe-based method, which is the more accurate and reliable of the two qRT-PCT methods. Using these techniques we can detect the presence of both chromatin remodelers at the *CUP1* promoter, and thus confirm the direct participation of these remodelers in *CUP1* induction.

4.2 Materials and Methods

4.2.1 Cross-linking, lysate preparation, input sample preparation and DNA quantification

All the stains including WT, *snf2Δ, isw1Δ, rsc3Δ and ino80Δ* were streaked from a single colony and were grown to mid-logarithmic phase. Cells were induced by adding 2mM $CuSO_4$. Cells were cross-linked by adding 1% formaldehyde and quenched by adding 400mM Glycine at room temperature for 5 minutes at 90rpm. Cells were collected and washed with TBS. Lysate was prepared by adding lysis buffer followed by sonication to shear the genomic DNA into small uniform fragments (600-1kb). Input samples were prepared and the DNA was quantified.

4.2.2 Immunoprecipitation

Based on DNA quantification, lysate that contained 5.5µg DNA were taken from each samples and prepared for immunoprecipitation. Antibodies against Snf2p, Ino80p, polIIp, histone H3p, histoneH4p, acetylated H3p and acetylated H4p were used. The antibodies and the concentrations used were as followed. 1.5µg anti-acetyl-histone H3 rabbit polyclonal antibody, 1.5µg anti-acetyl-histone H4 rabbit polyclonal antibody, 1.5µg anti-RNA polymerase II mouse monoclonal antibody, 2.5µg Arp8 rabbit polyclonal antibody, 1.5µg anti-Snf2 (yeast specific) rabbit polyclonal antibody, 1.5µg anti-histone H4 rabbit polyclonal antibody and 2µg anti-histone H3 rabbit polyclonal antibody were added to 5.5µg of each lysate sample for overnight immunoprecipitation. Samples were washed and eluted. Subsequently, samples were reverse

cross-linked and DNA was isolated followed by phenol chloroform extraction and ethanol precipitation (Figure 4.1).

4.2.3 qRT-PCR

The qPCR was used to determine the abundance of DNA fragments that were bound by the protein of interest. Three sets of probes were used, including probes that covered the TATA and UAS of *CUP1*, as well as the ORF region of *CUP1*.

TATA primers,

Forward: 5'AAAGACTACCAACGCAATATGGATT3'

Reversed: 5'GCAATTGATACAAGACAAGGAGTTA 3'

MGB Probe: 5' TCAGAATCATATAAAAGAGAAGC 3'

UAS primers,

Forward: 5'AAAAGACATTTTTGCTGTCAGTCACT 3'

Reverse: 5' GGAACGGTTCAGCGGAAA 3'

MGB Probe: 5' AAGAGATTCTTTTGCTGGCAT 3'

ORF primers,

Forward: 5' GCCAATGTGGTAGCTGCAAA 3'

Reverse: 5' ATGACTTCTTGGTTTCTTCAGACTTG 3'

MGB Probe: 5' AATGCCAAAAATCATG 3'

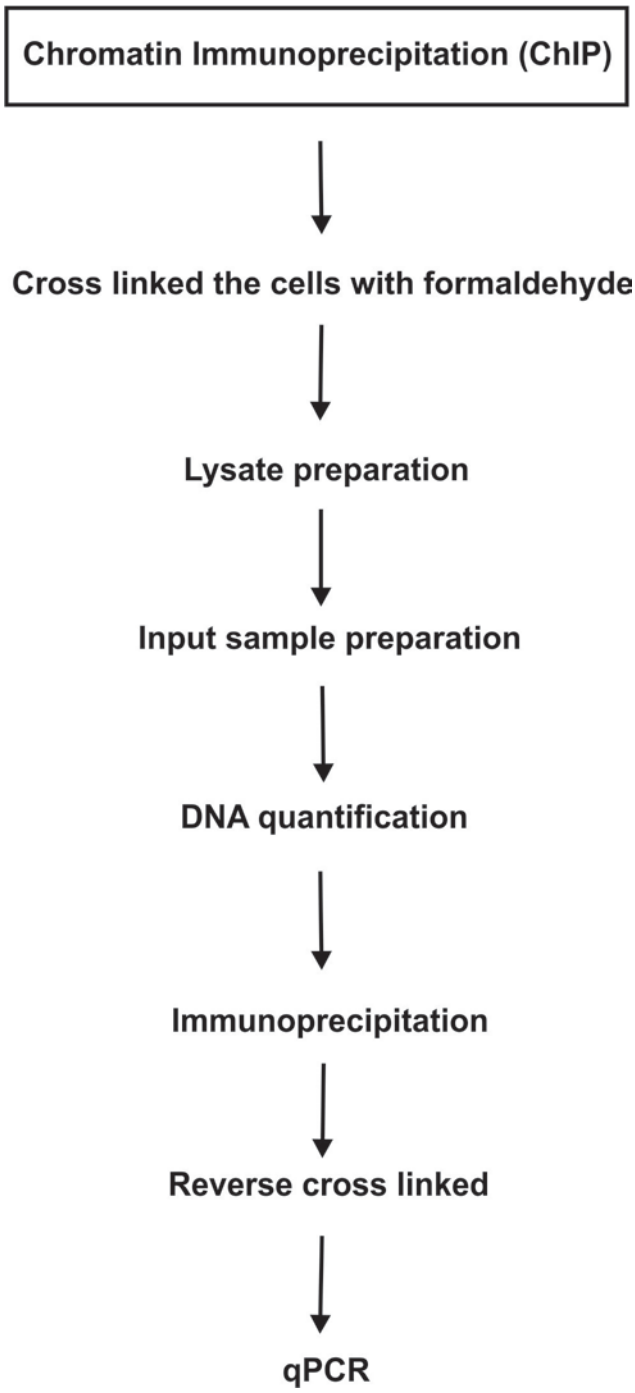

Figure 4.1 The flow chat represents the steps followed in the Chromatin Immunoprecipitation.

4.3 Results

4.3.1. Both SWI/SNF and INO80 are present at the *CUP1* promoter

For inducing and repressing WT cells, the IP signals of the Snf2p subunit of the SWI/SNF (Snf2-IP) and of the Arp8p subunit of INO80 (Arp8-IP) were observed at the *CUP1* upstream activation sequences (*UAS*), and part of the coding region of the *POL1* gene (*POL1*). *POL1* is often used as a control since it is relatively long and there should be no contributing signal fluctuation due to *POL1*. The input signals come from DNA extracted directly from cross-linked cells. The relative IP value (*UAS*/*POL1*) represented the ratio of *CUP1* IP DNA normalized to *CUP1* input to *POL1* IP DNA normalized to *POL1* input (Ford *et al*., 2008). The *UAS*/*POL1* ratio obtained from the Snf2p-IP was 0.66 for repressed chromatin, indicating that the amount of Snf2p at the *CUP1* promoter is 0.66 times less than the amount of Snf2p at the *POL1* coding region under repressing conditions (Figure 4.2). Furthermore, the *UAS*/*POL1* ratio was 17.75 for induced chromatin, suggesting that there is 17.75 times more Snf2p at the *CUP1* promoter than at the *POL1* coding region under inducing conditions (Figure 4.2). Based on these ChIP data, we concluded that Snf2p is absent at the promoter under repressing conditions, but there is a significant increase of Snf2p in the IP signals after *CUP1* induction. This indicates that a large amount of SWI/SNF was recruited to the *CUP1* promoter after induction. This increase implies that it is necessary to recruit a large quantity of SWI/SNF at the promoter during induction. These findings illustrate that SWI/SNF is present at the *CUP1* promoter, suggesting that SWI/SNF is involved in *CUP1* activation directly.

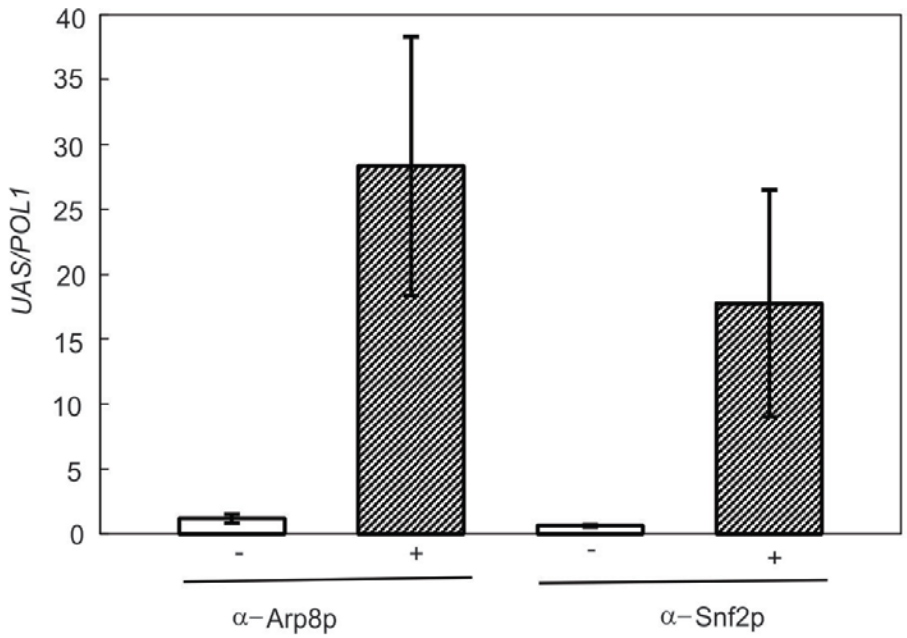

Figure 4.2 Both Arp8p and Snf2p are present at the *UAS* region in the WT cells under inducing conditions. ChIP analysis of WT cells grown under both repressing and inducing conditions. Antibodies raised against Arp8p (subunit of the INO80 remodeler complex) and Snf2p (subunit of the SWI/SNF remodeler complex) were used.

For INO80, the relative IP values obtained from the Arp8-IP were 1.19 and 28.33 for repressed and induced chromatin, respectively (Figure 4.2). This indicates that INO80 is absent at the *CUP1* promoter prior to induction but is also recruited to the promoter during induction. The IP signal again increases significantly following induction, indicating that INO80 arrives at the promoter after induction. As a result, we concluded that INO80 is also present at the *CUP1* promoter during induction.

To further illustrate the distribution of both chromatin remodelers during the induction process, we performed ChIP on the *CUP1* promoter regions including the *UAS* and the *TATA* region (*TATA*), as well as the open reading frame (*ORF*). Our results demonstrate that the relative IP values of the *UAS* and *TATA* for the ratio of inducing Snf2p-IP to the repressing Snf2p-IP were 2.85 and 3.24, respectively (Figure 4.3), suggesting that there are 2.85 folds and 3.24 folds more amount of Snf2p recruited to the promoter region under inducing conditions compared to the promoter region during repression. Meanwhile, the relative IP values for the ratio of inducing Snf2p-IP to the repressing Snf2p-IP at the *ORF* was about 1, suggesting that no significant amount of Snf2p was recruited to the *ORF* during induction. This result indicates that more Snf2p is recruited to the promoter region during activation. Similarly, the relative IP values for the ratio of inducing Arp8-IP to repressing Arp8p-IP were 2.04 and 1.77, respectively at the *UAS* and *TATA* (Figure 4.3), indicating that more Ino80p is also recruited to the conditions, respectively (Figure 4.4A). This result suggests that INO80 is present at the WT

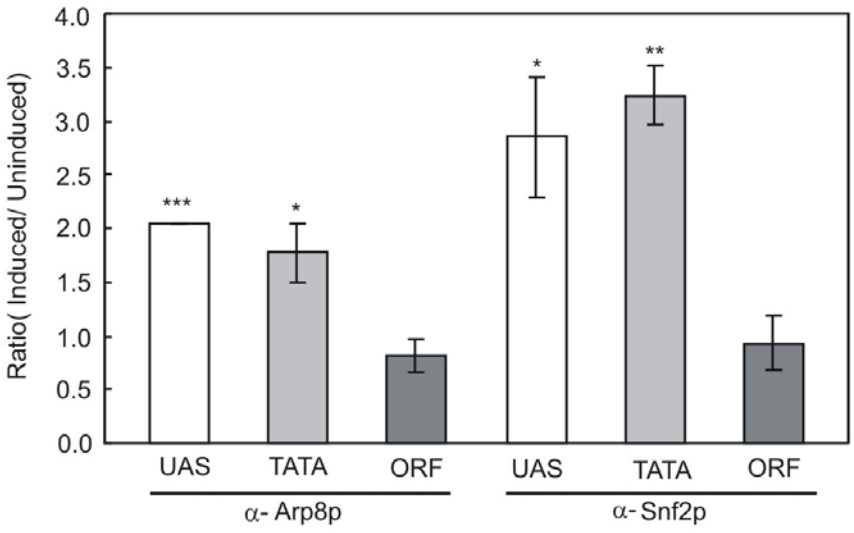

Figure 4.3 Both Arp8p and Snf2p present at *CUP1* promoter under inducing conditions. ChIP analysis of WT cells grown under repressing and inducing conditions. Antibodies raised against Arp8p (subunit of the INO80 remodeler complex) and Snf2p (subunit of the SWI/SNF remodeler complex) were used. *: p<0.1, **: p<0.05, ***: P<0.01.

CUP1 promoter but not at the *snf2Δ CUP1* promoter which means the recruitment of Ino80p depends on the presence of SWI/SNF. Similarly, the ratio of Snf2p-IP of *ino80Δ* cells to promoter region during activation. Since it has been demonstrated that *CUP1* induction results in gene-wide chromatin remodeling, perhaps, more remodelers are required for the nucleosome repositioning at the promoter than the *ORF* during induction.

Next, we wanted to know the inter-dependence of these two remodelers in *CUP1* induction. ChIP was performed with antibodies against Arp8p and Snf2p under both inducing and repressing conditions of various remodeler mutants. This experiment was repeated twice and each sample was replicated thrice in the qPCR. Our results showed that the ratio of Arp8p-IP of *snf2Δ* cells to Arp8p-IP of WT cells were 0.012 and 0.004 for repressing conditions and inducing Snf2p-IP of WT cells were 0.007 and 0.015 for repressing conditions and inducing conditions, respectively (Figure 4.4B). This implies that SWI/SNF is present at the WT *CUP1* promoter but not at the *ino80Δ CUP1* promoter under both conditions. For the control, we also examined the ratio of Arp8p-IP of *rsc3Δ* cells to Arp8p-IP of WT cells and the ratio of Snf2p-IP of *rsc3Δ* cells to Snf2p-IP of WT cells. Our result showed no significant difference between WT cells and *rsc3Δ* cells under inducing conditions, indicating that the deletion of Rsc3p does not influence the recruitment of both Ino80p and Snf2p (Figure 4.4). As such, both SWI/SNF and INO80 remodelers depend on each other to be recruited to the *CUP1* promoter.

A)

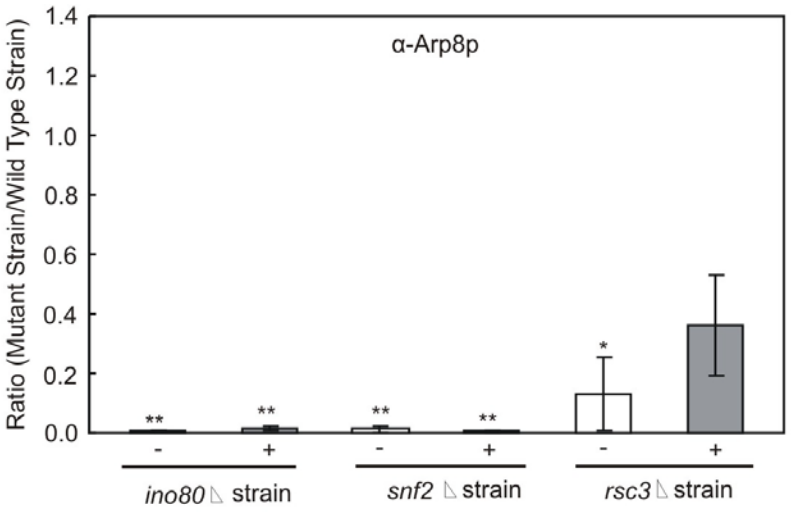

B)

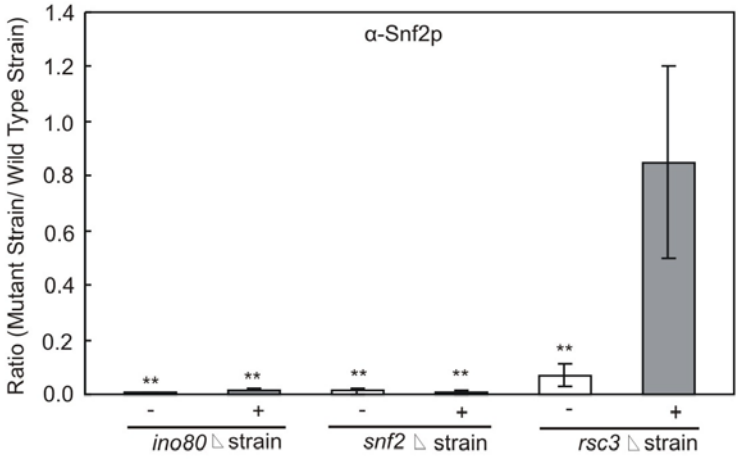

Figure 4.4 The inter-dependence of Snf2p and Ino80p at *CUP1* promoter. ChIP analysis of WT, *ino80*Δ, *snf2*Δ and *rsc3*Δ cells under both repressing and inducing conditions. Antibodies raised against (A) Arp8p (subunit of the INO80 remodeler complex) and (B) Snf2p (subunit of the SWI/SNF remodeler complex) were used. The ratios of mutant strain IP to WT IP were presented. *: $p<0.05$, **: $p<0.01$.

4.3.2 Both Ino80p and Snf2p are responsible for nucleosome repositioning at the *CUP1* promoter

We have established the evidence that both Ino80p and Snf2p remodelers are present at the *CUP1* promoter. We then wanted to confirm that they are directly responsible for the chromatin remodeling activities occurring at the promoter. To this end, we performed ChIP with antibodies against histone H3 and H4. Both histone H3 and H4 proteins are core histones, each nucleosome contains two copies of histone H3 and H4. As such, the distribution/density of H3 and H4 would provide the information of the nucleosome distribution/density, and thereby the chromatin structure. A lower density would suggest that the chromatin structures are disrupted and nucleosomes are mobile. Conversely, a higher density would indicate a silent chromatin structure.

ChIP analysis revealed that the relative histone H3 density of *UAS*/*POL1* for WT cells were 1.85 and 0.43 for both repressing and inducing conditions, and the relative histone H4 density were 0.92 and 0.49 (Figure 4.5). These results showed a significant reduction of nucleosome density at the *UAS* region under inducing conditions. The decrease of nucleosome density upon induction indicates that nucleosome repositioning is occurring at the *UAS* region under inducing conditions.

To further illustrate the change of the nucleosome density upon induction, we examined the ratio of the histone IP under inducing conditions to the histone IP under repressing conditions. For the *TATA* region, the ratios were 0.65 and 0.64 for H3 and H4 respectively

(Figure 4.6). The ratios for the *UAS* region were 0.65 and 0.49 for H3 and H4, respectively. The decreases of ratios were significant, suggesting less nucleosome density at the promoter region upon induction. For the *ORF*, the IP ratios were 0.94 and 0.85 for H3 and H4, respectively. Although the ratios were also decreased, the reduction was not as dramatic as in the promoter region.

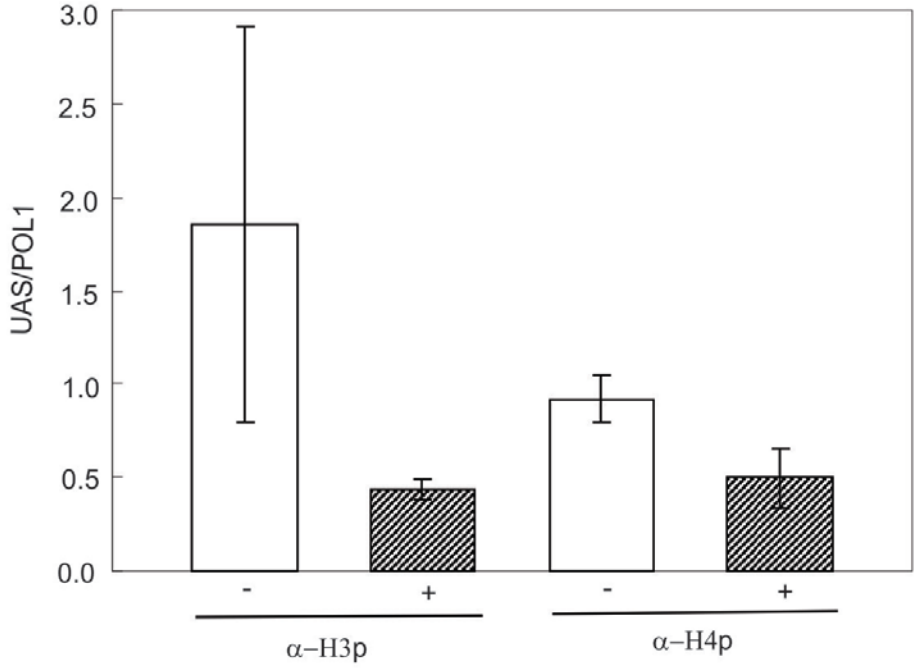

Figure 4.5 Nucleosome density at WT cells *UAS* region. ChIP analysis of WT cells grown under repressing and inducing conditions Antibodies raised against histone H3 and H4 were used.

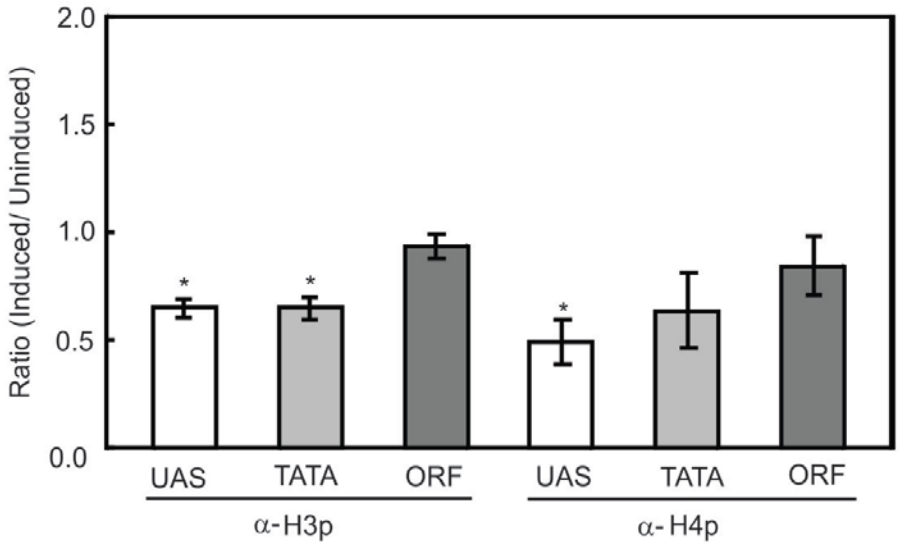

Figure 4.6 Nucleosome density at *CUP1* promoter and *ORF*. ChIP analysis of WT cells grown under both repressing and inducing conditions. Antibodies raised against histone H3 and H4 were used. *: $p<0.05$, **: $p<0.01$.

Next, we examined the effect of both Snf2p and Ino80p on the remodeling activities at the *CUP1* promote and coding region. As shown in Figure 4.7, both WT cells and *rsc3*Δ showed similar patterns at the *UAS*, *TATA* and *ORF* regions. They both showed significant reduction of ratios at the promoter regions upon induction, suggesting that the deletion of Rsc3p has no impact on the nucleosome repositioning. Conversely, such decreased ratios were not observed at *UAS* and *TATA* regions for both *snf2*Δ cells and *ino80Δ* cells. As such, both Snf2p and Ino80p are responsible for the chromatin remodeling activities during activation.

4.3.3 Histone acetylation level and gene activity at the *CUP1* promoter upon induction

Previously we have demonstrated that *CUP1* activation required the presence of chromatin remodelers Snf2p and Ino80p. To further explore the mechanism of gene expression, we asked whether histone acetylation is coupled with *CUP1* activation. ChIP coupled with real-time PCR analysis was again used to analyze the level of H3 and H4 histone acetylation at the *CUP1* promoter and its coding region in WT cells. For repressed and induced WT cells, the IP signals of di-acetylated H3 (acetylated on lysine residues 9 and 14; acH3-IP) or hyperacetylated H4 (acH4-IP) were observed at the *CUP1 UAS*, *TATA*, *ORF*, and *POL1*. Results showed that the relative IP values (*UAS*/*POL1*) obtained from acH3p-IP were 0.84 and 4.3 for repressed and induced chromatin, respectively (Figure 4.8). These results suggested that histone H3 at the *CUP1* promoter is not acetylated under repressing conditions. Upon induction, the relative IP value increases more than 5 times, indicating that histone H3 becomes acetylated under inducing conditions. For acH4-IP, the relative IP values were 0.89 and 1.62 for repressed and induced chromatin, respectively (Figure 4.8). Again, these results suggested that histone H4 at the *CUP1*

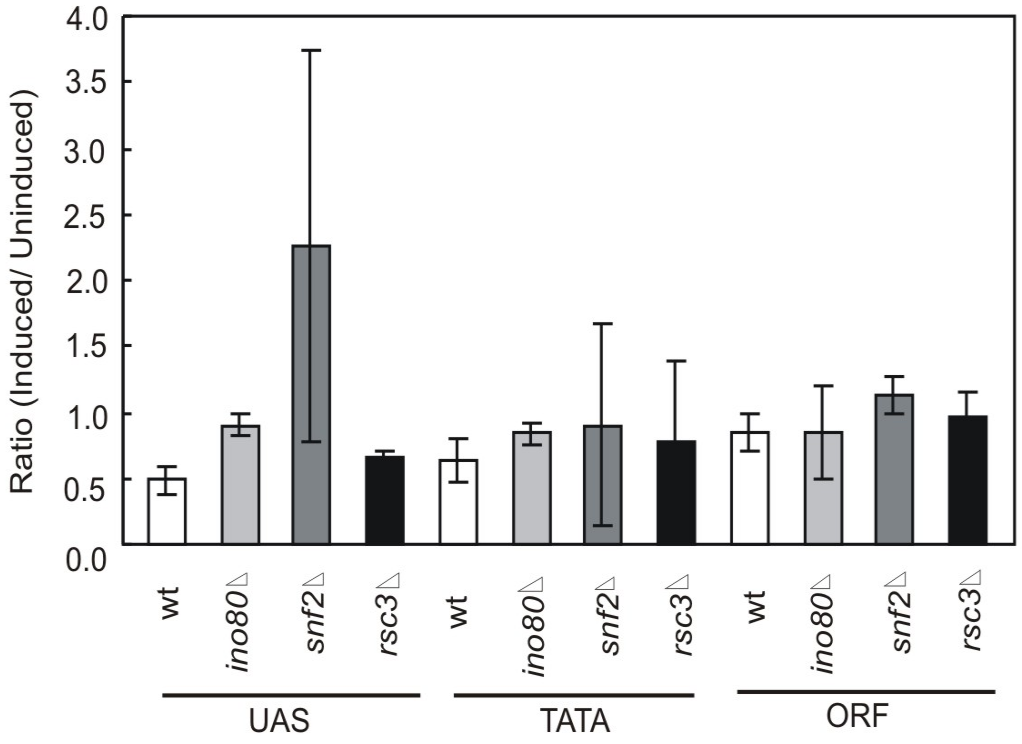

Figure 4.7 Nucleosome density analysis of *CUP1* promoter and *ORF*. H4p at UAS, TATA and ORF at *CUP1* gene in the WT, *ino80*Δ, *snf2*Δ and *rsc3*Δ cells. ChIP analysis of WT, *ino80*Δ, *snf2*Δ and *rsc3*Δ cells grown under repressing and inducing conditions. Antibody raised against histone H4 was used. *: $p<0.05$, **: $p<0.01$

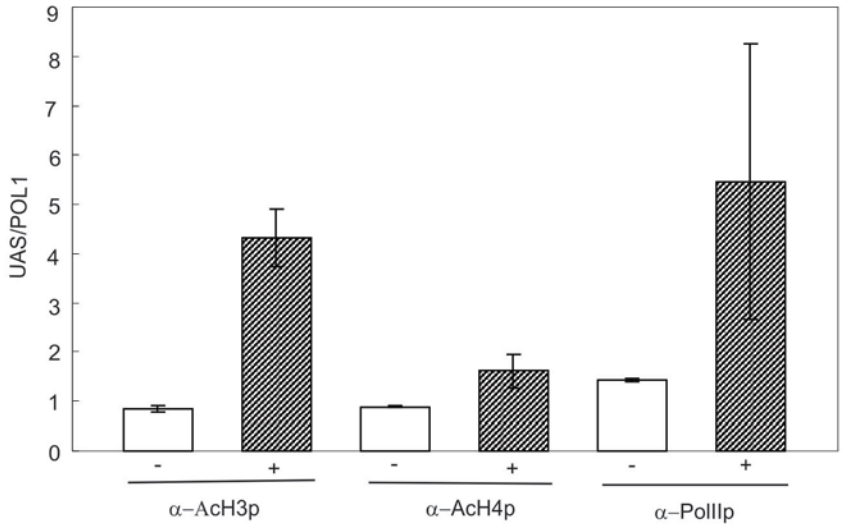

Figure 4.8 Acetylated histone H3, acetylated histone H4 and polymerase II are present at UAS regions in inducing WT cells. ChIP analysis of WT cells grown under repressing and inducing conditions. Antibodies raised against acetylated histone H3, acetylated histone H4 and *pol*II were used.

promoter is not acetylated under repressing conditions. Upon induction, the relative IP value increases almost 2 times, indicating that histone H4 becomes acetylated under inducing conditions. To connect this dramatic change to gene activity, we also looked at the *polII*-IP. The results showed that the relative IP values were 1.43 and 5.45 for repressed and induced chromatin, respectively (Figure 4.8). As such, the gene activity is accompanied by the increasing acetylated histone H3 and H4.

To further illustrate the change of the histone acetylation and gene activity from repressing conditions to inducing conditions, we examined the ratio of the acetylated histone IP under inducing conditions to the acetylated histone IP under repressing conditions. For the *UAS* region, the ratios were 1.5, 2.87 and 1.45 for acH3, acH4 and *pol*II respectively (Figure 4.9). The increases of ratios were significant for all at the *UAS* region, indicating increasing acetylation and gene activity at *UAS* region. The ratios for *TATA* region were 1.00, 2.06 and 2.27 for acH3, acH4 and *pol*II, respectively (Figure 4.9). The increase of ratios was only significant for *pol*II-IP, suggesting that no hyper-acetylation was observed at *TATA* but significant amount of PolIIp was recruited to *TATA* region under inducing conditions. For the *ORF*, the IP ratios were 0.99, 1.1 and 2.59 for acH3, acH4 and *pol*II, respectively (Figure 4.9). All these ratios are not significantly different between repressing and inducing chromatin, implying that no dramatic changes was observed at *ORF* region for acetylated histone and *pol*II amounts.

4.3.4 Both Snf2p and Ino80p are responsible for recruiting *pol*II to the CUP1 promoter

We have demonstrated that more *pol*II was recruited to *CUP1* at the *TATA* regions under inducing conditions. Next, we wanted to know if such recruitment is remodeler-dependent. WT, *snf2Δ*, *ino80Δ*, and *rsc3Δ* cells were used in ChIP analysis. Our results showed that the ratios of the *snf2Δ pol*II-IP to WT *pol*II-IP were 0.1 and 0.12 for the *TATA* and *ORF* under repressing conditions, respectively (Figure 4.10). Under inducing conditions, the ratios were 0.41 and 0.42 for *TATA* and *ORF*, respectively. These results suggest that the deletion of Snf2p results in more than 58% reduction of the *pol*II recruitment to *CUP1* upon induction.

Similarly, the ratios of the *ino80Δ pol*II-IP to WT *pol*II-IP were 0.02 and 0.02 for *TATA* and *ORF* under repressing conditions, respectively (Figure 4.10), whereas under inducing conditions, the ratios were 0.19 and 0.40 for *TATA* and *ORF*, respectively. These results suggest that the deletion of Ino80p results in more than 80% and 60% reduction of the recruitment of *pol*II to the *CUP1 TATA* and *ORF* upon induction, respectively.

For a control, we also examined the ratios of the *rsc3Δ pol*II-IP to WT *pol*II-IP and our results showed that the ratios were 0.98 and 0.87 for *TATA* and *ORF* under repressing conditions, respectively (Figure 4.10). Under inducing conditions, the ratios were 1.1 and 1.0 for *TATA* and *ORF*, respectively. As such, the deletion of Rsc3p has no effect on the recruitment of *pol*II to *CUP1* under both repressing and inducing conditions.

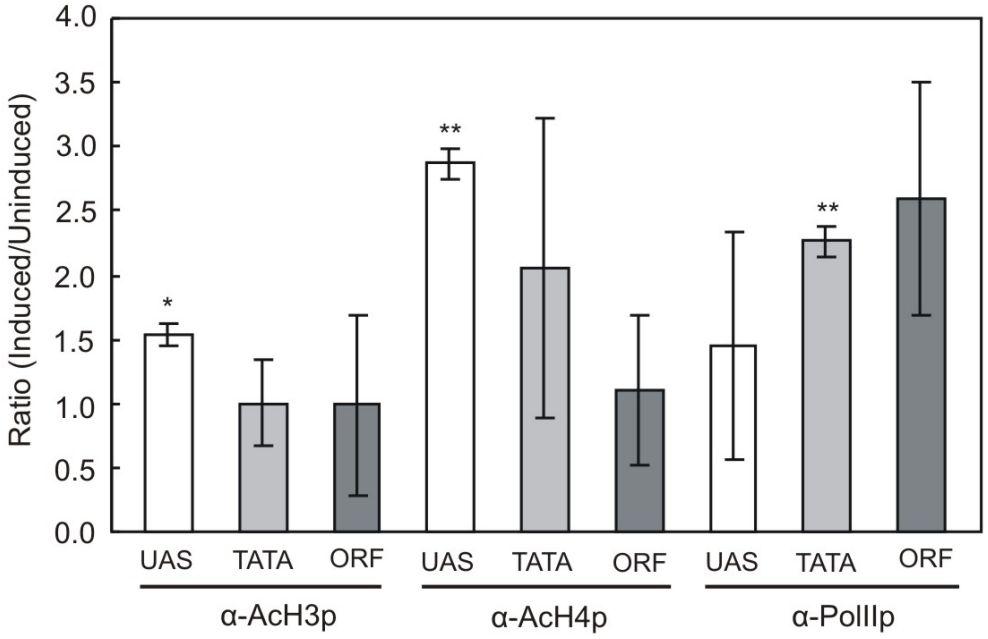

Figure 4.9 Gene activity and acetylation over the promoter and entire gene in WT cells. ChIP analysis of WT cells grown under repressing and inducing conditions. Antibodies raised against acetylated histone H3, acetylated histone H4 and *pol*II were used. *:$p<0.05$, **:$p<0.01$.

A)

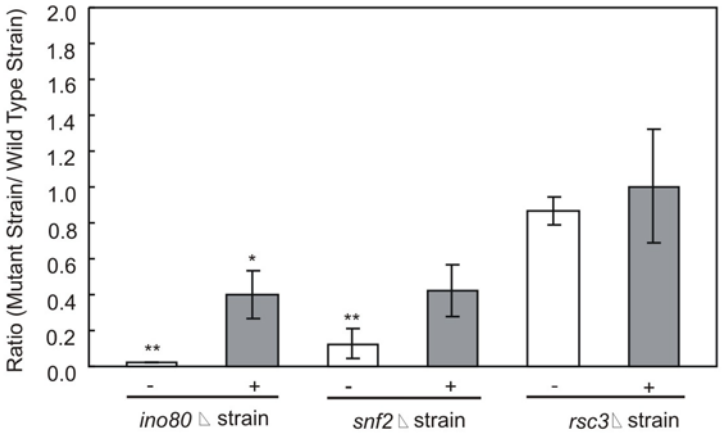

B)

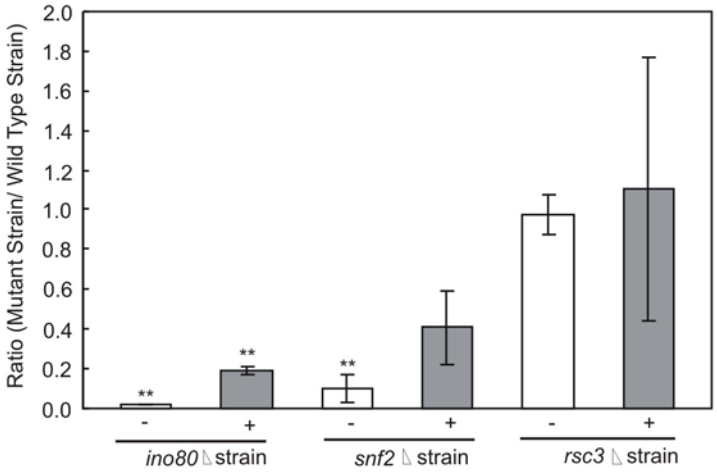

Figure 4.10 The presence of polymerase II at (A) *ORF* and (B) *TATA* regions of *CUP1* in WT, *ino80*Δ, *snf2*Δ and *rsc3*Δ cells. ChIP analysis of WT, *ino80*Δ, *snf2*Δ and *rsc3*Δ cells grown under both repressing and inducing conditions. Antibody raised against *pol*II was used. The ratios of mutant *pol*II IP to WT *pol*II IP were presented. *' $p<0.05$, **: $p<0.01$

4.4. Summary

In the previous chapter we have shown that both Snf2p and Ino80p are required for *CUP1* induction. To further, confirm that these two remodelers directly participate in *CUP1* induction, we performed ChIP coupled with qPCR analysis to examine the functional roles of these two transcriptional coactivators in *CUP1* activation.

We observed that both Snf2p and Ino80p are present at the *CUP1* promoter under inducing conditions and their distribution is limited to the promoter region only (Figure 4.2 and 4.3). This indicates that both remodelers are involved in *CUP1* induction directly. Furthermore, we observed the decrease of histone density at the *CUP1* promoter under inducing conditions but not at the *ORF* region, which suggests that the chromatin remodeling activities are limited to the promoter region and do not spread into the *ORF* region (Figure 4.5 and 4.6). These two observations are in accordance with each other. However, an earlier study demonstrated that *CUP1* induction resulted in gene-wide nucleosome repositioning activities (Shen *et al*., 2001). My observation is not in accordance with that study. It is possible that the systems used in these two studies are different. In that earlier study, the authors used a minichromosome-based system for the study of *CUP1* induction. Here, we study ChIP from the chromosomal *CUP1*, which could more closely resemble the real situation. Furthermore, the minichromosome used for chromatin remodeling activity is only 2.4 kb long, which might be easily influenced by a neighboring selective gene. Furthermore, the constraint of the closed circular covalent plasmid might also contribute to the variation observed. As such, the localized chromatin remodeling and remodeler distribution is more appropriate for the description of *CUP1* induction.

We have shown that H3 and H4 histone acetylation increased significantly at the *CUP1* promoter under inducing conditions. We also demonstrated that more *pol*II was recruited to the *CUP1* promoter under inducing conditions. This increase of histone acetylation and disappearance of *pol*II is observed in the absence of either Snf2p or Ino80p. These observations strongly suggest that the recruitment of histone acetylation and *pol*II depends on the presence of both chromatin remodelers. Furthermore, it is instructed to conclude that both remodelers arrive at the *CUP1* promoter first, which is then followed by the recruitment of histone acetylation and *pol*II. Previously, it had been shown that targeted histone acetylation was observed at the *CUP1* promoter and it happens at a very late stage of gene activation (Shen *et al*., 2002). Here, we further prove that such histone acetylation activity is a remodeler-dependent activity. Therefore, our results have provided further insight into the mechanism of *CUP1* activation.

CHAPTER 5

5 Activator-dependent recruitment of chromatin remodelers at *CUP1* promoter

5.1 Aims of this chapter

We have demonstrated that both SWI/SNF and INO80 are possible transcriptional co-activators in *CUP1* induction. To further confirm that they are transcriptional co-activator, we will need to demonstrate that they are recruited to the *CUP1* promoter by the transcriptional activator – Ace1p. The *ACE1* gene encodes a copper regulated DNA binding protein, known as Cup2p or copper regulated transcription activator. Ace1p is located at chromosome VII (Thiele *et al*., 1988). It contains a cysteine rich domain at the N- terminal, which is responsible for the binding of copper ions, for self-folding (Buchman *et al*., 1989; Szczypka *et al*., 1989; Furts *et al*., 1989). In this chapter, we used a yeast strain that carries the engineered *ACE1*-HA tag in the chromosome. We performed growth experiments and RNA analysis to prove that the engineered Ace1p is functional in the recombinant cells. Subsequently, ChIP assays were conducted to examine whether the recruitment of both Snf2p and Ino80p is activator-dependent.

5.2. Materials and Methods

5.2.1. Growth experiment for the *ace1* Δ, WT (BJ5459) and Rt-WT strains.

WT-BJ, *ace1Δ* and Rt-WT yeast strains (Table 5.1) were grown in the SC-Cu media (synthetic complete medium lacking copper) containing 2% glucose. These cultures were grown at 30^{o}C in the 300rpm. All strains were subjected to different copper concentrations (0, 1.0, 1.5 and 2.0 mM) and the growth curves were observed over a time period of 30 hours (spectrophotometer analysis 600 nm).

5.2.2. RNA Analysis for the *ace1* Δ, WT (BJ5459 and Rt-WT strains

Total RNA preparation, phenol-chloroform extraction and DNase treatment were performed as described in section 3.2.2 to 3.2.4. The SYBER Green ER Two-Step qRT-PCR kit was used for RNA analysis. Briefly, the c-DNA was made from the mRNA. In the second step, the q-PCR was performed to quantitate the amount of c-DNA template. Both *CUP1* and *ACT1* primers employed in the reaction were shown below.

CUP1 primers,

Forward Primer: 5'-GCAGCCAATGTGGTAGCTGCAAA- 3'

Reverse Primer: 5'-CATTTCCCAGAGCATGA-3'

ACT1 Primers,

Forward Primer: 5'-CCAAGCCGTTTTGTCCTTGT- 3'

Reverse Primer: 5' –ACCGGCCAAATCGATTCTC- 3'

Table 5.1 Yeast Strains used in this study

Strain	Genome Type
WT-BJ	*MATa ura3-52 trp1 lys2-801 leu2Δ1 his3Δ200 pep4::HIS3 prb1Δ1.6R can1 GAL cir+*
ace1 Δ	*MATa ura3-52 trp1 lys2-801 leu2Δ1 his3Δ200 pep4::HIS3 prb1Δ1.6R can1 GAL cir+ ace1Δ URA 3*
Rt-WT	*MATa ura3-52 trp1 lys2-801 leu2Δ1 his3Δ200 pep4::HIS3 prb1Δ1.6R can1 GAL cir+.ace1Δ URA 3:: ACE1HA*

5.2.3. Chromatin immunoprecipitation for the *ace1Δ*, WT-BJ and Rt-WT strains

All the stains were streaked from a single colony and grown to mid-logarithmic phase. Cells were induced by adding 2mM $CuSO_4$. Cells were cross-linked and harvested as described previously. Subsequently, DNAs were prepared as well.

Lysates that contains 5.5 μg total DNA were used for immunoprecipitation (IP) with antibodies against Snf2p, Ino80p, HAp and PolIIp, respectively. The amount of antibodies used in the IP reaction was: 1.5μg anti-RNA polymerase II mouse monoclonal antibody, 2.5μg anti-HA antibody, 2.5μg anti-Arp8 rabbit polyclonal antibody and 1.5μg anti-Snf2 (yeast specific) rabbit polyclonal antibody. After overnight IP, samples were washed once with low salt, high salt, and LiCl solution, respectively. Subsequently, samples were washed twice with 1X TE. DNA was collected after reverse cross-linked, and DNA elution was followed by phenol chloroform extraction and ethanol precipitation

The qPCR procedure was completed as was described previously in chapter 2 section 2.12.5. Three sets of primers and probes were used, with two sets that covered the TATA and UAS of promoter region of *CUP1* and the other set covered the *ORF* region of *CUP1* gene. We also used *POL1* primers which covered the *POL1 ORF* region.

TATA primers,

Forward: 5'AAAGACTACCAACGCAATATGGATT3'

Reversed: 5'GCAATTGATACAAGACAAGGAGTTA 3'

TATA MGB (Minor groove binder) Probe,

5’ TCAGAATCATATAAAAGAGAAGC 3’

UAS primers,

Forward: 5’AAAAGACATTTTTGCTGTCAGTCACT 3’

Reverse: 5’ GGAACGGTTCAGCGGAAA 3’

UAS MGB Probe,

5’ AAGAGATTCTTTTGCTGGCAT 3’

ORF primers,

Forward: 5’ GCCAATGTGGTAGCTGCAAA 3’

Reverse: 5’ ATGACTTCTTGGTTTCTTCAGACTTG 3’

ORF MGB Probe,

5’ AATGCCAAAAATCATG 3’

POL1 primers,

Forward: 5’ ATATGTGATATCGCCAATGAAATGG 3’

Reverse: 5’ ACATCATTTTGGTATTGTGGATTTTG 3’

POL1 MGB Probe,

5’ TCAATCATTAACACCCAAATG 3’

5.3. Results:

5.3.1. The recombinant Ace1p-HA can rescue *ace1Δ* cells from the toxic effect of copper

To examine whether Snf2p and Ino80p are activator-dependent, we used a yeast strain, Rt-WT that has been engineered to carry a chromosomal Ace1p-HA tag. This is because we needed to perform ChIP analysis but the anti-Ace1p antibody was not available. As the parental strain for Rt-WT is BJ5459, which is not the same WT (BY4741) we used previously, we performed biochemical analysis to prove that the Ace1p is functional followed by ChIP analysis. For the biochemical analysis, we used *ace1Δ* cells (BJ5459- *ace1Δ)*, WT-BJ (BJ5459) and Rt-WT strains (BJ5459-Ace1p-HA tag). The WT-BJ cells grew well in the absence of copper.

As the copper concentration was increased every 0.5 mM, the growth of the WT-BJ cells was influenced slightly. The WT-BJ cells were inviable when the concentration of copper was above 2 mM. These results suggested that the WT-BJ cells were resistant to copper up to 2 mM. The effect of copper on cell growth was shown in Table 5.2. Here, the A_{600} value (optical density at 600 nm) at 24^{th} hour for the presence of 1.0 mM copper was subtracted from the A_{600} value at 24^{th} hour for the absence of copper, and the value was divided by the original A_{600} value in the absence of copper. This can help us to identify the effect of copper on cell growth and to see if the recombinant Ace1p can

Table 5.2 Decrease of growth rate percentage at the 24th hour

Cell Type	O.D. at 0mM[Cu]	O.D. at 1.0 mM[Cu]	Decrease of Growth Rate (Drop off %)	Changes of cell doubling time (Folds)
WT-BJ	1.98	1.23	37.88	1.61
ace1 Δ	1.25	0.19	84.56	6.48
Rt-WT	4.70	2.45	47.87	1.92

rescue the growth of *ace1Δ* cells. We also calculated the length of cell doubling time (increased in folds). For WT-BJ cells, the decrease of growth rate was about 37.88%, indicating that the doubling time increased 62.12 % in the presence of 1.0 mM copper (Figure 5.1A), and that the doubling time increased 1.61 folds (Figure 5.2A). The *ace1*Δ cells grew well in the absence of copper, but were inviable in the presence of copper (Figure 5.1B). The decrease of growth rate was 84.56 % (Figure 5.2B), and the doubling time increased 6.48 folds (Figure 5.2A). This indicates that *ace1*Δ cells cannot survive in the presence of copper, which means *CUP1* expression has been repressed (Figure 5.1B). This result suggests that Ace1p is important in *CUP1* expression. The Rt-WT showed a similar pattern as the WT-BJ cells in both the absence and presence of copper (Figure 5.1A and C). The increase of cell doubling time was 1.92 folds in the presence of copper (Figure 5.2A), and the decrease of growth rate was 47.87% (Figure 5.2B). These results were very similar to WT-BJ cells (Table 5.2), suggesting that *ACE1-HA* is functional and can rescue the *ace1*Δ cells.

5.3.2. RNA Analysis for the WT-BJ, *ace1* Δ cells, and Rt-WT cells

The *ace1* Δ cells were sensitive to the toxic effect of copper, which suggested the lack of MT in the presence of the copper. The lack of MT could result from the defect of *CUP1* gene expression at the transcriptional or translational level. To further distinguish the difference, qRT-PCR was performed for Rt-WT, *ace1* Δ, and WT-BJ cells.

A.

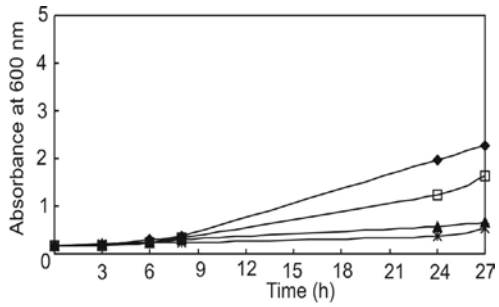

B.

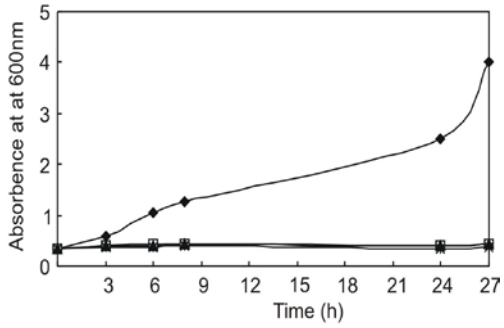

C.

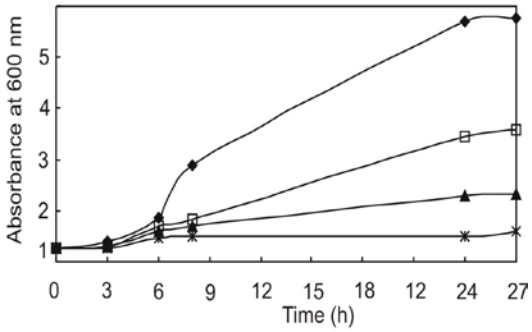

Figure 5.1 Ace1p protects cells from copper toxicity. The growth of yeast cells was monitored by A_{600}. Cells from overnight cultures grown in the absence of copper were inoculated into medium with different concentrations of copper (II) sulfate to an initial ptical density of about 0.2. (A)WT-BJ cells, (B) *ace1*Δ cells, (C)Rt-WT cells. (◆): 0 mM, (□): 1.0mM, (▲): 1.5mM, (*): 2.0mM.

A.

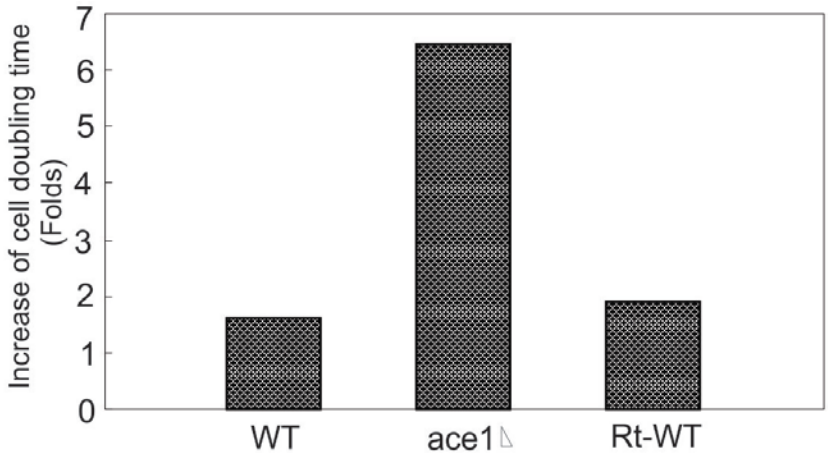

B.

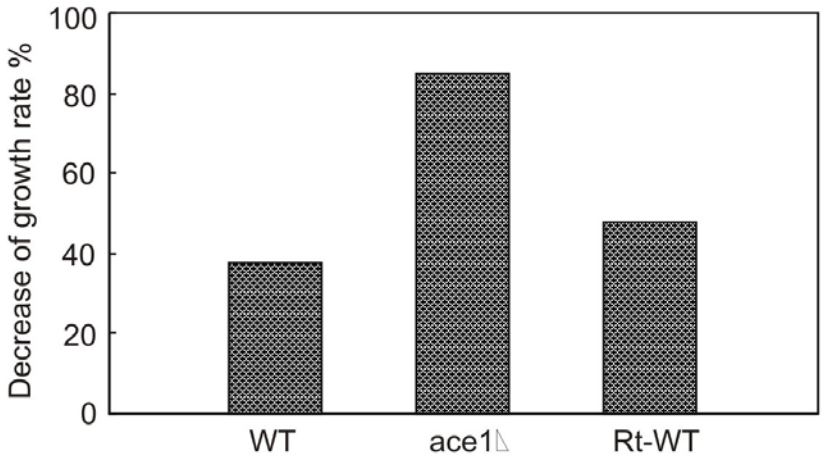

Figure 5.2 The toxic effect of copper on yeast cell growth. At 1mM copper concentration, (A) The increase of cell doubling time and (B) The decrease of growth rate percentages in *ace1*Δ, WT-BJ and Rt-WT cells.

In the WT-BJ cells, *CUP1* mRNA was induced by copper as soon as 15 minutes after induction. This *CUP1* mRNA level accumulated steadily and reached a maximum level at 60 minutes after induction. The maximum level of induction was about 8 folds compared to the uninduced cells (Figure 5.3A). The Rt-WT showed similar patterns of *CUP1* induction as the WT-BJ cells (Figure 5.3C). In *ace1*Δ cells, the level of *CUP1* mRNA showed no difference between uninduced and induced cells (Figure 5.3B). As such, these results provided the evidence to show that the Rt-WT cells acts similar to WT-BJ cells.

5.3.3. Chromatin immunoprecipitation analysis of the ace1 Δ, WT-BJ, Rt-WT cells

5.3.3.1 Ace1p is present at the *CUP1* promoter.

It has been demonstrated that Ace1p is present at the *CUP1* promoter (Buchman *et al*., 1989; Szczypka *et al*., 1989; Thiele *et al*., 1988; Furts *et al*., 1989). Here, ChIP analysis was performed to confirm that recombinant Ace1p-HA is present at the *CUP1* promoter in Rt-WT cells.

The IP ratio of the inducing Ace1p to the repressing Ace1p was 1.98 and 1.64 folds for *TATA* and *UAS* regions, respectively. The IP ratio of the inducing Ace1p to the repressing Ace1p was 0.51 for *ORF* region, suggesting an absence of Ace1p in the ORF region (Figure 5.4). These results suggest that Ace1p is present at the *CUP1* promoter under inducing conditions which further confirms that Ace1p functions the same as the endogenous Ace1p in the WT cells.

A.

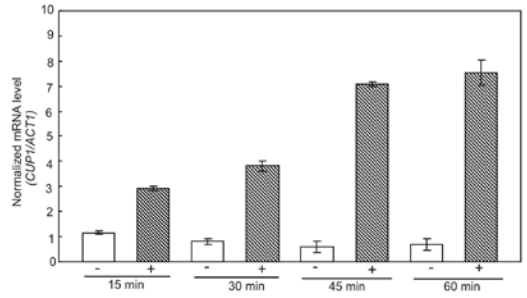

B.

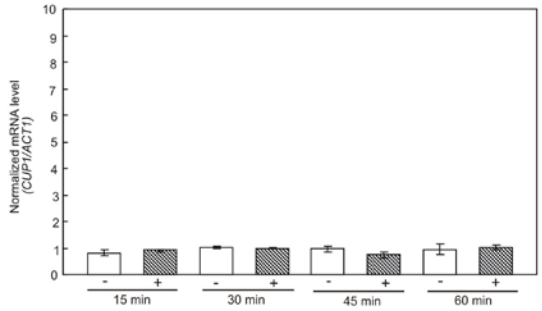

C.

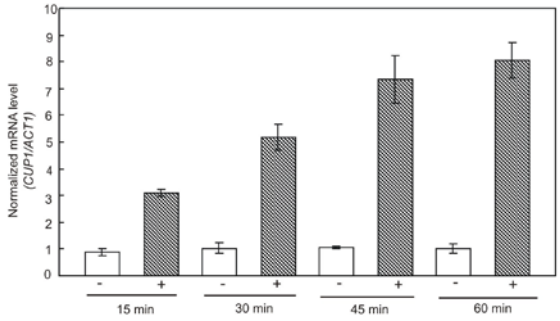

Figure 5.3 Induction of *CUP1*. (A)WT-BJ cells , (B)*ace1*Δ cells, (C)Rt-Wt cells were prepared from induced conditions (▨) or uninduced conditions (□) at different time intervals (15, 30, 45 and 60 minutes) after the addition of copper.

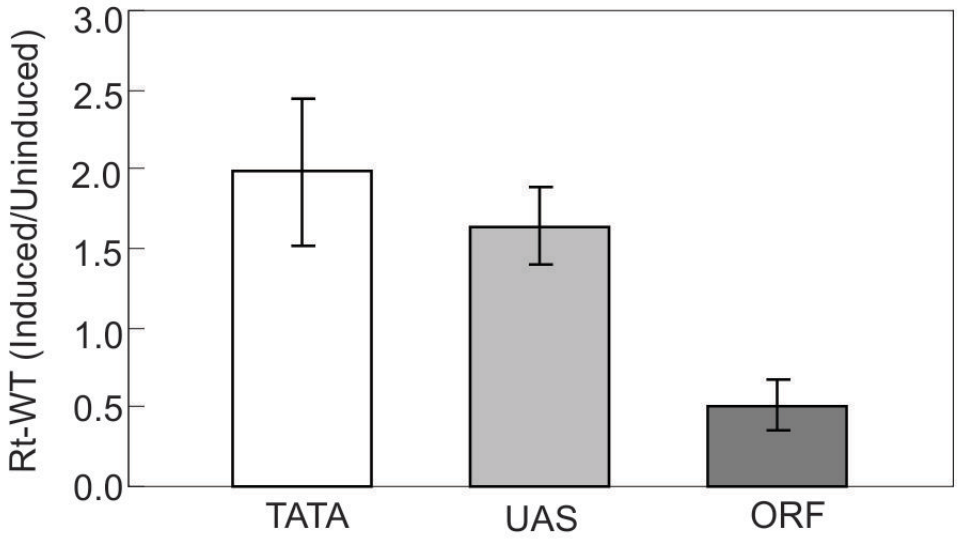

Figure 5.4 Ace1p is present at the *CUP1* promoter. ChIP analysis of Rt-WT cells grown under uninduced and induced conditions. Antibody against HA tag was used. *TATA*: open bar, *UAS*: light gray bar and *ORF*: dark gray bar.

5.3.3.2 Both INO80 and SWI/SNF remodeler are recruited to *CUP1* promoter by Ace1p

In the previous chapter, we have demonstrated that both Snf2p and Ino80p were recruited to *CUP1* promoter under inducing conditions. Next, we wanted to examine whether such recruitment is activator-dependent remodelers by using ChIP analysis with antibodies against Arp8p and Snf2p.

For INO80, the *UAS*/*POL* ratios obtained from the Arp8-IP were 1.09, 1.83 and 1.84 for repressed WT-BJ, *ace1Δ* and Rt-WT cells, respectively (Figure 5.5). Under inducing conditions, the *UAS*/*POL* ratios were 2.61, 0.59 and 7.2 for WT-BJ, *ace1Δ* and Rt-WT cells, respectively (Figure 5.5). This indicates that INO80 is absent at the *CUP1* promoter in the absence of Ace1p, but it is present at the *CUP1* promoter in the presence of Ace1p. These results strongly suggest that INO80 is an activator-dependent chromatin remodeler.

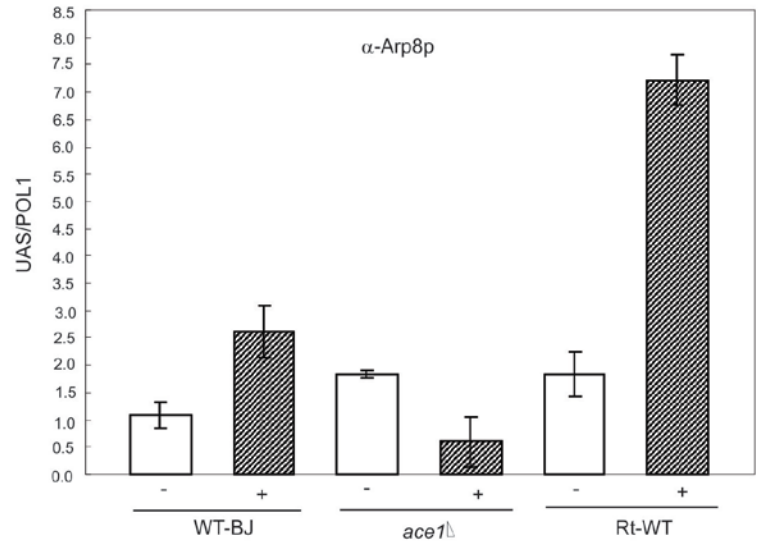

Figure 5.5 Ace1p is required for the recruitment of Ino80p.

ChIP was done using analysis of WT-BJ, *ace1* Δ and Rt-WT cells grown in the uninduced and induced conditions. An Antibody raised against Arp8p (subunit of the INO80 remodeler complex) was used. The ratio of Arp8-IP (*UAS*/*POL*) in WT-BJ cells.

For SWI/SNF, the *URS*/*POL* ratios obtained from the Snf2-IP were 0.89, 1.34 and 1.33 for the repressed WT-BJ, *ace1*Δ and Rt-WT cells, respectively (Figure 5.6). Under inducing conditions, the *UAS*/*POL* ratios were 2.2, 1.17 and 5.53 for WT-BJ, *ace1Δ* and Rt-WT cells, respectively (Figure 5.6). Likewise, this indicates that SWI/SNF is absent at the *CUP1* promoter in the absence of Ace1p but is present at the *CUP1* promoter in the presence of Ace1p. These results again strongly suggest that SWI/SNF is an activator-dependent chromatin remodeler.

From the above results, we have demonstrated that both Snf2p and Ino80p are recruited to the *CUP1* promoter by the transcriptional activator Ace1p. As such, both Snf2p and Ino80p are transcriptional co-activators in *CUP1* induction.

5.3.3.3 Activator-dependent chromatin remodeling activity

Next, we examined the histone density in WT-BJ, *ace1* Δ and Rt-WT stains under both induced and uninduced conditions by performing ChIP with the antibody against histone H4. Since histone H4 is one of the core histones, the density of histone H4 would indicate the distribution of the nucleosome at *CUP1*. For example, if the ratio of *UAS*/*POL*, *TATA*/*POL* or *ORF*/*POL* is less than 1, it would suggest the presence of repositioning activity. This is because fewer nucleosomes are present. If the ratio is 1 or greater, it would indicate no remodeling activity. Our ChIP data shows that the ratios of *UAS*/*POL* were 1.8, 1.26 and 1.08 for uninduced WT-BJ, *ace1*Δ and Rt-WT cells, respectively (Figure 5.7A). The IP ratios of *UAS/POL* were 0.53, 1.46 and 0.69 for

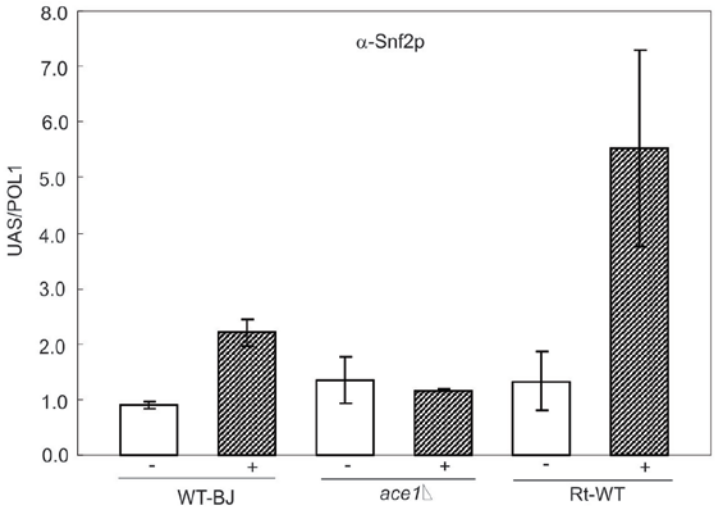

Figure 5.6 Ace1p is required for the recruitment of Snf2p.

ChIP analysis of WT-BJ, *ace1* Δ and Rt-WT cells grown in uninduced and induced conditions. Antibody raised against Snf2p was used. The ratio of Snf2-IP (*UAS*/*POL*) in WT-BJ cells.

induced WT-BJ, *ace1*Δ and Rt-WT cells, respectively. These results indicate that chromatin remodeling was observed in both WT-BJ and Rt-WT cells under inducing conditions at *UAS* region. This is similar to what we observed for WT cells in Chapter 4. Such remodeling activity disappears in *ace1*Δ cells.

We also examined the H4 IP ratios of *TATA/POL* and the ratios were 0.97, 0.66 and 0.97 for uninduced WT-BJ, *ace1*Δ and Rt-WT cells, respectively (Figure 5.7B). The IP ratios of *TATA/POL* were 0.36, 1.165 and 0.51 for induced WT-BJ, *ace1*Δ and Rt-WT cells, respectively (Figure 5.7B). These results indicate that chromatin remodeling was observed in both WT-BJ and Rt-WT cells and remodeling activity disappears in *ace1*Δ cells under inducing conditions.

Subsequently, we examined chromatin remodeling activity over *ORF* region. The IP ratios of *ORF/POL* were 0.95, 1.09 and 0.99, for uninduced WT-BJ, *ace1*Δ and Rt-WT cells, respectively. The IP ratios of *ORF/POL* were 0.44, 2.12 and 0.55 for induced WT-BJ, *ace1*Δ and Rt-WT cells, respectively (Figure 5.7C). These results indicate that chromatin remodeling was observed in both WT-BJ and Rt-WT cells under inducing conditions. Again, the chromatin remodeling activity disappears in *ace1*Δ cells under inducing condition.

We observed chromatin remodeling activity on *UAS*, *TATA* and *ORF* regions in both inducing WT-BJ and Rt-WT cells. Such remodeling activity was not observed in *ace1Δ* cells promoter or *ORF* regions. Therefore, our results demonstrated that the

A.

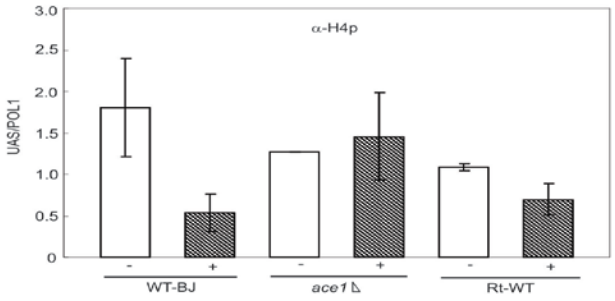

B.

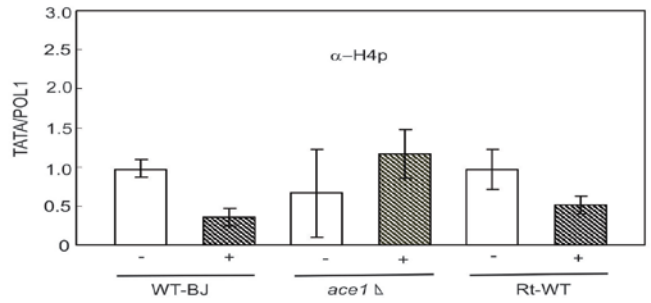

C.

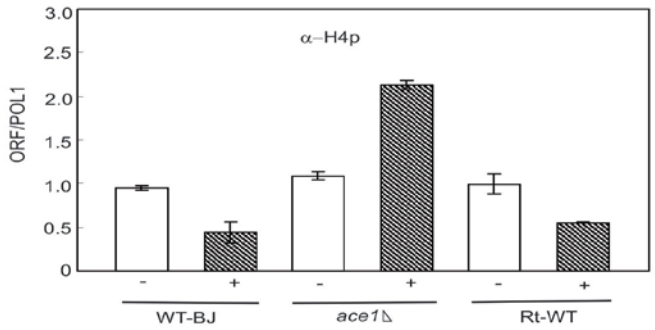

Figure 5.7 Ace1p is required for chromatin remodeling at *CUP1* promoter in induction. ChIP analysis of WT-BJ, *ace1* Δ and Rt-WT cells grown in uninduced and induced conditions. Antibody raised against histone H4 was used. **A.** IP ratio of *UAS*/*POL1* for H4p **B.** IP ratio of *TATA/POL1* for H4p. **C**. IP ratio of *ORF*/*POL1* for H4p.

chromatin remodeling activity at entire *CUP1* gene depends on the presence of the transcriptional activator Ace1p, and this findings supports our observations that chromatin remodelers Snf2p and Ino80p are activator-dependent.

5.3.3.4 Activator-dependent *CUP1* activity

Finally, we wanted to examine the effect of Ace1p on gene activity. To measure the gene activity, we performed ChIP with the antibody against *pol*II. The amount of *pol*II would indicate the gene activity. For uninducing conditions, the *UAS*/*POL* ratios were 0.72, 0.54 and 1.21 for WT-BJ, *ace1*Δ and Rt-WT cells, respectively (Figure 5.8 A).

Under inducing conditions, the *UAS*/*POL* ratios were 1.69, 0.56 and 8.52 for WT-BJ, *ace1*Δ and Rt-WT cells, respectively (Figure 5.8A). These results suggest that both WT-BJ and Rt-WT cells have very high gene activity, indicating an active transcriptional activity for both cells. Such activity was not observed in *ace1Δ* cells. As such, it showed that the transcriptional activator Ace1p is required for *CUP1* activation.

We then examined the distribution of *pol*II in the *TATA* region and *ORF* region. The *TATA*/*POL* ratios of WT-BJ, *ace1Δ* and Rt-WT cells were 0.79, 0.12 and 0.81 for uninduced condition, respectively (Figure 5.9B). Under inducing conditions, the *TATA*/*POL* ratios were 2.63, 0.39 and 5.62 for WT-BJ, *ace1*Δ and Rt-WT cells, respectively (Figure 5.8B). Again, this result indicates the absence of *pol*II at the *TATA* region in *ace1Δ* cells, but it presents at the *TATA* region for both WT-BJ and Rt-WT cells.

For the *ORF* region, the ratios of *ORF*/*POL* were 0.82, 0.49 and 0.99 for uninduced WT-BJ, *ace1*Δ and Rt-WT cells, respectively (Figure 5.8C). The IP ratios of *ORF/POL* were 2.05, 0.48 and 6.96 for induced WT-BJ, *ace1*Δ and Rt-WT cells, respectively (Figure 5.8C). Likewise, this result is similar to what we observed for *TATA* region. Therefore, the transcriptional activation *CUP1* depends on the presence of the transcriptional activator Ace1p.

A.

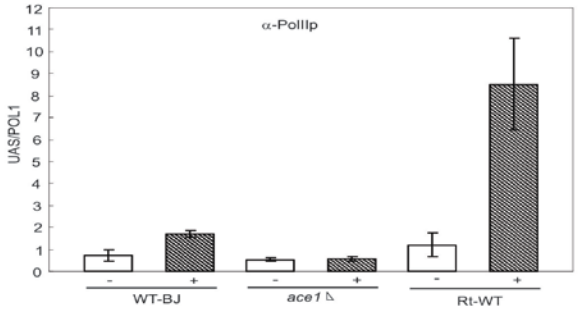

B.

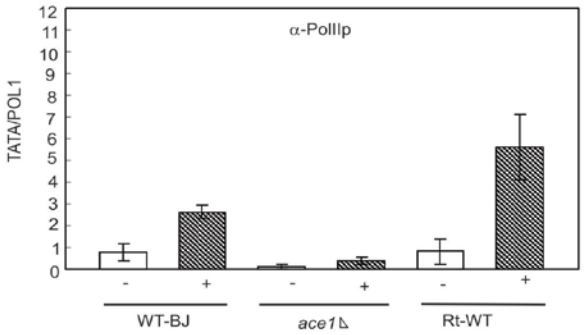

C.

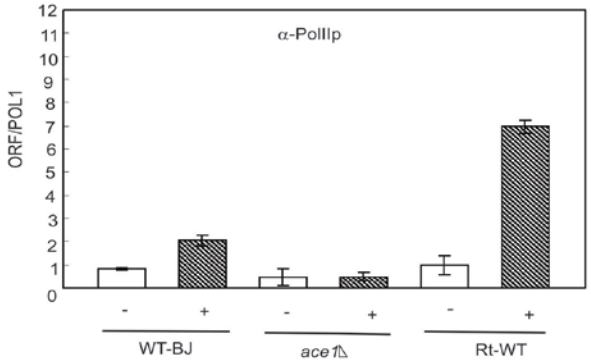

Figure 5.8 Ace1p is required for the recruitment of *pol*II at the *CUP1* promoter and *ORF*. ChIP analysis of WT-BJ, *ace1* Δ and Rt-WT cells grown in uninduced and induced conditions. Antibody raised against polII was used. **A.** IP ratio of *UAS*/*POL1* for *pol*II **B.** IP ratio of *TATA/POL1* for *pol*II. **C**. IP ratio of *ORF*/*POL1* for *pol*II.

5.4 Summary:

Here, we performed a series of biochemical analyses to demonstrate that the Rt-WT cells showed similar patterns as its parental strain WT-BJ. These analyses included survival experiments and RNA analysis. Our results also showed that both the Snf2p and Ino80p remodelers are activator-dependent. We then examined the functional role of Ace1p in *CUP1* expression through the histone density analysis and *pol*II distribution. Our results strongly demonstrated that both chromatin remodeling activity and the presence of *pol*II depends on the presence Ace1p, suggesting a critical role of Ace1p in *CUP1* expression.

CHAPTER 6

6 Discussion

We have chosen *CUP1* as the model to understand the mechanism of gene expression. To this end, it is important to identify which transcriptional co-activators work on the *CUP1* promoter and their functional interdependence in induction. To date, it is still unclear which co-activators are involved in *CUP1* activation. As one of the transcriptional co-activators, chromatin remodelers are responsible for the reconfiguration of chromatin structure during gene activation. Many yeast chromatin remodelers have been characterized recently, including SWI/SNF, RSC, INO80 and IWSI (Cairns *et al*., 1998; Muchardt *et al*., 1999; Ebbert *et al*., 1999; Shen *et al*., 2001; Mellor *et al*., 2004). Previous microarray analyses have suggested that some remodelers might be involved in *CUP1* expression. Based on these findings, we have chosen to test SWI/SNF, RSC, INO80 and IWSI remodeling complexes on *CUP1* gene activation.

From the growth experiments, we showed that both s*nf2*Δ and *ino80*Δ strains were highly sensitive to copper. Both *isw1Δ* and *rsc3Δ* strains displayed similar growth patterns as WT cells in the presence of copper (Figure 3.6). This observation suggests that ISW1 and RSC3 remodeling complexes have no positive effect in *CUP1* expression. On the other hand, the deletion of *SNF2* and *INO80* resulted in the death of cells in the presence of copper, indicating that both Snf2p and Ino80p might be responsible for *CUP1* expression.

The sensitivity of both s*nf2*Δ and *ino80*Δ strains to copper suggests a lack of metallothionein (MT) in these two strains in the presence of copper. We have proved that the

lack of MT was a result of a defect of *CUP1* gene expression at the transcriptional level by performing RNA analysis. Both the s*nf2*Δ strain and *ino80*Δ strain showed very low *CUP1* mRNA levels compared to the WT *CUP1* mRNA levels after induction (Figure 3.8). However, both the *isw1*Δ strain and *rsc3*Δ strain showed increasing amount of *CUP1* mRNA after induction. As such, we concluded that both SNF2 and INO80 remodeling complexes are involved in *CUP1* gene expression at the transcriptional stage. Both ISW1 and RSC3 remodeling complexes, however, may not be positively involved in *CUP1* gene expression.

To confirm that both SNF2 and INO80 remodeling complexes are directly involved in *CUP1* transcriptional activation, we confirmed their presence at the *CUP1* promoter during activation. To identify this DNA protein interaction we performed ChIP coupled with real-time PCR. Our data showed that both Snf2p and Ino80p are present at the *CUP1* promoter in the WT cells under inducing conditions and their distribution is limited to the promoter region only (Figure 4.2 and 4.3). This indicates that both SWI/SNF and INO80 remodelers are involved in *CUP1* induction directly. Furthermore, we demonstrated that both remodelers are activator-dependent. In the attempt to examine the inter-dependence of Snf2p and Ino80p by using *snf2Δ* and *ino80*Δ strains, our results showed that both SWI/SNF and INO80 remodelers depend on each other to be recruited to the *CUP1* promoter (Figure 4.4).

To confirm that both Snf2p and Ino80p are directly responsible for the chromatin remodeling activities occurring at *CUP1* promoter, we performed ChIP using antibodies against histone H3 and H4. A lower distribution would suggest that the chromatin structures are disrupted and nucleosomes are mobile. Conversely, a higher density would indicate a silent

chromatin structure. We observed the decrease of histone density at *CUP1* promoter under inducing conditions but not at the *ORF* region, which suggests that chromatin remodeling activities is limited to the promoter region and that it did not spread into the *ORF* region (Figure 4.5 and 4.6). These two observations are in accordance with each other. However, an earlier study has demonstrated that *CUP1* induction resulted in gene-wide nucleosome repositioning activities (Shen *et al*., 2001). Our observation is not in accordance with that study. It is possible that the systems used in these two studies are different. In that earlier study, the authors used a minichromosome-based system for the study of *CUP1* induction. Here in our study, we performed ChIP from the chromosomal *CUP1* which could be more closely resembled to the real situation.

To examine other remodeling activities at the *CUP1* promoter, we showed that H3 and H4 histone acetylation increased significantly at the *CUP1* promoter under inducing conditions. We also demonstrated that more *pol*II was recruited to the *CUP1* promoter under inducing conditions. Such an increase of histone acetylation and *pol*II was not observed in the absence of either Snf2p and Ino80p (Figure 4.7 and 4.10). These observations strongly suggest that the recruitment of histone acetylation and *pol*II depends on the presence of both chromatin remodelers.

Our results also showed that both the Snf2p and Ino80p remodelers are activator-dependent. Further we examined the functional role of Ace1p in *CUP1* expression through the histone density analysis and *pol*II distribution and our results strongly demonstrated that both chromatin remodeling activity and the presence of *pol*II depends on the presence Ace1p, suggesting a critical role of Ace1p in *CUP1* expression.

Furthermore, it is instructed to conclude that both remodelers arrive at the *CUP1* promoter before the recruitment of histone acetylation and *pol*II. Previously, it has been shown that targeted histone acetylation was observed at the *CUP1* promoter and that it happens at a very late stage of gene activation (Shen *et al*., 2002). Here, we further prove that such histone acetylation activity is a remodelers-dependent activity. Therefore, our results have provided a further insight into the mechanism of *CUP1* activation.

From our work and that of others, we propose a model to describe how several factors act on *CUP1* chromatin during gene activation (Figure 5.9). The first step in activation is the binding of copper-activated Ace1p. After the binding of Ace1p, it is proposed that both SWI/SNF and INO80 are recruited by Ace1p to create a dynamic chromatin structure for the promoter region, in which nucleosomes are moved continuously between positions. This process should render the underlying DNA sequence essentially transparent to binding factors. It is likely that the next step is the binding of TBP (*TATA* binding protein) and *pol*II to the TATA boxes at a moment when it is nucleosome free.

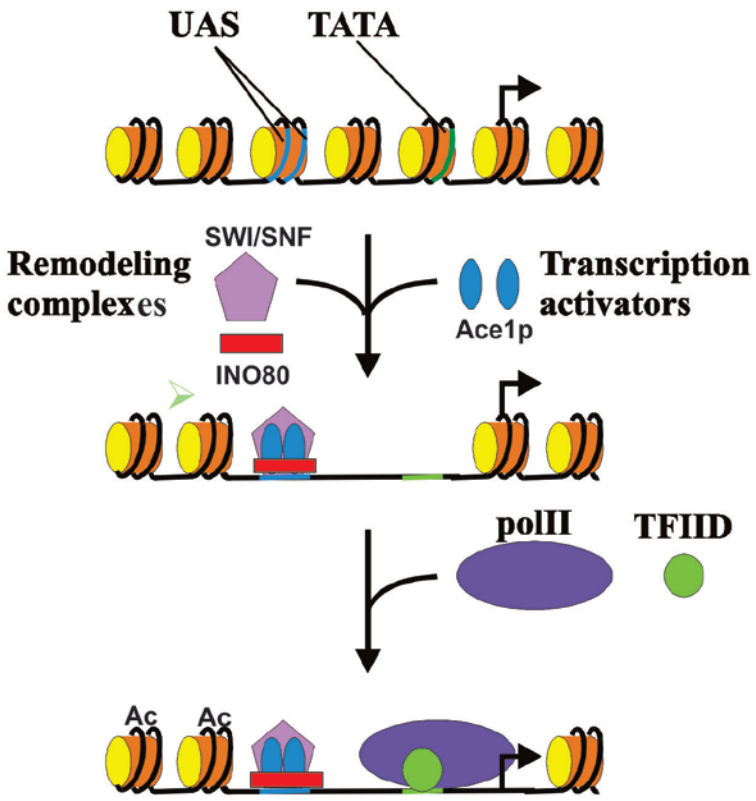

Figure 5.9 The model of *CUP1* gene activation

Orange cylinders –nucleosomes, Blue ovals- transcriptional activators (Ace1p), Purple oval- Polymerase II, Pink pentagon-SWI/SNF remodeling complex, Red rectangle- INO80 remodeling complex, Green circle- *TATA* binding protien (TFIID), Blue region on the thread- upstream activation region (*UAS*), Green region on the thread- *TATA* region, Black thread- gene, Ac represents the acetylation regions of the gene.

Finally, the HAT activity, which might be associated with TBP or might be recruited at an even later stage in initiation, acetylates nucleosomes at the promoter region. Therefore, our research has shown an insight into the mechanism of *CUP1* expression.

CHAPTER 7

7 Future direction and significant

Here, growth analysis, RNA analysis and ChIP analysis were performed to identify that both Ino80p and Snf2p are involved in *CUP1* transcriptional activation. The nucleosome density analysis showed that the deletion of either Ino80p or Snf2p resulted in the loss of remodeling activity at the *CUP1* promoter. As such, both Snf2p and Ino80p are inter-dependent and are required for *CUP1* induction. Furthermore, we showed that both remodelers were required to bring in RNA *pol*II. We also demonstrated that the recruitment of both remodelers is activator-dependent. Based on these observations, we have proposed a model to describe how several factors act on *CUP1* chromatin during gene activation.

In this research, we only tested four chromatin remodelers. It is not known whether Chd1p is involved in *CUP1* induction. In addition, it has not been determined which HAT is involved in *CUP1* induction. As such, mutant survival experiments, RNA analysis and ChIP assay should be performed to further identify any transcriptional coactivators that could be possibly involved in *CUP1* induction. It is also interesting to investigate and redefine the role of HAT in transcriptional activation. This is because a recent study showed that Gcn5 acetylates both histones and the Snf2 subunit of the SWI/SNF remodeler complex *in vitro* and *in vivo*, and such action promotes the dissociation of the SWI/SNF for the recycling purpose (Kim *et al*., 2010).

Above all, our *CUP1* activation model can serve as a starting point to study other genes in yeast that may exhibit similar patterns. Until now, over 6000 genes have been identified in yeast but only a few transcriptional coactivators are available. Some genes must use similar combination of the coactivators for transcriptional activation. It is reasonable to assume that they must share similar pattern of induction mechanism. Until now, only very few genes have been studied in detailed for the mechanism of gene activation, including *CUP1*, *INO1*, *HIS3*, and *SUC2* (Shen et al., 2002; Ford *et al*., 2008; Kim *et al*., 2006; Sudarsanam *et al*., 1999). They all have similar transcription coactivators. Here, we have provided further insight into the mechanism of *CUP1* activation, it is therefore imperative that we can use this as the starting point to further unveil the mechanism of gene activation.

Appendix I

Transcriptional Control of Genes Involved in Yeast Phospholipid Biosynthesis

The Journal of Microbiology (2011) Vol. 49, No. 2, pp.265-273

Transcriptional Control of Genes Involved in Yeast Phospholipid Biosynthesis[§]

Roshini Wimalarathna[1,3], Chen-Han Tsai[1], and Chang-Hui Shen[1,2,3*]

[1]*Department of Biology, College of Staten Island,* [2]*Institute for Macromolecular Assemblies, City University of New York, 2800 Victory Blvd, Staten Island, New York 10314, USA*

[3]*PhD Program in Biology, The Graduate Center, City University of New York, 356 Fifth Avenue, New York 10016, USA*

(Received March 14, 2011/ Accepted April 4, 2011)

Phospholipid biosynthetic genes encode enzymes responsible for phospholipid biosynthesis. They are coordinately regulated by the availability of phospholipid precursors through the inositol-sensitive upstream activating sequence (UAS_{INO}). However, not all phospholipid genes are UAS_{INO}-containing genes and not all

[*] For correspondence.E-mail:ChangHui.Shen@csi.cuny.edu; Tel: +1-718-982-3998; Fax: +1-718-982-3852

[§]Supplemental material for this article may be found at http://www.springer.com/content/120956

UAS$_{INO}$-containing genes have the same response to the phospholipid precursors. Therefore, the transcriptional regulation of phospholipid genes in response to the availability of phospholipid precursors is still unclear. Here, 22 out of 47 phospholipid biosynthetic genes were identified as UAS$_{INO}$-containing genes, including, *EKI1*, *EPT1*, *INM1*, *IPK2*, *KCS1*, *PAH1*, and *PIK1* which have never been

reported before. We also showed, using qRT-PCR technique, that 12 UAS$_{INO}$-containing genes are down-regulated by 100μM inositol in the wild type cells and up-regulated by the 100μM inositol in the *ino2*Δ cells. Therefore, it is possible that these genes are transcriptionally regulated by the UAS$_{INO}$ through the negative response of Ino2p to inositol. One other UAS$_{INO}$-containing gene might be regulated by the positive response of Ino2p to 100μM inositol. Surprisingly, we found 9 UAS$_{INO}$-containing genes are not dependent on the response of Ino2p to 100μM inositol, indicating that they may be regulated by other pathway. Furthermore, we identified 9 and 3 non-UAS$_{INO}$-containing genes that are possibly regulated by the negative and positive response of Ino2p to 100μM inositol, respectively. Therefore, these observations provide insight into the understanding of the co-regulated phospholipid biosynthetic genes expression.

Keywords: phospholipid biosynthesis, gene expression, UAS$_{INO,}$ Ino2p, qRT-PCR

Phospholipid structural genes play an important role in regulating yeast cellular rocesses. These genes encode enzymes responsible for phospholipid synthesis, which define the structural integrity of cells during mitosis. For example, one of the essential phospholipids, phosphatidylinositol (PI), and its metabolites regulate a diverse set of cellular processes such as glycolipid anchoring of proteins (Shields and Arvan, 1999), signal transduction (Divecha and

Irvine, 1995; Ohanian and Ohanian, 2001), mRNA export from the nucleus (Odom *et al*., 2000; Saiardi *et al*., 2000a, 2000b; Shears, 2000), vesicle trafficking (Czech, 2000; Martin, 2001) and also serve as reservoirs of second messengers (Greenberg and Lopes, 1996; Henry and Patton-Vogt, 1998; Carman and Henry, 1999).

In the budding yeast *Saccharomyces cerevisiae*, phospholipid metabolism is coordinately regulated by the response to the availability of phospholipid precursor molecules, inositol and choline, in the growth medium (Kelley *et al*., 1988; Dowd *et al*., 2001; Loewen *et al*., 2004; Boumann *et al*., 2006; Gaspar *et al*., 2006). The addition of inositol to yeast cells starved for inositol induces a rapid and significant change in the pattern and synthesis of membrane phospholipids (Kelley *et al*., 1988; Loewen *et al*., 2004) and inositol-containing sphingolipids (Alvarez-Vasquez, 2005). The synthesis of PI, and the consumption of phosphatidic acid (PA) and cytidinediphosphatediacylglycerol
(CDP-DAG) are increased in the presence of inositol. Recent studies have also demonstrated that the addition of phospholipid precursor molecules to actively growing yeast cultures caused changes in the expression of genes and in the phospholipid synthesis and turnover (Santiago and Mamoun, 2003; Jesch *et al*., 2005; Gaspar *et al*., 2006).

Our current understanding of phospholipid gene expression comes from the study of *INO1* expression. *INO1* encodes a key enzyme required in the inositol biosynthetic pathway (Fig. 1). The *de novo* synthesis of PI, one of the major membrane phospholipids in mitotically active cells, requires the product of *INO1* expression. The regulation of *INO1* requires chromatin remodeling activities (Ford *et al*., 2007, 2008; Esposito *et al*., 2009) and the binding of

heterodimeric transcriptional activator, Ino2p/Ino4p, to its promoter (Ambroziak and Henry, 1994; Schwank *et al*., 1995). The binding site for the transcriptional activator is a 10-bp *cis*-acting promoter element, the inositol sensitive upstream activating sequence (UAS_{INO}) (Lopes *et al*., 1991; Koipally *et al*., 1996). The promoters of some yeast phospholipid structural genes contain variants of a 10-bp UAS_{INO} element. It is believed that the coordinated regulation of those phospholipid genes is influenced by the binding of Ino2p to the UAS_{INO} element and such binding depends on its response to the availability of phospholipid precursors. However, not all of the phospholipid genes have the UAS_{INO} element in their promoters and not all UAS_{INO}-containing genes have the same response to the phospholipid precursors. Therefore, our understanding of how cells regulate the phospholipid gene expression in response to the availability of phospholipid precursor molecules is still unclear.

In the present study, sequence analysis was used to search for the UAS_{INO}-containing phospholipid genes. We also used quantitative real-time PCR (qRT-PCR) to examine transcriptional regulation of structural genes in the presence or absence of inositol. We have shown that the addition of inositol to logarithmically growing yeast cells results in major and rapidchanges of the expression of phospholipid biosynthetic genes. The regulation of most of the phospholipid biosynthetic genes that contain at least one copy of the UAS_{INO} element in their promoter depends on the response of Ino2p to

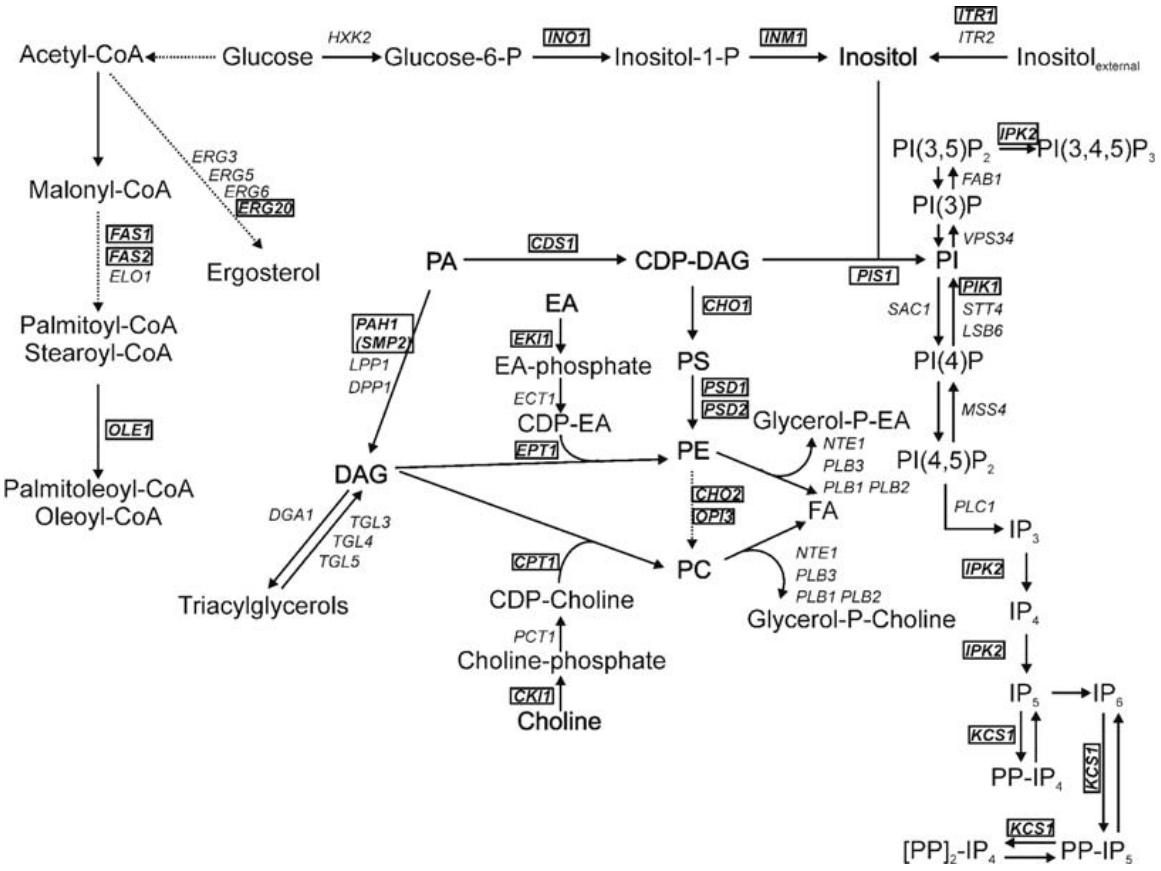

Fig.1. Phospholipid biosynthetic pathways of *S. cerevisiae*. UAS_{INO}-containing structural genes are highlighted in boxes. PA, phosphatidic acid; PS, phosphatidylserine; PE, phosphatidylethanolamine; PC, phosphatidylcholine; EA, ethanolamine; FA, fatty acid; CDP-DAG, cytidinediphosphate diacylglycerol; DAG, diacylglycerol; IP_3, IP_4, IP_5, IP_6, PP-IP_4, PP-IP_5, $[PP]_2$-IP_4, inositol polyphosphates; PI(3)P, PI(4)P, PI(3,5)P_2, PI(4,5)P_2, PI(3,4,5)P_3, phosphoinositides.

inositol availability. Furthermore, our results identified genes that do not have the UAS_{INO} element might also depend on the response of Ino2p to the inositol availability. Taken together, these observations provide insight into the understanding of the coregulated genes expression in the phospholipid biosynthetic pathway.

Materials and Methods

Yeast strains and growth conditions

Wild-type (WT) yeast strain BY4741 (*MATa his3Δ1 leu2Δ0 met15Δ0 ura3Δ0*) and *ino2*Δ strain (*MATa his3Δ1 leu2Δ0 met15Δ0 ura3Δ0 ino2Δ)* were used in this study. WT cells were grown at 30^{o}C in SC (synthetic complete media) containing 2% glucose (w/v) with 10 μM inositol, 100 μM inositol or without inositol. For *ino2*Δ cells, yeast culture was grown at 30^{o}C in SC with 10 μM inositol. When the optical density reached 0.9-1.1, cells were harvested by centrifugation and washed twice with SC without inositol to completely remove inositol. Cells were then resuspended in SC with 10 μM inositol, 100 μM inositol or without inositol, and incubated for 2 h at 30^{o}C.

RNA preparation and first strand cDNA synthesis

The total RNA was prepared as described previously (Ford *et al*., 2007). Briefly, 250 ml cells were harvested and resuspended in 400 μl lysis solution (10 mM Tris HCl; pH 7.5, 10 mM EDTA, 0.5% SDS). Subsequently, equal volume of acid phenol (pH 4.3) was added to the cells suspension. After 1 h incubation at 65^{o}C, the mixture was subject to centrifugation, and the aqueous phase was mixed with an equal volume of acid phenol again. After 5 min of incubation on ice, the aqueous phase was subject to chloroform extraction, ethanol precipitation, and was resuspended in 50 μl DEPC-treated H2O.

Equal amounts (10 μg) of total RNA were treated with RNase-free DNase (QIAGEN cat.#79254) at 37^{o}C for 1 h, and purified by phenol/ chloroform (3:1) extraction and ethanol precipitation. One microgram of pure RNA was used in SYBR GreenER Two-Step qRT-PCR kit (Invitrogen cat#11765-100) for first strand cDNA synthesis and real-time PCR reaction preparation as described in manufacture's manual.

Real-time PCR analysis

Phospholipid biosynthetic genes chosen for this study are shown in Fig. 1. All real-time PCR primers are listed in the supplementary materials. All experiments were repeated twice, and in each experiment, PCR reactions were done in triplicate in a 7,500 sequence detection system (Applied Biosystems, USA). Target DNA sequence quantities were estimated as described previously (Ford *et al*., 2008). Briefly, target DNA sequence quantities were estimated from the threshold amplification cycle number (C_T) using Sequence Detection System software (Applied Biosystems). Each DNA quantity was normalized to the *ACT1* DNA quantity by taking the difference between each gene's C_T and *ACT1*'s C_T value. Furthermore, a ΔC_T value was calculated for each gene by subtracting the C_T value for the sample prepared from SC with 10 μM inositol or 100 μM inositol from the C_T value for the sample prepared from SC without inositol. Each relative RNA fold change was then calculated with the following formula: $2^{(-\Delta C)}{}_T$.

Results

Search of UAS_{INO}-containing phospholipid genes

It has been shown that transcriptional activation of a UAS_{INO}-containing gene, *INO1,* is regulated through the response of Ino2p to the availability of inositol and choline (Lopes and Henry, 1991; Lopes *et al*., 1991; Ambroziak and Henry, 1994; Schwank *et al*., 1995; Koipally *et al*., 1996). The consensus sequence of 5'-WYTTCAYRTG-3' has been derived as the UAS_{INO} element (Schuller *et al*., 1995; Hoppen *et al*., 2005). Our aim is to understand the coordinated transcriptional control of genes with or without the UAS_{INO} element in the phospholipid biosynthetic pathway. Sequence analysis was performed to search genes that contain a UAS_{INO} element. The DNA sequence of each gene was obtained from the *Saccharomyces* Genome Database (http://yeastgenome.org). Each gene's DNA sequence covered 1 kb upstrea of the translation start site and the entire open reading frame. Serial Cloner (Version 1.3r11) was used to search for the consensus sequence 5'-WY TTCAYRTG-3' (Schuller *et al*., 1995; Hoppen *et al*., 2005). Our results showed that 22 genes out of the 47 genes in the phospholipid pathway contained at least one UAS_{INO} element (Table 1). The locations of the UAS_{INO} elements in these genes fell within the intergenic region, except in *KCS1, OPI3, PIK1*, and *PSD1*, which fell into their neighboring genes' open reading frame. Most of these UAS_{INO}-containing genes had only one copy of the UAS_{INO} element within their promoter region, except for *CHO2, FAS1*, *INO1, ITR1* and *KCS1*, which had two or more copies of the UAS_{INO} element within their promoter region.

Table 1. Compilation of phospholipid biosynthetic genes containing UAS_{INO} consensus sequence[a] in their promoter regions

Gene	Sequence	Location[b]	Distance from the nearest gene[c]
CDS1	ATGTGAAAA	-160	550
CHO1	CTTTCACAT	-162	505
CHO2	TGTGAAAA	-402	617
	ATGTGAATT	-334	617
	ATGTGAAGA	-265	617
CKI1	TATTCACATG	-196	290
CPT1	ATGTGAAAA	-162	414
EKI1	ATGTGAAAA	-215	889
EPT1	ATTTCACA	-154	495
ERG20	TTTTCACAT	-423	586
FAS1	ATGTGAAAA	-866	1030
	ACTTCACAT	-707	1030
FAS2	TTTTCACAT	-235	505
INM1	TTTTCACG	-445	455
INO1	TCTTCACGT	-357	439
	CATGTGAAAA	-241	439
	ATGTGAAAT	-290	439
	TTCACATG	-179	439
IPK2	TTTTCACAT	-6	478
ITR1	TCTTCACATG	-285	376
	ATGTGAAAA	-219	376
KCS1	TTTCATAT	-463	403
	TTTCATAT	-368	403
OLE1	TGTGAAAT	-868	1007
OPI3	TGTGAAAT	-190	160
PAH1	ATTTCACAT	-593	739
PIK1	TTTCACAT	-684	493
PIS1	CATATGAAGT	-274	348
PSD1	ATGTGAAA	-400	359
PSD2	ATATGAAAA	-244	477

[a] UAS_{INO} consensus sequence: WYTTCAYRTG (Schuller *et al.*, 1995; Hoppen *et al.*, 2005).

[b] Location: the position of the ICRE sequence relative to the translation start site (+1).

[c] Distance from the nearest gene: the distance between the two neighboring genes' translation start sites.

In our sequence analysis, 15 out of those 22 genes that contained at least one UAS_{INO} element have been identified in previous studies (Schuller *et al*., 1995; Santiago and Mamoun, 2003; Jesch *et al*., 2005, 2006). The other 7 phospholipid genes that contained at least one UAS_{INO} element have not been previously reported as UAS_{INO}-containing genes. These 7 genes include *EKI1*, *EPT1*, *INM1*, *IPK2*, *KCS1*, *PAH1*, and *PIK1*. *PAH1* catalyzes the dephosphorylation of PA to yield diacylglycerol (DAG) (Fig. 1). *EKI1* and *EPT1* contribute to the cytidinediphosphate (CDP)-choline pathway (Kennedy pathway) for the synthesis of phosphatidylcholine (PC) from DAG. *INM1* is involved in the biosynthesis of inositol. *IPK2*, *KCS1*, and *PIK1* are involved in the PI second messenger system.

Transcriptional profile of phospholipid genes

Next, we used the qRT-PCR strategy to examine the transcription profile of phospholipid genes in response to the presence or absence of the phospholipid precursor inositol. A cDNA probe was prepared from poly$(A)^+$ RNA isolated from WT cells cultivated in SC medium with 10 μM, 100 μM, or without inositol. The transcript levels of 29 phospholipid genes decreased in the presence of 100 μM inositol (Table 2), whereas the transcript levels of 18 phospholipid genes increased in the presence of 100 μM inositol (Table 3). 18 out of 29 of these genes which were repressed by 100 μM inositol contained at least one copy of the UAS_{INO} element. These genes were *CDS1, CHO1, CHO2, CKI1, EKI1, EPT1, ERG20, FAS1, FAS2, INO1*, *IPK2*, *ITR1, OLE1, OPI3, PAH1, PIK1, PSD1*, and *PSD2*. The other 11 genes, *DGA1*, *ECT1, ERG3, ERG5, ITR2,*

Table 2. Genes down-regulated by inositol for WT cells

Gene	Fold change[a]			
	10 μM inositol		100 μM inositol	
	Avg.[b]±SD[c]	*p* value	Avg.±SD	*p* value
CDS1	0.605±0.213	0.20	0.108±0.010	<0.01
CHO1	0.077±0.015	<0.01	0.005±0.002	<0.01
CHO2	0.632±0.626	0.62	0.039±0.023	<0.01
CKI1	0.452±0.038	<0.01	0.486±0.042	<0.01
DGA1	0.237±0.104	0.02	0.081±0.016	<0.01
ECT1	0.195±0.173	0.04	0.492±0.103	0.04
EKI1	0.219±0.053	<0.01	0.144±0.074	<0.01
EPT1	0.631±0.045	0.01	0.104±0.008	<0.01
ERG3	0.316±0.232	0.10	0.082±0.030	<0.01
ERG5	0.752±0.343	0.54	0.055±0.017	<0.01
ERG20	0.00005±0.00003	<0.01	0.137±0.023	<0.01
FAS1	0.267±0.056	<0.01	0.162±0.034	<0.01
FAS2	0.018±0.009	<0.01	0.005±0.001	<0.01
INO1	0.241±0.162	0.04	0.013±0.002	<0.01
IPK2	0.262±0.008	<0.01	0.126±0.004	<0.01
ITR1	0.129±0.101	0.01	0.019±0.011	<0.01
ITR2	0.379±0.164	0.06	0.041±0.010	<0.01
LSB6	0.160±0.059	<0.01	0.426±0.092	0.02
MSS4	0.961±0.443	0.94	0.186±0.029	<0.01
NTE1	0.897±0.228	0.70	0.596±0.033	<0.01
OLE1	0.036±0.015	<0.01	0.002±0.0002	<0.01
OPI3	0.006±0.004	<0.01	0.078±0.001	<0.01
PAH1	0.005±0.0009	<0.01	0.430±0.074	0.02
PIK1	0.434±0.194	0.10	0.046±0.012	<0.01
PLC1	0.587±0.073	0.03	0.052±0.002	<0.01
PSD1	0.0005±0.0001	<0.01	0.002±0.001	<0.01
PSD2	0.337±0.044	<0.01	0.213±0.026	<0.01
SAC1	0.401±0.287	0.17	0.075±0.036	<0.01
TGL3	0.083±0.0003	<0.01	0.276±0.036	<0.01

[a] Fold change: the ratio of a specific gene's relative RNA quantity to *ACT1* re-lative RNA quantity. Each gene's relative RNA quantity has been normalized to its corresponding RNA quantity obtained from no inositol treatment.
[b] Avg.: average fold change
[c] SD: standard deviation

Table 3. Genes up-regulated by inositol for WT cells

Gene	Fold change[a]			
	10 μM inositol		100 μM inositol	
	Avg.[b]±SD[c]	*p* value	Avg.±SD	*p* value
CPT1	2.518±1.566	0.43	7.787±1.467	0.04
DPP1	0.847±0.061	0.13	1.502±0.192	0.12
ELO1	0.258±0.046	<0.01	1.302±0.045	0.02
ERG6	1.999±0.430	0.09	2.421±0.407	0.07
FAB1	0.870±0.255	0.66	1.306±0.220	0.30
HXK2	0.234±0.066	<0.01	1.916±0.126	0.02
INM1	3.172±1.718	0.33	4.190±0.218	<0.01
KCS1	2.285±0.705	0.21	3.966±0.411	0.02
LPP1	0.072±0.025	<0.01	3.761±0.833	0.08
PCT1	1.323±1.191	0.81	3.34±0	<0.01
PIS1	1.720±0.172	0.05	3.834±0.279	<0.01
PLB1	0.834±0.650	0.82	5.382±1.298	0.08
PLB2	4.218±3.563	0.46	26.35±7.71	0.08
PLB3	0.888±0.378	0.80	6.332±1.893	0.11
STT4	1.416±0.476	0.08	1.973±0.489	0.18
TGL4	0.266±0	<0.01	6.353±1.111	0.04
TGL5	0.769±0.066	0.07	1.994±0.179	0.03
VPS34	11.196±10.812	0.45	21.160±2.265	0.01

Annotation were as described in the footnote of Table 2.

LSB6, MSS4, NTE1, PLC1, SAC1, and *TGL3*, which were repressed by 100 μM inositol do not have any UAS_{INO} elements. There was no significant difference in the increased transcript levels in the absence of inositol between the UAS_{INO} containing genes and non-UAS_{INO}-containing genes.

All 6 genes, *CDS1, CHO1, CHO2, OPI3, PSD1,* and *PSD2,* involved in the phosphatidylethanolamine (PE) methylation pathway contained at least one copy of the UAS_{INO} element and were down-regulated in the presence of 100 μM inositol (Fig. 1, Table 1, and Table 2). Genes that are involved in the synthesis of PE via DAG and the Kennedy pathway, including *PAH1, EKI1, ECT1,* and *EPT1,* were also down-regulated in the presence of 100 μM inositol, except for *LPP1* and *DPP1*, which do not have any UAS_{INO} elements. Fatty acid biosynthetic genes *FAS1, FAS2,* and *OLE1* contain at least one copy of the UAS_{INO} element and were down-regulated in the presence of 100 μM inositol. *ERG3, ERG5*, and *ERG20* are ergosterol biosynthetic genes and were down-regulated in the presence of 100 μM inositol, but only *ERG20* is a UAS_{INO}-containing gene. *PIK1, IPK2, LSB6, MSS4, PLC1,* and *SAC1* are in the PI second messenger system and were down-regulated in the presence of 100 μM inositol. From the above genes, only *IPK2* is a UAS_{INO}-containing gene.

Four genes, *CPT1, INM1, KCS1,* and *PIS1,*that contain at least one copy of the UAS_{INO} element were up-regulated in response to the presence of 100 μM inositol (Table 3). *CPT1* is involved in the process of PC synthesis, *INM1* is involved in PI synthesis, *KCS1* is involved in the PI second messenger system, and *PIS1* is required for PI synthesis from CDP-DAG. The other 14 genes, *DPP1, ELO1, ERG6, FAB1, HXK2, LPP1, PCT1, PLB1, PLB2, PLB3, STT4,*

TGL4, *TGL5*, and *VPS34*, which were up-regulated by 100 μM inositol do not have any UAS_{INO} elements (Table 3). Therefore, our results showed that the transcriptional regulation of most UAS_{INO}-containing genes (18 out of 22) is negatively controlled by the presence of 100 μM inositol.

Role of Ino2p in phospholipid biosynthetic genes expression

It has been demonstrated that only Ino2p is required to bind to the UAS_{INO} element of *INO1* promoter for transcriptional activation (Schwank *et al*., 1995). Furthermore, we have shown transcriptional response of 47 phospholipid biosynthetic genes to the availability of inositol. To further examine the role of Ino2p in the regulation of other phospholipid biosynthetic gene expression, the same qRT-PCR strategy was used to determine the transcription profile of phospholipid genes in the presence or absence of the phospholipid precursor inositol for the yeast *ino2*Δ strain. By comparing the transcription profiles between WT cells and *ino2*Δ cells, we can examine how these genes respond to inositol through Ino2p.

Our results showed that the mRNA levels of 12 phospholipid genes decreased in the presence of 100μM inositol (Table 4), and the mRNA levels of 35 phospholipid genes increased in the presence of 100μM inositol in *ino2*Δ strain (Table 5). For the genes repressed by inositol in *ino2*Δ strain, 7 out of 12 genes, *CHO1*, *EKI1*, *INM1*, *ITR1*, *PAH1*, *PSD1*, and *PSD2*, contained at least one copy of UASINO element (Tables 1 and

Table 4. Genes down-regulated by inositol for *ino2*Δ cells

Gene	Fold change[a]			
	10 μM inositol		100 μM inositol	
	Avg.[b]±SD[c]	*p* value	Avg.±SD	*p* value
CHO1	1.542±0.397	0.31	0.412±0.004	<0.01
EKI1	1.392±0.139	0.11	0.116±0.022	<0.01
ERG3	1.546±0.635	0.48	0.399±0.054	<0.01
ERG6	0.0012±0.0002	<0.01	0.016±0.005	<0.01
INM1	0.061±0.057	<0.01	0.014±0.006	<0.01
ITR1	1.042±0.348	0.91	0.060±0.021	<0.01
LPP1	0.111±0.062	<0.01	0.051±0.017	<0.01
PAH1	1.566±1.403	0.73	0.205±0.056	<0.01
PLC1	18.956±16.797	0.40	0.651±0	0.40
PSD1	2.349±1.306	0.41	0.068±0.009	<0.01
PSD2	0.511±0.216	0.20	0.511±0.076	0.02
TGL5	0.115±0.082	<0.01	0.722±0.082	0.08

Annotation were as described in the footnote of Table 2.

Table 5. Genes up-regulated by inositol for *ino2*Δ cells

Gene	Fold change[a]			
	10 μM inositol		100 μM inositol	
	Avg.[b]±SD[c]	*p* value	Avg.±SD	*p* value
CDS1	29.74±27.547	0.41	64.387±62.729	0.42
CHO2	5.205±0	<0.01	2.332±0.785	0.23
CKI1	0.288±0.279	0.13	1.802±1.336	0.61
CPT1	5.225±2.396	0.22	9.623±0.433	<0.01
DGA1	4.350±0.151	<0.01	0.994±0.325	0.99
DPP1	0.560±0.549	0.51	17.065±3.328	0.04
ECT1	0.003±0.001	<0.01	1.634±0.540	0.36
ELO1	0.038±0.030	<0.01	2.207±0.221	0.03
EPT1	8.923±7.873	0.42	34.572±33.077	0.42
ERG5	95.10±1.43	0.41	13.378±12.435	0.42
ERG20	32.486±31.072	0.42	27.787±23.128	0.37
FAB1	23.16±8.840	0.13	15.616±5.205	0.11
FAS1	33.58±33.138	0.43	30.225±27.455	0.40
FAS2	62.000±50.206	0.35	83.393±43.723	0.20
HXK2	4.711±4.044	0.46	81.126±22.843	0.07
INO1	0.436±0.312	0.21	1.476±0.138	0.07
IPK2	3.093±2.804	0.53	6.595±1.461	0.06
ITR2	7.108±1.830	0.08	5.406±2.268	0.19
KCS1	70.838±39.059	0.22	17.393±1.503	<0.01
LSB6	4.603±2.862	0.34	35.576±34.459	0.42
MSS4	33.366±0.694	<0.01	2.603±0	<0.01
NTE1	1.349±0.075	0.04	1.432±0.346	0.34
OLE1	6.621±5.255	0.40	94.113±78.333	0.40
OPI3	70.524±47.260	0.28	359.80±270.54	0.32
PCT1	8.445±6.798	0.39	166.770±57.637	0.10
PIK1	3.510±3.181	0.17	115.14±104.65	0.39
PIS1	0.260±0.189	0.06	34.287±2.727	<0.01
PLB1	2.225±1.693	0.54	6.522±0.113	<0.01
PLB2	4.150±0.878	0.07	97.567±33.122	0.10
PLB3	0.105±0.043	<0.01	7.735±0.722	0.01
SAC1	3.740±2.116	0.32	1.489±0.205	0.14
STT4	21.990±10.909	0.19	4.969±0.310	<0.01
TGL3	8.856±0.993	0.02	7.459±1.542	0.05
TGL4	0.323±0.079	0.01	4.737±1.119	0.08
VPS34	25.872±2.769	0.01	22.7±9.523	0.15

Annotation were as described in the footnote of Table 2.

4). *CHO1*, *EKI1*, *ITR1*, *PAH1*, *PSD1*, and *PSD2* were also repressed by 100 μM inositol in WT cells (Table 2), indicating genes depends on the presence of 100 μM inositol rather than the presence of Ino2p. These results suggest that these UAS_{INO}-containing genes might be negatively regulated by 100 μM inositol and the transcriptional control of these genes is irrelevant to the UAS_{INO} element. *INM1* was up-regulated by 100 μM inositol in WT cells but down-regulated by 100 μM inositol in *ino2*Δ cells, suggesting that transcriptional regulation of *INM1* might depend on the binding of Ino2p to its UAS_{INO} element through the positive response of Ino2p to inositol. The other 5 genes repressed by 100 μM inositol in the absence of Ino2p were *ERG3, ERG6, LPP1, PLC1*, and *TGL5*. The expression of *ERG3* and *PLC1* was also repressed by 100 μM inositol in WT cells, indicating that their expression is repressed by inositol and is irrelevant to the Ino2p. On the other hand, *ERG6, LPP1*, and *TGL5* which were repressed by 100 M inositol in *ino2*Δ, cells were induced by 100 μM inositol in WT cells, suggesting that transcriptional regulation of these genes might depend on the indirect positive response of Ino2p to inositol.

For those genes which were up-regulated by 100 μM inositol in ino2Δ cells, 15 out of 35 genes contained at least one copy of the UAS_{INO} element, but only *CDS1, CHO2, CKI1, EPT1, ERG20, FAS1, FAS2, INO1, IPK2, OLE1, OPI3,* and *PIK1* were repressed by 100 μM inositol in WT cells (Tables 2 and 5). It has been shown that transcriptional regulation of *INO1* depends on the binding of Ino2p to the UAS_{INO} element through the negative response of Ino2p to inositol (Lopes and Henry, 1991; Lopes *et al*., 1991; Ambroziak and Henry, 1994; Schwank *et al*., 1995; Koipally *et al*., 1996). Therefore, it is possible that all these genes have the same mechanism of transcriptional regulation as I*NO1*. The other three UAS_{INO}-containing genes *CPT1, KCS1,* and *PIS1* were induced by 100 μM inositol in both WT and *ino2*Δ cells, indicating that the

expression of these three genes is regulated by the availability of inositol and is irrelevant to the presence of Ino2p (Tables 3 and 5). The rest of the other genes up-regulated by 100 μM inositol are non-UAS_{INO}-containing genes. *DGA1, ECT1, ERG5, ITR2, LSB6, MSS4, NTE1, SAC1*, and *TGL3* were up-regulated by 100 μM inositol in *ino2*Δ cells, but down-regulated by 100 μM inositol in WT cells, suggesting that transcriptional regulation of these genes probably depends on the negative response of Ino2p to inositol (Tables 2 and 5). The other 11 genes, *DPP1, ELO1, FAB1, HXK2, PCT1, PLB1, PLB2, PLB3, STT4, TGL4,* and *VPS34*, were up-regulated by 100 μM inositol in both WT and *ino2*Δ cells (Tables 3 and 5). Therefore, the expression of these genes was directly influenced by the availability of the inositol positively.

Discussion

In the yeast Saccharomyces cerevisiae, the transcription of structural genes, which encode many phospholipid biosynthetic enzymes, is believed to be coordinately regulated by a cis-acting promoter element named UAS_{INO} element (Carman and Henry, 1989; Carman and Henry, 1999; Kagiwada and Zen, 2003; Jesch *et al*., 2006; Jani and Lopes, 2008). The binding of the Ino2p activator to the UAS_{INO} element is in response to the availability of inositol in the environment (Ambroziak and Henry, 1994; Schwank *et al*., 1995). However, some phospholipid biosynthetic genes do not have any UAS_{INO} element in their promoter region. The availability of inositol could also influence their transcriptional activation. Therefore, a complete description of the transcriptional changes of the phospholipid biosynthetic genes can help us to understand the regulation of the coordinated phospholipid signaling pathway.

From sequence analysis, we found that 22 out of 47 phospholipid biosynthetic genes contained at least one or more copies of the UAS_{INO} element in their promoter. Seven of them have never been reported before, including *EKI1, EPT1, INM1, IPK2, KCS1, PAH1,* and *PIK1*. We have also shown that the addition of inositol to logarithmically growing yeast cells resulted in major and rapid changes of the transcription profile. Based on our findings, we propose that these phospholipid biosynthetic genes can be divided into 2 different categories depended on their regulation or lack of regulation by 100 μM inositol through Ino2p (Table 6). Each category can be further divided into up-regulated by and down-regulated by 100 μM inositol. Twenty-one genes, *CDS1, CHO2, CKI1*,

Table 6. Categories of inositol-regulated phospholipid biosynthetic genes

Regulation through inositol directly				Regulation through the response of Ino2p to inositol			
Up-regulation		Down-regulation		Up-regulation		Down-regulation	
UAS_{INO}	Non-UAS_{INO}	UAS_{INO}	Non-UAS_{INO}	UAS_{INO}	Non-UAS_{INO}	UAS_{INO}	Non-UAS_{INO}
CPT1	*DPP1*	*CHO1*	*ERG3*	*INM1*	*ERG6*	*CDS1*	*DGA1*
KCS1	*ELO1*	*EKI1*	*PLC1*		*LPP1*	*CHO2*	*ECT1*
PIS1	*FAB1*	*ITR1*			*TGL5*	*CKI1*	*ERG5*
	HXK2	*PAH1*				*EPT1*	*ITR2*
	PCT1	*PSD1*				*ERG20*	*LSB6*
	PLB1	*PSD2*				*FAS1*	*MSS4*
	PLB2					*FAS2*	*NTE1*
	PLB3					*INO1*	*SAC1*
	STT4					*IPK2*	*TGL3*
	TGL4					*OLE1*	
	VPS34					*OPI3*	
						PIK1	

DGA1, ECT1, EPT1, ERG5, ERG20, FAS1, FAS2, INO1, IPK2, ITR2, LSB6, MSS4, NTE1, OLE1, OPI3, PIK1, SAC1, and *TGL3,* are regulated by the negative response of Ino2p to inositol either directly or indirectly. Only 4 genes, *ERG6, INM1, LPP1,* and *TGL5,* are positively regulated by the response of Ino2p to inositol. The other 22 phospholipid biosynthetic genes are directly regulated by 100 μM inositol (Table 6).

The expression of *INO1* has been studied intensively (Ambroziak and Henry, 1994; Kagiwada and Zen, 2003; Ford *et al*., 2007, 2008; Esposito *et al*., 2009). The regulation of *INO1* transcription is dependent on the binding of Ino2p to the UAS_{INO} element, which is in response to inositol availability. Here, we showed that *INO1* expression was up-regulated in the absence of inositol for WT cells (Table 2). The expression of *INO1* was down-regulated in the absence of inositol for *ino2*Δ cells. This result confirms that *INO1* expression depends on the negative response of Ino2p to 100 μM inositol. Eleven other UAS_{INO}-containing genes displayed a similar pattern as *INO1*, including *CDS1, CHO2, CKI1, EPT1, ERG20, FAS1, FAS2, IPK2, OLE1, OPI3,* and *PIK1* (Table 6). Therefore, 12 out of 22 UAS_{INO}-containing structural genes are negatively regulated by inositol through Ino2p. Of these, *CDS1, CHO2, CKI1, ERG20, FAS1, FAS2, OLE1,* and *OPI3* had been previously shown to exhibit a negative response of Ino2p to the inositol (Santiago and Mamoun, 2003; Jesch *et al*., 2005, 2006). The present study is the first report to show that *EPT1, IPK2,* and *PIK1* are co-regulated with *INO1* and are likely to be Ino2p targets. One other UAS_{INO}-containing gene, *INM1*, is positively regulated by inositol through Ino2p. The other 9 UAS_{INO} element-containing genes that are not directly regulated by the Ino2p may be regulated by inositol directly or through other signals generated by ongoing phospholipid metabolism (Henry and Patton-Vogt, 1998).

Previous studies showed that 4 UAS_{INO}-containing genes, *CHO1, ITR1, PSD1*, and *PSD2*, displayed a similar negative response to 100 μM inositol as *INO1* (Jesch *et al*., 2005, 2006). This is in accord with our findings for WT cells (Table 2). In the present study, we further examined the response of these genes to 100 μM inositol in *ino2*Δ cells and found they did not show similar patterns as *INO1*, indicating that their response to inositol was not related to the UAS_{INO} element. It is possible that these four genes along with *EKI1, ERG3, PAH1*, and *PLC1* are negatively regulated by inositol directly and not through the response of Ino2p to inositol (Tables 2, 4, and 6). Furthermore, we found that 3 other UAS_{INO}-containing genes, *CPT1, KCS1* and *PIS1*, are positively regulated by 100 μM inositol directly (Table 6). Therefore, our results demonstrated the evidence that the expression of UAS_{INO}-containing genes is not completely regulated by Ino2p.

Our results showed that genes involved in the PE methylation pathway and genes involved in the PE synthesis via DAG were up-regulated in the absence of inositol. These observations suggest that PC synthesis is increased in the absence of inositol. Since PC synthesis is increased, PI synthesis is expected to drop (Fig. 1). Indeed, we observed that *PIS1* was down-regulated in the absence of inositol, indicating the decrease of PI synthesis (Table 3). This 3.8-fold repression of *PIS1* is in accord with previous findings (Jani and Lopes, 2008). Previous studies have also demonstrated that the rate of PI synthesis dramatically increased and PC synthesis decreased when inositol was added to the growth medium of WT cells (Loewen *et al*., 2004; Gaspar *et al*., 2006). Therefore, our findings provide a detailed explanation for such physiological reactions.

In this report, we identified some structural genes that do not have the UAS_{INO} element and might be either positively or negatively regulated by the response of Ino2p to 100 μM inositol (Table 6). It is possible that Ino2p regulates these genes via indirect effects which could represent ongoing phospholipid metabolism. We have also shown that the positive or negative regulation of most of the UAS_{INO}-containing genes depends on the response of Ino2p to inositol availability. Taken together, these observations suggest that Ino2p is mediating either repression or activation of these genes in response to inositol through either direct or indirect effect. Further biochemical analysis, including chromatin immunoprecipitation coupled with real-time PCR analysis and/or promoter site-direct mutagenesis, can provide insight into the coordinated regulation of phospholipid gene expression.

Acknowledgement

We thank Michelle Esposito and Paulina Konarzewska for helpful discussion and comments on the manuscript. We are grateful to our laboratory colleagues for technical assistance. This work was supported by an NSF Grant (MCB-0919218) and PSC-CUNY awards (61164-0039 and 62180-0040) to C.-H. S.

References

Alvarez-Vasquez, F., K.J. Sims, L.A. Cowart, Y. Okamoto, E.O. Voit, and Y.A. Hannun. 2005. Simulation and validation of modeled sphingolipid metabolism in *Saccharomyces cerevisiae.* *Nature* 433, 425-430.

Ambroziak, J. and S.A. Henry. 1994. *INO2* and *INO4* gene products, positive regulators of phospholipid biosynthesis in *Saccharomyces cerevisiae*, form a complex that binds to the *INO1* promoter. *J. Biol. Chem*. 269, 15344-15349.

Boumann, H.A., J. Gubbens, M.C. Koorengevel, C.S. Oh, C.E. Martin, A.J. Heck, J. Patton-Vogt, S.A. Henry, B. de Kruijff, and A.I. de Kroon. 2006. Depletion of phosphatidylcholine in yeast induces shortening and increased saturation of the lipid acyl chains: evidence for regulation of intrinsic membrane curvature in a eukaryote. *Mol. Biol. Cell* 17, 1006-1017.

Carman, G.M. and S.A. Henry. 1989. Phospholipid biosynthesis in yeast. *Annu. Rev. Biochem.* 58, 635-669.

Carman, G.M. and S.A. Henry. 1999. Phospholipid biosynthesis in the yeast *Saccharomyces cerevisiae* and interrelationship with other metabolic processes. *Prog. Lipid Res*. 38, 361-399.

Czech, M.P. 2000. PIP2 and PIP3: complex roles at the cell surface. *Cell* 100, 603-606.

Divecha, N. and R.F. Irvine. 1995. Phospholipid signaling. *Cell* 80, 269-278.

Dowd, S.R., M.E. Bier, and J.L. Patton-Vogt. 2001. Turnover of phosphatidylcholine in *Saccharomyces cerevisiae*. The role of the CDPcholine pathway. *J. Biol. Chem*. 276, 3756-3763.

Esposito, M., P. Konarzewska, O. Odeyale, and C.H. Shen. 2009. Genewide histone acetylation at the yeast *INO1* requires the transcriptional activator Ino2p. *Biochem. Biophys. Res. Commun.* 391, 1285- 1290.

Ford, J., O. Odeyale, A. Eskandar, N. Kouba, and C.H. Shen. 2007. A SWI/SNF- and INO80-dependent nucleosome movement at the *INO1* promoter. *Biochem. Biophys. Res. Commun*. 361, 974-979.

Ford, J., O. Odeyale, and C.H. Shen. 2008. Activator-dependent recruitment of SWI/SNF and INO80 during *INO1* activation. *Biochem. Biophys. Res. Commun.* 373, 602-606.

Gaspar, M.L., M.A. Aregullin, S.A. Jesch, and S.A. Henry. 2006. Inositol induces a profound alteration in the pattern and rate of synthesis and turnover of membrane lipids in *Saccharomyces cerevisiae*. *J. Biol. Chem*. 281, 22773-22785.

Greenberg, M.L. and J.M. Lopes. 1996. Genetic regulation of phospholipid biosynthesis in *Saccharomyces cerevisiae*. *Microbiol. Rev*. 60, 1-20.

Henry, S.A. and J.L. Patton-Vogt. 1998. Genetic regulation of phospholipid metabolism: yeast as a model eukaryote. *Prog. Nucleic Acid Res. Mol. Biol.* 61, 133-179.

Hoppen, J., A. Repenning, A. Albrecht, S. Geburtig, and H.J. Schuller. 2005. Comparative analysis of promoter regions containing binding sites of the heterodimeric transcription factor Ino2/Ino4 involved in yeast phospholipid biosynthesis. *Yeast* 22, 601-613.

Jani, N.M. and J.M. Lopes. 2008. Transcription regulation of the *Saccharomyces cerevisiae PIS1* gene by inositol and the pleiotropic regulator, Ume6p. *Mol. Microbiol*. 70, 1529-1539.

Jesch, S.A., P. Liu, X. Zhao, M.T. Wells, and S.A. Henry. 2006. Multiple endoplasmic reticulum-to-nucleus signaling pathways coordinate phospholipid metabolism with gene expression by distinct mechanisms. *J. Biol. Chem*. 281, 24070-24083.

Jesch, S.A., X. Zhao, M.T. Wells, and S.A. Henry. 2005. Genome-wide analysis reveals inositol, not choline, as the major effector of Ino2p- Ino4p and unfolded protein responsetarget gene expression in yeast. *J. Biol. Chem*. 280, 9106-9118.

Kagiwada, S. and R. Zen. 2003. Role of the yeast VAP homolog, Scs2p, in *INO1* expression and phospholipid metabolism. *J. Biochem*. 133, 515-522.

Kelley, M.J., A.M. Bailis, S.A. Henry, and G.M. Carman. 1988. Regulation of phospholipid biosynthesis in *Saccharomyces cerevisiae* by inositol. Inositol is an inhibitor of phosphatidylserine synthase activity. *J. Biol. Chem*. 263, 18078-18085.

Koipally, J., B.P. Ashburner, N. Bachhawat, T. Gill, G. Hung, S.A. Henry, and J.M. Lopes. 1996. Functional characterization of the repeated UAS_{INO} element in the promoters of the *INO1* and *CHO2* genes of yeast. *Yeast* 12, 653-665.

Loewen, C.J., M.L. Gaspar, S.A. Jesch, C. Delon, N.T. Ktistakis, S.A. Henry, and T.P. Levine. 2004. Phospholipid metabolism regulated by a transcription factor sensing phosphatidic acid. *Science* 304, 1644-1647.

Lopes, J.M. and S.A. Henry. 1991. Interaction of trans and cis regulatory elements in the *INO1* promoter of *Saccharomyces cerevisiae*. *Nucleic Acids Res*. 19, 3987-3994.

Lopes, J.M., J.P. Hirsch, P.A. Chorgo, K.L. Schulze, and S.A. Henry. 1991. Analysis of sequences in the *INO1* promoter that are involved in its regulation by phospholipid precursors. *Nucleic Acids Res*. 19, 1687-1693.

Martin, T.F. 2001. PI (4,5)P(2) regulation of surface membrane traffic. *Curr. Opin. Cell Biol.* 13, 493-499.

Odom, A.R., A. Stahlberg, S.R. Wente, and J.D. York. 2000. A role for nuclear inositol 1,4,5-trisphosphate kinase in transcriptional control. *Science* 287, 2026-2029.

Ohanian, J. and V. Ohanian. 2001. Sphingolipids in mammalian cell signaling. *Cell. Mol. Life Sci.* 58, 2053-2068.

Saiardi, A., J.J. Caffrey, S.H. Snyder, and S.B. Shears. 2000a. Inositol polyphosphate multikinase (ArgRIII) determines nuclear mRNA export in *Saccharomyces cerevisiae*. *FEBS Lett*. 468, 28-32.

Saiardi, A., J.J. Caffrey, S.H. Snyder, and S.B. Shears. 2000b. The inositol hexakisphosphate kinase family: Catalytic flexibility and function in yeast vacuole biogenesis. *J. Biol. Chem.* 275, 24686-24692.

Santiago, T.C. and C.B. Mamoun. 2003. Genome expression analysis in yeast reveals novel transcriptional regulation by inositol and choline and new regulatory functions for Opi1p, Ino2p, and Ino4p. *J. Biol. Chem*. 278, 38723-38730.

Schuller, H.J., K. Richter, B. Hoffmann, R. Ebbert, and E. Schweizer. 1995. DNA binding site of the yeast heteromeric Ino2p/Ino4p basic helix-loop-helix transcription factor: structural requirements as defined by saturation mutagenesis. *FEBS Lett*. 370, 149-152.

Schwank, S., R. Ebbert, K. Rautenstrauss, E. Schweizer, and H.J. Schuller. 1995. Yeast transcriptional activator *INO2* interacts as an Ino2p/Ino4p basic helix-loop-helix heteromeric complex with the inositol/choline-responsive element necessary for expression of phospholipid biosynthetic genes in *Saccharomyces cerevisiae*. *Nucleic Acids Res.* 23, 230-237.

Shears, S.B. 2000. Transcriptional regulation: a new dominion for inositol phosphate signaling? *Bioessays* 22, 786-789.

Shields, D. and P. Arvan. 1999. Disease models provide insights into post-golgi protein trafficking, localization and rocessing. *Curr.Opin. Cell Biol*. 11, 489-494.

Appendix II

Histone Modifications and Gene Activation

In: Histones: Class, Structure and Function
Editor: Chang-Hui Shen, pp.
ISBN 978-1-62100-274-1

Chapter 5

Histone Modifications and Gene Activation

Roshini Nilupama Wimalarathna[1,3,*] and Chang-Hui Shen[1,2,3]

[1]Department of Biology, College of Staten Island, City University of New York, 2800 Victory Blvd, Staten Island, New York 10314, USA

[2]Institute for Macromolecular Assemblies, City University of New York, 2800 Victory Blvd, Staten Island, New York 10314, USA

[3]PhD Program in Biology, The Graduate Center, City University of New York, 365 Fifth Avenue, New York 10016, USA

ABSTRACT

Histones are subjected to post translational modifications such as acetylation, deacetylation, methylation, phosphorylation, ubiquitination sumoylation, ADP ribosylation, glycosylation, biotinylation and carbonylation. The first four post-translational modifications (acetylation, deacetylation, methylation and phosphorylation) have been studied extensively in comparison to the other types of modification. Histone

* Corresponding author. E-mail: Roshini.Wimalarathna@csi.cuny.edu.

modification activity has been shown to participate in a variety of cellular processes including, but not limited to, gene activity. In this chapter, we will discuss current findings of histone modifications and its connection to gene activity.

1. INTRODUCTION

The nucleosome is the basic structural repeat unit of chromatin. A nucleosome contains 147 bp of DNA wrapped in 1.75 superhelical turns around a central octamer. This central octamer is composed of two of each of the four core histones H2A, H2B, H3 and H4. The chromatin structure helps to package a vast amount of DNA into the cellular nucleus, but this compaction of DNA creates a barrier in the accessibility of the information encoded within the DNA for many DNA template-based cellular activities, such as transcription, replication, recombination and repair. To overcome the repressive effects of chromatin on RNA polymerase II-mediated transcription, the chromatin structure must be perturbed at promoter regions prior to or during transcriptional activation [1]. There are two types of proteins that work on the nucleosomes which allow for the access of the DNA to *trans-acting* factors. The first type is ATP-dependent chromatin remodelers, which typically form complexes with protein partners and use the free energy generated by ATP hydrolysis to remodel the chromatin structure [2, 3]. The other type of protein covalently modifies histone proteins by acetylation [4], deacetylation [5], methylation [6], phosphorylation [7], ubiquitynation [8], sumoylation [9], ADP ribosylation [10], biotinylation [11] glycosylation and carbonylation. Acetylation, deacetylation, methylation, and phosphorylation have been studied extensively, whereas relatively little is known about the other

types of modification. In this chapter, we will discuss these post-translational modifications as well as the connection of histone modification and gene activity.

2. HISTONE ACETYLATION

Acetylation of lysine residues on the core histones N-terminal tails is normally associated with transcriptionally active genes. In general, histone H3 Lys 9, Lys 14, Lys 18 and Lys 23, histone H4 Lys 5, Lys 8, Lys 12 and Lys 16, histone H2A Lys 5 and Lys 9, and histone H2B Lys 5, Lys 12, Lys 15 and Lys 20 are targets for acetylation [3, 12, 13]. Histone acetyltransferases (HATs) are the enzymes responsible for the transfer of an acetyl group to the ε-amine group of lysine residues. HATs consist of both large multi-subunit complexes and transcriptional co-activators which are recruited to promoters by interactions with DNA-bound activator proteins [14]. HATs not only acetylate histone proteins but also modify non-histone proteins such as tumor suppressor protein p53 [15] and minichromosome maintenance 3 protein [16].

Based on sequence homology HATs can be grouped into different families such as Hat1p, Gcn5p/PCAF, p300/CBP, MYST, p160,CIITA, Atf2p, $TAF_{II}250$, TFIIC, Nut1p, Elp3p, CDY, Hpa2p, TFIIB, MCM3AP, Eco1p and Ard1p [17, 18; Table 1]. In terms of sub-cellular location, HATs can be categorized into two types, Type A and Type B. Type A HATs are normally found in the nucleus. This type of HAT acetylates histone in the chromatin context and may play important roles in the regulation of gene expression by functioning as transcriptional co-activators. PCAF, CBP, p300, $TAF_{II}250$, ACTR, Tip60p, Esa1p and Elp3p are type A HATs [4, 19-24]. Type B HATs can be found in the cytoplasm and are involved in the acetylation of nascent histones H3 and histone H4. Hat1p is the only currently known type B HAT [19, 25-26],

however, recent evidence has shown that Hat1p may be present in multiple locations [19, 27], and thus may not precisely fit into this classification.

The Gcn5p/PCAF family is one of the nuclear HATs, which consists of Gcn5p, PCAF, and related proteins. Yeast Gcn5p contains a HAT domain and a bromodomain which is highly homologous to the human PCAF and Gcn5p. Gcn5p was the first type A HAT discovered in *Tetrahymena thermophila* [28]. Later, homologs of Gcn5p were found in humans, mice, *Schizosaccharomyces pombe* and *Drosophila melanogaster*, suggesting that its function is highly conserved throughout eukaryotes [29- 32]. Gcn5p primarily acetylates histone H3 Lys14 and histone H4 Lys 8 and Lys 16 [33]. Yeast Gcn5p is required for normal progression through the G2/ M boundary [34] and mitotic gene expression [35]. The gene for PCAF, which is also referred to as P/CAF, was originally identified from a human cDNA database on the basis of its homology to Gcn5p. PCAF preferentially acetylates histone H3 Lys 14 and weakly acetylates histone H4 Lys 8 [36]. Although PCAF was originally characterized as a HAT, it can also acetylate various non-histone transcription related proteins such as the chromatin proteins HMG17 and HMGI(Y), transcriptional activator p53 and MyoD, and general transcription factors TFIIE and TFIIF [15, 32].

The MYST family is the most diverse nuclear HAT family, and is important in transcriptional activation, DNA repair and gene silencing. Yeast Sas2p, Sas3p and Esa1p are members of MYST family. Both Sas2p and Sas3p are involved in gene silencing [32, 37-38], and Esa1p is essential for cell cycle progression [39]. It has been shown that Esa1p can acetylate free histones H4 Lys 5 with high efficiency, and acetylate H4 Lys 8, Lys 12 and Lys 16 with moderate efficiency *in vitro* [40]. Histone H3 Lys14 and histone H2A Lys 4 are potentially major targets, and histone H3 Lys 4 and histone H2A Lys 7 are potentially moderate targets. Furthermore, the

esa1 mutants succeed in replicating their DNA but fail to proceed through mitosis and cytokinesis, suggesting a role of Esa1p in cell cycle progression.

Both p300 and CBP (CREB binding protein) are transcriptional co-activators which can acetylate both histones and non-histone proteins [17]. They are recruited to specific promoters through interactions with transcription factors, including E1A and phosphorylated CREB [41, 42]. P300/CBP contain putative zinc finger domains, a bromodomain, a HAT domain, and at least two independent regions that interact with multiple transcription factors [42, 43]. Mutations of p300 are associated with certain cancers such as leukemia [17], colorectal carcinomas, and gastric carcinomas [44, 45]. The p300/CBP is able to acetylate all four histones within the nucleosome as well as free histones.

Yeast Hat1p is the only type B HAT which is found in the cytoplasm and can acetylate newly synthesized histones H3 and H4. Hat1p preferentially acetylates H4 Lys 5 and Lys 12 [19, 46]. Hat2p is usually co-purified with Hat1p from the cytosolic extracts. Hat2p is not required for the catalytic activity of Hat1p but acts as a regulatory subunit when in complex with Hat1p. It has been shown that the catalytic activity of Hat1p increases 10 fold when Hat2p binds to Hat1p compared to the activity of the Hat1p alone [47]. Although Hat1p is mainly localized in the cytoplasm, a recent study has shown that Hat1p can be translocated into the nucleus for telomeric silencing. This process is mediated mainly through H4 Lys 12, thus in contrast to other HATs, Hat1p is involved in transcriptional repression rather than gene activation [19].

It is commonly accepted that histone acetylation is important in transcriptional activation, although some exception do exist such as the acetylation of histone H4 Lys 12 which is a mark for the silent chromatin state as described above [19, 48, 49]. Histone acetylation can modulate gene transcription at two levels: global histone acetylation and promoter –specific histone

acetylation. While global histone acetylation correlates with general transcription activity [50], promoter-specific acetylation is a critical mechanism for the control of specific gene activity [51].

Table 1. Classification of histone acetyltransferases [17, 18]

Family	HATs	Organism	Histone	Site	Function
Hat1	Hat1	*S.cerevisia*	H4	K5	Histone deposition
		to		K12	Gene silencing, Histone deposition
		mammals	H2A	K7	?
Gcn5/P	Gcn5	*S.cerevisia*	H2B	K11	Transcriptional activation
CAF		to		K16	Transcriptional activation
		mammals	H3	K9	Transcriptional activation
				K14	Transcriptional activation
				K18	Transcriptional activation
					DNA repair
				K27	Transcriptional activation
			H4	K8	Transcriptional activation
				K16	Transcriptional activation
	PCAF		H3	K14	Transcriptional activation
		Mammals	H4	K8	Transcriptional activation
p300/C	CBP	*C.elegans*	H2A	K5	Transcriptional activation
BP		to	H2B	K12	Transcriptional activation
		mammals		K15	
			H3	K18	DNA replication
				K23	Transcriptional activation
	P300		H2A	K5	Transcriptional activation
		Mammals	H2B	K12	Transcriptional activation
				K15	
				K20	Transcriptional activation
			H3	K14	Transcriptional activation
				K18	DNA replication
				K23	Transcriptional activation
MYST	Sas2	*S.cerevisia*	H3	K14	Gene silencing
			H4	K16	Gene silencing
	Sas3	*S.cerevisia*	H3	K14	Transcriptional activation,
					Elongation
			K23		DNA repair
	Eas1	*S.cerevisia*	H2A	K4	Transcriptional activation
				K7	Transcriptional activation
			H2B	K16	Transcriptional activation
			H3	K4	Transcriptional activation
				K14	Transcriptional activation,
					DNA repair
			H4	K5	Transcriptional activation,
					DNA repair
				K8	Transcriptional activation
				K12	Transcriptional activation,
					DNA repair
				K16	DNA repair
	Mof	*Drosophila*	H4	K16	Gene dosage compensation

	TIP60	Mammals	H2A	K5	Transcriptional activation
			H3	K14	Transcriptional activation, DNA repair
			H4	K5	Transcriptional activation, DNA repair
				K8	Transcriptional activation, DNA repair
				K12	Transcriptional activation, DNA repair
	MOF	Mammals	H4		Transcriptional activation
	HBO1	Mammals	H3/H4		DNA replication, Transcriptional repressor
	MOZ	Mammals	H3/H4		Transcriptional activation
	MORF	Mammals	H3/H4		Transcriptional activation
p160	SCR-1	Mammals	H3	K9	Transcriptional activation
				K14	Transcriptional activation
	ACTR	Mammals	H3/H4		Transcriptional activation
CIITA	CIITA	Mammals	H4		Transcriptional activation
ATF2	ATF2	Mammals	H2B	K5	Transcriptional activation
				K12	Transcriptional activation
				K15	Transcriptional activation
			H4	K5	Transcriptional activation
				K8	Transcriptional activation
				K16	Transcriptional activation
TAF_{II} 250	$TAF_{II}230$	*Droso[hila*	H3/H4		Transcription initiation
	$TAF_{II}250$	Mammals	H3/H4		Transcriptional initiation, kinase and ubiquitin ligase
TFIIIC	hTFIIIC90	*S.cerevisia*	H3	K14	RNA polymerase III transcription
	TFIIIC subunits	to mammals	H4		Transcriptional initiation
Nut1	Nut1	*S.cerevisia*	H3/H4		Transcriptional initiation
Elp3	Elp3	*S.cerevisia*	H3	K14	Transcriptional elongation
		to	H4	K8	Transcriptional elongation
		mammals			
CDY	CDY	Humans	H4		Histone to protamine transition
	CDYL	Mammals	H4		during spermatogenesis
Hpa2	Hpa2	*S.cerevisia*	H3	K4	Unknown
				K14	Unknown
			H4	K5	Unknown
				K12	Unknown
	Hpa3	*S.cerevisia*			Unknown
			H3/H4		

At the promoter-specific level, it has been shown that the induction of *CUP1* in *Saccharomyces cerevisiae* with copper resulted in targeted acetylation of both H3 and H4 at the *CUP1* promoter [52]. Nucleosomes containing upstream activating sequences of *CUP1* and sequences farther upstream were also the targets for acetylation. It has also been shown that the levels of H3 and H4 histone acetylation at the *INO1* promoter and *ORF* (open reading frame) increased under inducing conditions [53]. Such an increase of histone acetylation is not due to the increase of the nucleosome number; instead, it is because the acetylation level per nucleosome increased significantly. Therefore, these experiments demonstrate the direct connection between promoter-specific histone acetylation and gene activation.

At the global level, it has been reported that histone H4 Lys 5 and Lys12 are preferentially bound by the TAFII250 bromodomains *in vitro*, and these interactions promote acetylation-stimulated global transcription [54].

3. HISTONE DEACETYLATION

Histone deacetylases (HDACs) oppose the effects of HATs by deacetylating acetylated lysine residues. Histone deacetylation reverses the charged, neutralizing effect of the acetyl group on histone tails to a charged tail state and promote the interaction between DNA and histone tails. As such, histone deacetylation causes the condensation of chromatin fibers and promotes gene repression. HDACs are also called lysine deacetylases (KDAC). HDAC not only perform histone deacetylation, but can also deacetylate non-histone proteins such as α-tubulin [55].

HDACs can be divided into four classes based on their function and protein sequence similarity [Table 2]. The class I and class II HDACs are classical HDACs and their activities can be inhibited by trichostatin A (TSA), whereas the class III HDACs are a family of NAD+-

dependent proteins which are not affected by TSA. HDAC1, HDAC2, HDAC3 and HDAC8 belong to class I HDACs. HDAC1, HDAC2 and HDAC8 are primarily found in the nucleus, whereas HDAC3 can be found in both the nucleus and cytoplasm. The yeast reduced potassium dependency 3 (Rpd3p) is also a class I HDAC.

HDAC4, HDAC5, HDAC6, HDAC7, HDAC9a, HDAC9b and HDAC10 are class II HDACs. Yeast histone deacetylase 1 (Hda1p) is also a class II HDAC [5,56]. Class II HDACs can be shuttled in and out of the nucleus in response to certain cellular signals [57-58]. HDAC6 is mainly localized in the cytoplasm and responsible for deacetylation of α-tubulins.

Mammalian Sirtuins including SIRT1, SIRT2, SIRT3, SIRT4, SIRT5, SIRT6 and SIRT7 belong to class III HDACs. Yeast silent information regulator 2 (Sir2p) is also a class III HDAC [5, 58]. HDAC11 is the only class IV HDAC [55, 58-59] and is localized in the nucleus, although it has been shown that it can be co-precipitated with the cytoplasmically localized HDAC6 [60]. HDAC11 has a catalytic domain situated at the N-terminus, with proven HDAC activity that can be inhibited by trapoxin (a TSA analogue). There is no association of HDAC11 with any of the known HDAC complexes, suggesting the distinct biochemical function of HDAC11 [60].

Table 2. Classification of Histone Deacetylases [58]

Class I	Class II	Class III	Class IV
HDAC1, HDAC2, HDAC3, HDAC8	HDAC4, HDAC5, HDAC6, HDAC7, HDAC9a, HDAC9b, HDAC10	Sirtuins in mammals SIRT1, SIRT2, SIRT3, SIRT4, SIRT5, SIRT6, SIRT7	HDAC11
RPD3 in the yeast (*Saccharomyces cerevisiae*)	HDA1 in the yeast (*Saccharomyces cerevisiae*)	SIR2 in the yeast (*Saccharomyces cerevisiae*)	

4. HISTONE METHYLATION

Histone methylation was discovered over 35 years ago, however, only recently has this process been investigated. Methylation occurs at lysine and arginine residues on the histone tails of histones H3 and H4 and is associated with both transcriptional activation and repression. Histone methyltransferases (HMTs) are the enzymes responsible for these modifications. Based on their substrate specificity HMTs can be grouped into two families. Histone lysine methyltransferases (HKMTs) catalyze the methylation of lysine residues. On the other hand, protein arginine methyltransferases (PRMTs) catalyze the methylation of arginine residues. The PRMTs contain a conserved catalytic domain and an *S*-adenosyl methionine-binding region. Specificity with respect to the particular arginines methylated varies, as does the number of methyl groups attached. PRMTs can attach one or two methyl groups to arginine residues allowing for variation in the symmetry of these groups [6, 16, 61]. The HKMTs contain the evolutionarily conserved SET domain. The SET domain is the catalytic motif and is approximately 130 amino acids in length [62-66]. Based on the sequence homology within and surrounding the SET domain, SET-containing HKMTs can be divided into six different subfamilies including SET1, SET2, SUV39, EZH, SMYD, and PRDM [62-63, 67-68].

Table 3. Histone methyltransferases and their targeted residues [131]

HMTs	Histone	Site
PRMT1	H4	R3
PRMT5	H3 H4	R8 R3
NSD1	H3 H4	K36 K20
PR-SET7/SET8, SUV4-20H1, SUV4-20H2	H4	K20
EZH2	H3	K27
CARM1	H3	R26 R17
SET1, MLL/HRX/ALL1, MLL2/HRX2, MLL3/HALR, ASH1, SMYD3	H3	K4
SUV39H1, SUV39H2, G9a, EuHMTase, SETDB1/ESET, RIZ1	H3	K9
DOT1	H3	K79

Methylation of lysine residues is known to occur on histone H3 Lys 4, Lys 9, Lys14, Lys 27, Lys 36 and Lys 79, and histone H4 Lys 20. Histone H3 Lys 4 methylation is a mark for transcriptionally active genes [69; Table 3]. There are usually three different states of H3 Lys 4 methylation. The mono- and di-methylated state is associated with both transcriptionally active and inactive genes, respectively, whereas the tri-methyated state occurs exclusively at transcriptionally active genes [70].

Studies of fission yeast mating type loci have shown that a large stretch of silent heterochromatin (20kb) that contains histones methylated at H3 Lys 9 but are devoid of H3 Lys 4 methylation. In contrast, the surrounding actively transcribed regions have H3 Lys 4 methylation but not H3 Lys 9. Removal of a boundary element results in the spreading of H3 Lys 9 methylation into the active domain, resulting in depletion of H3 Lys 4 methylation. This result suggests that methylation of H3 Lys 9 is associated with gene silencing, while methylation of H3 Lys 4 is associated with transcriptional activation [71-72].

The methylation of arginine residues is known to occur on histone H3 Arg 2, Arg 17 and Arg 26, and histone H4 Arg 26 [73-74]. Arginines can be either mono-methylated or di-methylated on the guanidino amine (or imine). The methylation of H3 Arg 17 has a positive influence on transcription [69].

5. HISTONE PHOSPHORYLATION

Histone phosphorylation is involved in transcriptional activation and chromatin condensation during mitosis. Histone phosphorylation occurs at serine, threonine and tyrosine residues. The

ratio of phosphorylation for serine, threonine, and tyrosine residues is approximately 1000:100:1, respectively [75].

The phosphorylation of histone H3 Ser 10 is conserved throughout eukaryotes and is crucial for chromosomal condensation and cell cycle progression during mitosis and meiosis [7]. In addition, it is important during interphase because H3 Ser10 phosphorylation enables an increase in gene transcription which is activated as a consequence of a variety of cell-signaling events [76]. It has been shown that histone H3 phosphorylation is necessary for the initiation of chromosome condensation in *Tetrahymena thermophila* [7] and in mammalian cells [77]. Furthermore, it has been observed that phosphorylation of histone H3 Ser 10 enhances gene expression after neuronal activation through the administration of agonists which activate dopaminergic, muscarinic acetylcholine, and ionotropic glutamate receptors in hippocampal neurons [78].

It has been shown that H3 Ser 28 phosphorylation occurred in chromosomes predominately during early mitosis and coincided with the initiation of mitotic chromosome condensation [79]. Furthermore, histone H3 phosphorylation at Ser 28, together with Ser 10 phosphorylation, is a conserved event and is likely to be involved in mitotic chromosome condensation. The phosphorylation of linker histones has also been related to mitotic chromosome condensation [80]. Cyclin-dependent kinases participate in cell cycle-dependent phosphorylation of linker histones [81]. Histone H2A from *Tetrahymena pyriformis* has been shown to be hyper-phosphorylated at its C-terminal tail [82], and this hyper-phosphorylation might be important for chromosome stability. H2A.X phosphorylation was shown to correlate with double stranded breakage [83].

6. HISTONE UBIQUITINATION

Ubiquitin is an 8.6-kDa, 76 amino acid protein that is highly conserved and is "ubiquitously" distributed throughout eukaryotes. It is a globular protein in which residues 1-72 are tightly folded and 73-76 are in a random coil configuration [84]. Ubiquitin is activated by an ATP-dependent reaction involving an ubiquitin activating enzyme, followed by its conjugation via a thioester bond to a cysteine residue in an ubiqutin-conjugating enzyme. In the final enzymatic step, ubiquitin is transferred from ubiqutin-conjugating enzyme to targeted lysine residue in a particular substrate protein by ubiquitin-protein isopeptide ligase [85].

Ubiquitination occurs on the ε-amino group of lysine residues of H2A, H2B, H3, H4, H2A.Z and H1 [8, 86-90]. The C-terminal glycine residue of ubiquitin protein can form an iso-peptide bond with the ε-amino group of lysine. Most of the ubiquitination occurs in the cytosol and is associated with proteolytic breakdown and degradation of proteins within proteosomes. Studies in *Drosophlia* and mammalian cells showed that the ubiquitinated forms of histones H2A and H2B are associated specifically with actively transcribed genes [91-92]. Histone H2A Lys 119 and H2B Lys 120 can be reversibly ubiquitinated within their C-terminal domains [93]. It has been shown that H2A and H2B are polyubiquitinated [87]. Although H2B is generally known to be mono-ubiquitinated at Lys 123, a recent study has shown that H2B can be poly-ubiquitinated at Lys 123 and it is dependent on the Rad6-Bre1 ubiquitination machinery [94].

Ubiquitination is a reversible histone modification like acetylation. In vertebrate cells, ubiquitinated histones have been found to be in a non-ubiquitinated state during the mitosis specifically. Deubiquitination may be accomplished by a family of ubiquitin–specific proteases [86-87, 95-97]. In *Saccharomyces cerevisiase,* the deubiquitinating enzyme Ubp3p interacts with

Sir4p, a protein involved in *MAT* silencing and heterochromatin formation [98]. In contrast, ubiquitinated histones are associated with transcriptionally active genes [91, 99]. Mono-ubiquitination of H2B is required for the optimal expression of two highly inducible yeast genes, *GAL1* and *SUC2* [99]. Furthermore, Ubp8p, a stable component of the SAGA complex, is capable of deubiquitinating H2B both *in vivo* and *in vitro*. Substitution of the histone H2B ubiquitination site or deletion of Ubp8p decreased transcription, suggesting that deubiquitination of H2B are required for optimal expression of *GAL1* [99].

7. HISTONE SUMOYLATION

Small ubiquitin related modifier (SUMO), a 100 amino acid poly-peptide is conserved in all eukaryotes and is a member of a growing family of ubiquitin like protein involved in post-translational modifications (sumoylation) which occur on lysine residues [100-101]. The three members of the SUMO family which include SUMO-1, SUMO-2 and SUMO-3 are found in mammals [102-103]. It has been shown that histone H4 is modified by SUMO both *in vivo* and *in vitro* - this process requiring two enzymes, SUMO-activating enzyme (E1) and SUMO-conjugating enzyme (E2). Histone H4 binds to SUMO-conjugating enzyme Ubc9, and can be sumoylated in an E1- and E2-dependent manner. Although the actual attachment sites have not been determined, it is believed that histone sumoylation mediates gene silencing through the recruitment of histone deacetylase and heterochromatin protein 1 **[**9].

It has been demonstrated that histone sumoylation occur at all four core histones in *S. cerevisiae.* Histone H2B Lys 6 and Lys 7, histone H4 Lys 5, Lys 8, Lys 12, Lys 16 and Lys 20, and histone H2A Lys 126 are targets for sumoylation. Sumoylation may also have a negative effect on gene

expression. It has been shown that the genes *GAL1*, *SUC2* and *TRP3* are negatively controlled by histone sumoylation [101]. It is believed that histone sumoylation may present in a dynamic interplay with histone acetylation and ubiquitination - as histone sumoylation may recruit HDACs to deacetylate neighboring sites [104].

8. HISTONE ADP-RIBOSYLATION

ADP-ribosylation is important in many physiological and pathological processes, including intercellular and intracellular signaling, transcription, DNA repair pathways, cell cycle regulation, mitosis, necrosis and apoptosis [10]. ADP-ribosylation involves the attachment of a homopolymer of ADP-ribose (ADPr) units to a specific protein. These polymers can vary in length and can form either linear or branched structures, or a combination of both linear and branched structures. Polymers differ in both size and complexity. The short and linear structures are referred to as oligo (ADP-ribosyl) homopolymers. The longer and branched structures are referred to as poly (ADP-ribosyl)(pADPr) homopolymers that contain as many as 200 units *in vitro* [105]. The addition of the ADPr units is catalyzed by poly (ADP-ribose) polymerase, which is a 113- kDa enzyme and appears to be ubiquitous throughout eukaryotes except for yeast [105-106].

In eukaryotes, histones are covalently modified by mono-ADPr. It has been shown that mono-ADP-ribosylation occurs at glutamate residues of H2A, arginine residues of H2A, H2B, H3, and H4, and the phosphate group of phosphoserine in histone H1, H2A, H2B, H3 and H4 [107-110]. Although all histones can be poly(ADP-ribosyl)ated, H1 and H2B are the main targets [111-113]. It has been shown that poly(ADP-ribosyl)ation can negatively regulate transcription.

Mouse lymphoma cells treated with DNA-damaging agents have lower RNA polymerase activity, suggesting a decrease in mRNA and rRNA synthesis [114]. Reduction of RNA synthesis can be prevented by 3-aminobenzamide, a specific inhibitor of poly(ADP-ribose) synthetase, indicating the negative effect of poly-(ADP-ribosyl)ation in transcription. The transcriptional activity of the p53 tumor suppressor protein has also been shown to be regulated by poly(ADP-ribosyl)ation *in vitro* and *in vivo*[111,115].

9. HISTONE BIOTINYLATION

Histone biotinylation occurs through covalent linkage of the vitamin, biotin, to histones. This covalent linkage is mediated by holocarboxylase synthetase and biotinidase [116-117]. Biotinidase belongs to the nitrilase superfamily [118] and promotes the process of biotinylation of histones through the hydrolytic cleavage of biocytin, followed by the transfer of the biotinyl residue to the free amine groups of histones [116].

The biotinylation of histones by holocarboxylase synthetase requires the presence of ATP and biotin [119]. Biotinylation of histones may play a role in diverse cellular processes including gene silencing [11], cell proliferation [119], DNA repair and apoptosis [11, 120]. Biotinylation sites have been identified within histones, such as histone H2A Lys 9, Lys 13, Lys 125, Lys 127 and Lys 129 [121], histone H3 Lys 4, Lys 9 and Lys 18 [122], and histone H4 Lys 8 and Lys 12 [123]. Biotinylation of histone H4 Lys 12 is a mark for repeat regions and heterochromatin. Furthermore biotinylation of histone H4 Lys 12 is co-localized with the repression marker of histone H3 Lys 9 di-methylation [120, 124]. As such, biotinylation of histone H4 Lys 12 may play a role in gene repression.

10. THE EPIGENETIC HISTONE CODE

The “histone code hypothesis” has been proposed in recent years and suggests that histone tail modifications constitute an epigenetic code to be read by other proteins. The epigenetic code occurs either sequentially or in combination as words in a language or symbols in a code. Consequently, the response to the histone code triggers downstream events resulting in a unique and specific biological outcome, such as gene expression, gene silencing, heterochromatin formation, DNA replication, and chromosome segregation.

It has been shown that yeast Gcn5p binds to histone H3 which is phosphorylated at Ser 10 by Snf1p kinase. Subsequently, H3 Lys 9 and Lys 14 are acetylated followed by *INO1* induction [76, 125-126]. Thus, phosphorylation of Ser 10 facilitates the sequential acetylation of histone H3 Lys 9 and Lys 14. Here, phosphorylation and acetylation are targeted to the same histone through coordinated patterns of histone modification and as such, this histone code leads to gene activation [126]. Also histone H3 Lys 4 methylation by an HKMT facilitates subsequent H3 and H4 acetylation through p300. Histone H3 Lys 9 methylation, however, inhibits acetylation events as it impairs subsequent Ser 10 phosphorylation which leads to the acetylation of histone H3 Lys 9 and Lys 14 [127-128]. The PRMT1-mediated histone H4 Arg 3 methylation is severely impaired by histone H4 acetylation, whereas histone H4 Lys 8 and histone H4 Lys 12 acetylation is elevated after methylation of histone H4 Arg 3 [129]. Moreover, histone H4 Lys 20 methylation and histone H4 Lys 16 acetylation were found to preclude each other [130]. In yeast Rad6-mediated histone H2B Lys 123 ubiquitination is required for subsequent histone H3 Lys 4 and Lys 79 methylation [131-132].

11. CONCLUSIONS

It is established that histone acetylation is associated with gene activation, and such a connection can be regulated by an upstream epigenetic histone code as described above. However, it is still unclear about the interplay between the epigenetic histone code and chromatin remodeling activity in the mechanism of gene activation. This is so, because it requires the detail of chromatin repositioning and the change of histone modification status. So far, relatively few genes have obtained detailed information as in the case of *CUP1* [52, 133], *PHO5* [134], *PHO8* [135], *HO* [136], and *INO1* [53]. These studies have demonstrated that different roles of histone acetylation in the mechanism of gene activation are possible. For example, histone acetylation is not required until the very late stage when TATA-binding protein binds to the TATA box in *CUP1* induction whereas a histone acetylase is recruited by the chromatin remodeler at an early stage in *PHO8* and *HO* induction. Clearly, histone acetylation is needed for gene activation at different stages. As such, a comprehensive analysis of histone modification status and nucleosome repositioning pattern at a defined time and in a precise context would be helpful to further understand the mechanism of gene expression.

ACKNOWLEDGEMENTS

We thank Mohammed Hassan Bhuiyan for critical reading of this chapter. This work was supported by an NSF Grant (MCB-0919218) and PSC-CUNY awards (62180-0040 and 64243-0042).

REFERENCES

[1] Kim, Y., McLaughlin, N., Lindstrom, K., Tsukiyama, T. & Clark, D. J. (2006). Activation of Saccharomyces cerevisiae HIS3 results in Gcn4p-dependent, SWI/SNF-dependent mobilization of nucleosomes over the entire gene. *Mol Cell Biol, 26,* 8607-8622.

[2] Smith, C. & Peterson, C. L. (2005). ATP-dependent chromatin remodeling. *Curr Top Dev, 65,* 115-148.

[3] Tsukiyama, T., Palmer, J., Landel, C.C., Shiloach, J. & Wu C. (1999). Characterization of the imitation switch subfamily of ATP-dependent chromatin-remodeling factors in Saccharomyces cerevisiae1. *Genes Dev, 13,* 686-697.

[4] Ogryzko, V. V., Schiltz, R. L., Russanova, V., Howard, B. H. & Nakatani, Y. (1996). The transcriptional coactivators p300 and CBP are histone acetyltransferases. *Cell, 87,* 953-959.

[5] Bjerling, P., Silverstein, R. A., Thon, G., Caudy, A.,Grewal, S. & Ekwall, K. (2002). Functional divergence between histone deacetylases in fission yeast by distinct cellular localization and in vivo specificity. *Mol Cell Biol, 22,* 2170-2181.

[6] O'Carroll, D., Scherthan, H., Peters, A. H., Opravil, S., Haynes, A. R., Laible, G., Rea, S., Schmid, M., Lebersorger, A., Jerratsch, M., Sattler, L., Mattei, M. G., Denny, P., Brown, S. D., Schweizer, D. & Jenuwein, T. (2000). Isolation and characterization of Suv39H2, a second histon H3 methyltransferase gene that displays testis-specific expression. *Mol Cell Biol, 20,* 9423-9433.

[7] Wei,Y., Mizzen, C. A., Cook, R. G., Gorovsky, M. A. & Allis, C. D. (1998). Phosphorylation of histone H3 at serine 10 is correlated with chromosome condensation during mitosis and meiosis. *Pro Natl Acad Sci U S A, 95,* 7180- 7484.

[8] Chen, H. Y., Sun, J. M., Zhang, Y., Davie, J. D. & Meistrch, M. L. (1998). Ubiquitination of Histone H3 in Elongating spermatids of Rat testes. *J Biol Chem, 273,* 13165-13169.

[9] Shiio, Y. & Eisenman, R. N. (2003). Histone sumoylation is as sociated with transcriptional repression. *Proc Natl Acad Sci, 10,* 13225-13230.

[10] Hassa, P. O., Haenni, S. S., Elser, M. & Hottiger, M. O. (2006). Nuclear ADP-Ribosylation reaction in mammalian cells: Where are we today and where are we going? *Microbiol Mol Biol Rev, 70,* 789-829.

[11] Peters, D. M., Griffin, J. B., Stanley, J. S., Beck, M. M. & Zempleni, J. (2002). Exposure to UV light causes increased biotinylation of histones in Jurkat cells. *Am J Physiol Cell Physiol, 283,* C878-C884.

[12] Marmorstein, R. (2001). Protein Modules that manipulate histone tails for chromatin regulation. *Nat Rev Mol Cell Biol, 2,* 422-431.

[13] Roth, S. Y., Denu, J. M. & Allis, C. D. (2001). Histone Acetyltransferases. *Annu Rev Biochem, 70,* 81-120.

[14] Utley, R. T., Ikeda, K., Grant, P. A., Cote, J., Steger, D. J., Eberharter, A., John, S. & Workman, J. L. (1998). Transcriptional activators direct histone acetyltransferase complexes to nucleosomes. *Nature, 98,* 498-502.

[15] Gu, W. & Roeder, R. G. (1997). Activation of p53 sequence-specific DNA binding by acetylation of the p53 C-terminal domain. *Cell, 90,* 595-606.

[16] Tachibana, M., Sugimoto, K., Fukushima, T. & Shinkai, Y. (2001). Set domain containing protein, G9a, is a novel lysine-preferring mammalian histone methyltransferase with hyperactivity and specific selectivity to lysines 9 and 27 of histone H3. *J Biol Chem, 276,* 25309-25317.

[17] Yang, X-J. (2004). The diverse super family of lysine acetyltransferases and their roles in leukemia and other diseases. *Nucleic Acid Res, 32,* 959-976.

[18] Peterson, C. L. & Laniel, M. C. (2004). Histones and histone modifications. *Curr Biol, 14,* R546- R551.

[19] Kelly, T. J., Qin, S., Gottschling, D. E. & Parthun, M. R. (2000). Type B histone acetyltransferase Hat1p participates in telomeric silencing. *Mol Cell Biol, 20,* 7051-7058.

[20] Yamamoto, T. & Horikoshi, M. (1997). Novel substrate specificity of the histone acetyltransferase activity of HIV-1-Tat interactive protein Tip60. *J Biol Chem, 272,* 30595-30598.

[21] Spencer, T. E., Jenster, G., Burcin, M. M., Allis, C. D., Zhou, J., Mizzen, C. A., McKenna, N. J., Onate, S. A., Tsai, S. Y., Tasai, M. J. & O'Maley, B. W. (1997). Steroid receptor coactivator-1 is a histone acetyltransferase. *Nature, 389,* 194-198.

[22] Mizzen, C. A., Yang, X. J., Kokubo, T., Brownell, J. E., Bannister, A. J., Owen-Hughes, T., Workman, J., Wang, L., Berger, S. L., Kouzarides, T., Nakatani, Y. & Allis, C. D. (1996). The TAF(II)250 subunits of TFIID has histone acetyltransferase activity. *Cell, 87,* 1261-1270.

[23] Clarke, A. S., Lowell, J. E., Jacobson, S. J. & Pilus, L. (1999). Esa1p is an essential histone acetyltransferase required for cell cycle progression. *Mol Cell Biol, 19,* 2515-2526.

[24] Chen, H., Lin, R. J., Schiltz, R. L., Chakravarti, D., Nash, A., Nagy, A., Nagy, L., Privalsky, M. L., Nakatani, Y. & Evans, R. M. (1997). Nuclear receptor coactivetor ACTR is a novel histone acetyltransferase and forms a multimeric activator compex with P/CAF and CBP/p300. *Cell, 90,* 569-580.

[25] Parthun, M. R. (2007). Hat1: the emerging cellular roles of a type B acetyltransferase. *Oncogene, 26,* 5319-5328.

[26] Brownell, J. E. & Allis, C. D. (1996). Special HATs for special occasions: linking histone acetylation to chromatin assembly and gene activation. *Curr Opin Genet Dev, 6,* 176-184.

[27] Poveda, A., Pamblanco, M., Rafrov, S., Tordera, V., Srernglanz, R. & Sendra, R. (2004). Hif1 is component of yeast histone acetyltransferacse b, a complex mainly localized in the nucleus. *J Biol Chem, 279,* 16033-16043.

[28] Brownell, J. E., Zhou, J., Ranalli, T., Kobayashi, R., Edmondson, D. G., Roth, S. Y. & Allis, C. D. (1996). *Tetrahymena* histone acetyltransferase A: a transcriptional co-activator linking gene expression to histone acetylation. *Cell, 84,* 843-851.

[29] Candau, R., Moore, P.A., Wang, L., Barlev, N., Ying, C. Y., Rosen, C. A. & Berger, S. L. (1996). Identification of human proteins functionally conserved with the yeast putative adaptors ADA2 and GCN5. *Mol Cel Biol, 16,* 593-602.

[30] Xu, W., Edmondson, D. G. & Roth, S. Y. (1998). Mammalian GCN5 and P/CAF acetyltransferases have homologous amino-terminal domain important for recognition of nucleosomal substrates. *Mol Cell Biol, 18,* 5659-5669.

[31] Smith, E. R., Belote, J. M., Schiltz, R. L., Yang, X. J., Moore, P. A., Berger, S. L., Nakatani, Y. & Allis, C. D. (1998). Cloning of Drosophila GCN5: conserved features among metazoan GCN5 family members. *Nucleic Acids Res, 26,* 2948-2954.

[32] Sterner, D. E. & Berger, S. L. (2000). Acetylation of Histones and Transcription-Related Factors. *Microbio Mole Biol Rev, 64,* 435-459.

[33] Kuo, M.-H., Broenell, J. E. Sobel, R. E., Ranalli, T. A., Cook, R. G., Edmonoson, D. G., Roth, S. Y. & Allis, C. D. (1996). GCN5p, a yeast nuclear histone acetyltransferase, acetylates specific lysine in histone H3 and H4 that differ from deposition-related acetylation sites. *Nature, 383,* 269-272.

[34] Kreb, J. E., Fry, C. J., Samuels, M. L. & Peterson, C. L. (2000). Global role for chromatin remodeling enzymes in mitotic gene expression. *Cell, 102,* 587-598.

[35] Wenzheng Zhang, W., Bone, J. R., Edmondson, D. G., Turner, B. M. & Roth, S. Y. (1998). Essential and redundant functions of histone acetylation revealed by mutation of target lysines and loss of the Gcn5p acetyltransferase. *EMBO J, 17,* 3155-3167.

[36] Schiltz, R. L., Mizzen, C. A., Vassilev, A., Cook, C. D., Allis, C. D. & Nakatani, Y. (1999). Overlapping but distinc patterns of histone acetylation by the human coactivators p300 and PCAF within nucleosomal substrates. *J Biol Chem, 274,* 1189-1192.

[37] Carrozza, M. J., Utley, R. T., Workman, J. L. & Cote, J. (2003). The diverse functions of histone acetyltransferase complexes. *Trends Genet, 19,* 321-329.

[38] Xu, L., Lavinsky, R. M., Dasen, J. S., Flynn, S. E., McInerney, E. M., Mullen, T. M., Heinzel, T., Szeto, D., Koruzus, E., Kurokawa, R., Aggarwal, A. K., Rose, D. W., Glass, C. K. & Rosenfeld, M. G. (1998). Singal-specific co-activator domain requirements for Pit-1 activation. *Nature, 395,* 301-306.

[39] Smith, E. R., Eisen, A., Gu, W., Sattah, M. Pannuti, A., Zhou, R. G., Cook, J. C., Lucchesi, J. C. & Allis, C. D (1998). ESA1 is a histone acetyltrasferase that is essential for growth in yeast. *Proc Natl Sci USA, 95,* 3561-3565.

[40] Clarke, A. S., Lowell, J. E., Jacobson, S. J. & Pillus, L. (1999). Esa 1p is an essencial histone acetyltransferase required for cell cycle progression. *Mol Cell Biol, 19,* 2515-2526.

[41] Kwok R. P, Lundblad, J. R., Chrivia, J. C., Richards, J. P., Bachinger, H. P., Brennan, R. G., Roberts, S. G., Green, M. R. & Goodman, R. H. (1994). Nuclear protein CBP is a coactivator for the transcription factor CREB. *Nature, 370,* 223-226.

[42] Janknecht, R. & Hunter, T. (1996). Transcription. A growing coactivator network. *Nature*, 383, 22-23.

[43] Shikama N., Lyon, J. & La Thangue, N. B. (1997). The p300/CBP family: integrating signals with transcription factors and chromatin. *Trends Cell Biol, 7,* 230-236.

[44] Giles, R. H., Peter, D. J. & Breuning, M. H. (1998). Conjugation dysfunction:CBP/p300 in human disease. *Trends Genet, 14,* 178-183.

[45] Muraoka, M., Konishi, M., Kikuchi-Yanoshita, R., Tanaka, K., Shitara, N., Chong, J. M., Iwama, T. & Miyaki, M., (1996). p300 gene alterations in colorectal and gastric carcinomas. *Oncogene, 12,* 1565-1569.

[46] Kleff, S., Andrulis, E. D., Anderson, C. W. & Sternglanz, R. (1995). Identification of a gene encoding a yeast histone H4 acetyltransferase. *J Biol Chem, 270,* 24674-24677.

[47] Parthun, M. R., Widmon, J. & Gottschling, D. E., (1996). The Major Cytoplasmic Histone Acetyltransferase in Yeast: Links to Chromatin Replication and Histone Metabolism. *Cell, 87,* 85-94.

[48] Quana, A. S., Buschbeck, M. & Croce, L. Di. (2006). Chromatin structure and epigenetics. *Biochemical Pharmacology, 72,* 1563-1569.

[49] Lancher, M., O' Sulliva, R. J. & Jenuwein, T. (2003). An epigenetic road map for histone lysine methylation. *J Cell Sci, 116,* 2117-2124.

[50] Gottesfeld, J. M. & Forbes, D. J., (1997). Mitotic repression of the transcriptional machinery. *Trends Biochem Sci, 22,* 197-202.

[51] Vaissiere, T., Sawan, C. & Herceg, Z. (2008). Epigenetic interplay between histone modifications and DNA methylation in gene silencing. *Mutation Research, 659,* 40-48.

[52] Shen, C-H.,Leblanc, B. P., Neal, C., Akhaven, R. & Clark, D. J. (2002). Targeted histone acetylation at the yeast *CUP 1* promoter requires the transcriptional activator, the TATA boxes, and the putative histone acetylase encoded by *SPT10*. *Mol Cell Biol, 22,* 6406-6416.

[53] Esposito, M., Konarzewska, P., Odeyale, O. & Shen, C-H. (2010). Gene-wide histone acetylation at yeast *INO1* requires the transcriptional activator Ino2p. *Biochem Biophys Res Commun, 391,* 1285-1290.

[54] Jacobson, R. H., Ladumer, A. G., King, D. S. & Tjian, R. (2000). Structure and function of a human TAFII250 double bromodomain module. *Science, 288,* 1422-1425.

[55] Hubbert, C., Guardiola, A., Shao, R., Kawaguchi, Y., Ito, A., Nixon, A., Yoshida, M., Wang, X. F. & Yao, T. P. (2002). HDAC6 is a microtubule-associated deacetylase. *Nature, 417,* 455-458.

[56] Sengupta, N. & Seto, E., (2004). Regulation of histone deacetylase activities. *J Cell Biochem, 93,* 57-67.

[57] Longworth, M. S. & Laimins, L. A. (2006). Histone deacetylase 3 localizes to the plasma membrane and is a substrate of Src. *Oncogene, 25,* 4495-500.

[58] de Ruijter, A. J. M., van Gennip, A. H., Caron, H. N., Kemp, S. & van Kuilenburg, A. B. P. (2003). Histone deacetylases (HDACs): characterization of the classical HDAC family. *Biochem J, 370,* 737-749.

[59] Fischle, W., Dequiedt, F., Hendezel, M. J.,Guenther, M. G., Lazar, M. A., Voelter, W. & Verdin, E. (2002). Enzymatic activity associated with class II HDACs is dependent on a multiprotein complex containing HDAC3 and SMRT/N-CoR. *Mol Cell, 9,* 45-57.

[60] Gao, L., Cueto, M. A., Asselbergs, F. & Atadja, P. (2002). Cloning and functional characterization of HDAC11, a novel member of the human histone deacetylase family. *J Biol Chem, 277,* 25748-25755.

[61] Yang, L., Xia, L., Wu, D. Y., Wang, H., Chansky, H. A., Schubach, W. H., Hickstein, D. D. & Zhang, Y. (2002). Molecular cloning of ESET, a novel histone H3 specific methyltransferase that interacts with ERG transcription factor. *J Biol Chem, 277,* 148-152.

[62] Cheng, X., Collins, R. E. & Zhang, X. (2005). Structural and sequence motifs of protein (histone) methylation enzymes. *Annu Rev Biophys Biomol Struct, 34,* 267-294.

[63] Dillon, S. C., Zhang, X., Trievel, R. C. & Cheng, X. (2005). The SET-domain protein superfamily: protein lysine methyltransferases. *Genome Biol, 6,* 227.

[64] Qian, C. & Zhou, M. M. (2006). SET domain protein lysine methyltransferases: structure, specificity and catalysis. *Cell Mol Life Sci, 63,* 2755-2763.

[65] Couture, J. F. & Trievel, R. C. (2006). Histone-modifying enzymes: encrypting an enigmatic epigenetic code. *Curr Opin Struct Biol, 16,* 753-760.

[66] Cheng, X. & Zhang, X. (2007). Structural dynamics of protein lysine methylation and demethylation. *Mutat Res, 618,* 102-115.

[67] Volkel, P. & Angrand, P. O. (2007). The control of histone lysine methylation in epigenetic regulation. *Biochimie, 89,* 1-20.

[68] Upadhyay, A. K. & Cheng, X. (2011). Dynamics of Histone Lysine Methylation: Structures of Methyl Writers and Eraser. *Prog Drug Res, 67,* 107-124.

[69] Noma, K. I., Allis, C. D. & Grewal, S. I. S. (2001). Transitions in distinct histone H3 methylation patterns are the heterochromatin domain boundaries. *Science, 293,* 1150-1155.

[70] Santos-Rosa, H., Schneider, R., Bannister, A. J., Sherriff, J., Bernstein, B. E., Emre, N. C., Schreiber, S. L., Mellor, J. & Kouzarides, T. (2002). Active genes are tri-methylated at K4 of histone H3. *Nature, 419,* 407-411.

[71] Stec, I., Wright, T. J., van Ommen, G. J., de Boer, P. A., van Haeringen, A., Moorman, A. F., Altherr, M. R. & den Dunnen, J. T. (1998). WHSC1, a 90kb SET domain-containing gene, expressed in early development and homologous Drosophila dysmorphy gene maps in the Wolf-Hirschhorn syndrome critical region and is fused to IgH in t(4;14) multiple myeloma. *Hum Mol Genet, 7,* 1071-1082.

[72] Kouzarides, T. (2002). Histone methylation in transcriptional control. *Curr Opin Gene Devel, 12,* 198-208.

[73] McBrige, A. E. & Silver, P. A. (2001). State of the Arg: protein methylation at arginine comes of age. *Cell, 106,* 5-8.

[74] He, H. & Lehming, N. (2003). Global effect of histone modifications. *Briefings in functional genomics and proteomics, 2,* 234-243.

[75] Dieker, J. & Muller, S. (2010). Epigenetic histone code and Autoimmunity. *Clinic Rev Allerg Immunol, 39,* 78-84.

[76] Nowak, S. J. & Corces, V. G. (2004). Phosphorylation of histone H3: balancing act between chromosome condensation and transcriptional activation. *Trends Genet, 20,* 214-220.

[77] Van Hooser, A., Goodrich, D. W., Allis, C. D. & Brinkley, B. R. (1998). Histone H3 phosphorylation is required for the initiation, nut not maintenance, of mammalian chromosome condensation. *J Cell Sci, 111,* 3497-3506.

[78] Crosio, C., Heitz, E., Allis, C. D., Borelli, E. & Sassone-Corsi, P. (2003). Chromosome remodeling and neuronal response: multiple signaling pathways induce specific histone H3 modifications and early gene expression in hippocampal neurons. *J Cell Sci, 116,* 4905-4914.

[79] Goto, H., Tomono, Y., Ajiro, K., Kosako, H., Fujita, M., Sakurai, M., Okawa, K., Iwamatsu, A., Okigaki, T., Takahashi, T. & Inagaki, M. (1999). Identification of a novel phosphorylation site on histone H3 coupled with mitotic chromosome condensation. *J Biol Chem, 274,* 25543-25549.

[80] Bradbury, E. M. (1992). Reversible histone modifications and the chromosome cell cycle. *Bioessays, 14,* 9-16.

[81] Davie, J. R. & Chadee, D. N. (1998). Regulation and regulatory parameters of histone modifications. *J Cell Biochem, 30,* 203-213.

[82] Fusauchi, Y. & Iwai, K. (1984). Tetrahymena histone H2A. acetylation in the N-terminal sequence and phosphorelation in the C-terminal sequence. *J Biochem, 95,* 147-154.

[83] Hunter, N. & Borner, G. V. (2001). Gamma-H2AX illuminates meiosis. *Nat Genet, 27,* 236-238.

[84] Vijay-Kumar, S., Bugg, C. E., Wilkinson, K. D., Vierstra, R. D., Hatfeild, P. M. & Cook, W. J. (1987). Comparison of three dimensional structures of human, yeast, and oat ubiquitin. *J Biol Chem, 262,* 6396-6399.

[85] Weake, V. M. & Workman, J. L. (2008). Histone ubiquitination: Triggering gene activity. *Mol Cell, 29,* 653-663.

[86] Muller, R., Yasuda, H., Hatch, C., Bonner, W. & Bradbury, E. (1985). Identification of ubiquitinqted histones 2A and 2B in physarum polycephalum. Disappearance of these proteins at metaphase and reappearance at anaphase. *J. Biol Chem, 26,* 5147-5153.

[87] Nickel, B. E., Roth, S. Y., Cook, R. G., Allis, C. D. & Davie, J. R. (1987). Changes in the histone H2A variant H2A.Z and polyubiquitinated histone species in developing trout testis. *Biochemistry, 26,* 4417-4421.

[88] Robzyk, K., Recht, J. & Osley, M. A. (2000). Rad6-dependent ubiquitination of histone H2B in yeast. *Science, 287,* 501-504.

[89] Murantani, M. & Tansey, W. P. (2003). How the ubiquitin-proteasome system controls transcription. *Nat Rev Mol Cell Biol, 3,* 192-201.

[90] Kanda, F., Sykes, D. E., Yasuda, H., Sandberg, A. A. & Matsui, S. (1986). Substrate recognition of isopeptidase: specific cleavage of the epsilon-(alpha-glycyl)lysine linkage in ubiquitin-protein conjugates. *Biochim Biophys Acta, 870,* 64-75.

[91] Levinger, L. & Varshavsky, A. (1982). Selective arrangement of ubiquitinated and D1 protein-containing nucleosomes within the *Drosophila* genome. *Cell, 28,* 375-385.

[92] Huang, S. Y., Barnard, M. B., Xu, M., Matsui, S., Rose, S. M. & Garrard, W. T. (1986). The active immunoglobulin kappa chain gene is packaged by non-ubiquitin-conjugated nucleosomes. *Proc Natl Acad Sci USA, 83,* 3738-3742.

[93] Goldknopf, I. L. & Busch, H. (1977). Isopeptide linkage between non-histone and histone 2A polypeptides of chromosomal conjugated-protein A24. *Proc Natl Acad Sci U S A, 74,* 864-868.

[94] Geng, F. & Tansey, W. P. (2008). Polyubiquitylation of histone H2B. *Mol Biol Cell, 9,* 3616-3624.

[95] Kao, C.-F. & Osely, M. A. (2003). In vivo assays to study histone ubiquitylation. *Methods, 31,* 59-66.

[96] Cai, S. Y., Babbit, R. W. & Marchesi, V. T. (1999). A mutant deubiquitinating enzyme (Ubp-M) associates with mitotic chromosomes and blocks cell division. *Proc Natl Acad Sci USA, 96,* 2828-2833.

[97] Kerscher, O., Felberbaum, R. & Hochstrasser, M. (2006). Modification of protein by ubiquitin and ubiquitin like protein. *Annu Rev Cell Dev Biol, 22,* 159-180.

[98] Moazed, D. & Johnson, A. D. (1996). A deubiquitinating enzyme interacts with SIR4 and regulates silencing in S. cerevisiae. *Cell, 86,* 667-677.

[99] Henry, K. W., Wyce, A., Lo, W-S., Duggan, L. J., N.C. Tolga Emre, N. C. T., Kao, C-F., Pillus, L., Shilatifard, A., Osley, M. A. & Berger, S. L. (2003). Transcriptional activation via sequential histone H2B ubiquitylation and deubiquitylation, mediated by SAGA-associated Ubp8. *Genes Dev, 17,* 2648-2663.

[100] Johnson, E. S. & Gupta, A. A. (2001). An E3- like factor that promotes SUMO conjugation to the yeast septins. *Cell, 106,* 735-744.

[101] Nathan, D., Ingvarsdottir, K. & Sterner, D. E. (2006). Histone sumoylation is a negative regulator in *Saccharomyces cerevisiae* and shows dynamic interplay with positive-acting histone modifications. *Genes & Dev, 20,* 966-976.

[102] Picher, A., Knipscheer, P., Saithh, H., Sixma, T. K. & Melchior, F. (2004). The RanBP2 SUMO E3 ligase is neither HECT- nor RING-type. *Nature Stru Mole Biol, 11,* 984- 991.

[103] Tatham, M. H., Jaffray, E., Vaughan, O. A., Desterro, J. M. & Botting, C. H. (2001). Polmeric chains of SUMO-2 and SUMO-3 are conjugated to protein substrates by SAE1/SAE2 and Ubc9. *J Biol Chem, 276,* 35368-35374.

[104] Yang, S.-H. & Sharrocks, A. D. (2004). SUMO promotes HDAC-mediated transcriptional repression. *Mol Cell, 13,* 611-617.

[105] Diefenbach, J. & Burkle, A. (2005). Introduction to poly (ADP-ribose) metabolism. *Cell Mol Life Sci, 62,* 721-730.

[106] Burkle, A., (2005). Poly (ADP-ribose) The most elaborate metabolic of NAD+. *FEBS J, 18,* 4576-4589.

[107] Golderer, G. & Grobner, P. (1991). ADP-ribosylation of core histones and their acetylated subspecies. *Biochem J, 277,* 607-610.

[108] Ord, M. G. & Stocken, L. A. (1977). Adenosine diphosphate ribosylated histones. *Biochem J, 161,* 583-592.

[109] Smith, J. A. & Stoken, L. A. (1975). Chemical and metabolic properties of adenosine diphosphate ribose derivatives of nuclear proteins. *Biochem J, 147,* 523-529.

[110] Tanigawa, Y., Tsuchiya, M., Imai, Y. & Shimoyama, M. (1984). ADP-ribosyltransferase from hen liver nuclei. Purification and characterization. *J Biol Chem, 259,* 2022-2029.

[111] D' Amours, D., Desnoyers, S., D' Silva, I. & Poirier, G. G. (1999). Poly (ADP-ribosyl) ation reactons in the regulation of nuclear functions. *Biochem J, 342,* 249-268.

[112] Malanga, M., Atorino, L., Tramontano, F., Farina, B. & Quesada, P. (1998). Poly (ADP-ribose) binding properties of histone H1 variants. *Biochem Biophys Acta, 1399,* 154-160.

[113] Ausio, J., Abbott, D. W., Wang, X. & Moore, S. C. (2001). Histone variants and histone modifications: a structural perspective. *Biochem Cell Bio, 79,* 693-708.

[114] Taniguchi, T., Aggmori, M., Kameshita, I., Nishikimi, M. & Shiznta, Y.(1982). Participation of poly(ADP-ribosyl)ation in the depression of RNA synthesis caused by treatment of mouse lymphoma cells with methylnitrosourea. *J Biol Chem, 257,* 4027-4030.

[115] Wang, X., Ohnoshi, K., Takahashi, A. & Ohnishi, T. (1998). Poly(ADP-ribosyl)ation is required for p53-dependent signal transduction induced by radiation. *Oncogene, 17,* 2819-2825.

[116] Narang, M. A., Dumas, R., Ayer, L. M. & Gravel, R. A. (2004). Reduced histone biotinylation in multiple carboxylase deficiency patients: a nuclear role for holocarboxylase synthetase. *Hum Mol Genet, 13,* 15-23.

[117] Camporeale, G.,Giordano, E., Rendina, R., Zempleni, J. & Eisseenberg, J. C. (2006). Drosophila holocarboxylase synthetase is a chromosomal protein required for normal histone biotinylation, gene transxription patterns, lifespan and heat toleance. *J Nutr, 136,* 2735-2742.

[118] Brenner, C. (2002). Catalysis in the nitrilase superfamily. *Curr Opin Struct Biol*, *12*, 775- 782.

[119] Zempleni, J. (2005). Uptake, localization and noncarboxylase role of biotin, *Annu Rev Nutr, 25,* 175-195.

[120] Kothapalli, N., Sarath, G. & Zempleni, J. (2005). Biotinylation of K12 in histone H4 decreases in response to DNA double-strand breaks in human JAr choriocarcinoma cells. *J Nutr, 135,* 2337-2342.

[121] Chew, Y. C., Camoreale, G., Kothapalli, N., Sarath, G. & Zempleni, J. (2006). Lysine residues in N-and C-terminal regions of human histone H2Aare targets for biotinylation by biotinidase. *J Nutr Biochem, 17,* 225-233.

[122] Kobaza, K., Comporeale, G., Rueckert, B., Kuch, A., Griffin, J. B., Sarath, G. & Zempleni, J. (2005). K4, K9 and K18 in human histone H3 are targets or biotinylation by biotinidase. *FEBS J, 272,* 4249-4259.

[123] Camporeale, G., Shubert, E. E., Sarath, G., Cerny, R. & Zempleni, J. (2004). K8 and K12 are biotinylated in human histone H4. *Eur J Biochem, 271,* 2257-2263.

[124] Camporeale, G., Oommen, A. M., Griffin, J. B., Sarath, G., Zempleni, J. (2007). K12-biotinylated histone H4 marks heterochromatin in human lymphoblastoma cells. *J Nutr Biochem, 18,* 760-768.

[125] Lo, W. S., Trievel, R. C., Rojas, J. R., Duggan, L., Hsu, J.-Y., Allis, C. D., Marmorsten, R. & Berger, S. L. (2000). Phosphorylation of serine 10 in histone H3 is functionally linked *in vitro* and *in vivo* to Ggcn5-mediated acetylation at lysine 14. *Mol Cell, 5,* 917-926.

[126] Lo, W. S., Duggan, L., Emre, T. N. C., Lane, Belotserkovsky, R., Lane, W. S., Shiekhsttar, R. & Berger, S. L. (2001). Snf1- a histone kinase that works in concert with the histone acetyltransferase Gcn5 to regulate transcription. *Science, 293,* 1142-1146.

[127] Wang, H. Cao, R., Xia, L., Erdjument-Bromzge, H., Borchres, C., Tempst, P. & Zhang, Y. (2001). Purification and Functional Characterization of a Histone H3-Lysine 4-Specific Methyltransferase . *Mol Cell, 8,* 1207-1217.

[128] Rea, S., Eisenhaber, F., O'Carrol, D., Strahl, B. D., Sun, Z. W., Schmid, M., Opravil, S., Mechtler, K., Ponting, C. P., Allis, C. D. & Jenuwein, T. (2000). Regulation of chromatin structure by site-specific histone H3 methyltransferases. *Nature, 406,* 593-599.

[129] Wang, H., Huang, Z. Q., Xia, L., Feng, Q., Erdjument-Bromzge, H., Strahl, B. D., Briggs, S. D., Allis, C. D., Wong, J., Tempst, P. & Zhang, Y.(2001). Methylationof histone H4 at arginine 3 facilitating transcriptional activation by nuclear hormone receptor. *Science, 298,* 853-857.

[130] Nishioka, K., Rice, J. C., Sarma, K., Erdjument-Bromzge, H., Werner, J., Wang, Y., Chuikov, S., Valenzuela, P., Tempst, P., Steward, R., Lis, J. T., Allis, C. D. & Reinberg, D. (2002). PR-Set7 is a nucleosome-specific methyltransferase that modifies lysine 20 of histone H4 and is associated with silent chromatin. *Mol Cell, 9,* 1201-1213.

[131] Margueron, R., Trojer, P. & Reinberg, D. (2005). The key to development: interpreting the histone code? *Curr Opin Genet Dev, 15,* 163-176.

[132] Ng, H. H., Xu, R. M., Zang, Y. & Struhl, K. (2002). Ubiquitination of histone H2B by Rad6 is required for Dot1-medated methylation of histone H3 lysine 79. *J Biol Chem, 277,* 34655-34657.

[133] Shen, C-H., Leblance, B. P., Alfieri, J.A. & Clark, D. J. (2001). Remodeling of yeast *CUP1* chromatin involves activator-dependent repositioning of nucleosomes over the entire gene and flanking sequences. *Mol Cell Biol, 21,* 534-547.

[134] Svaren, J. & Ho rs, W.(1997). Transcription factor vs. nucleosomes: regulation of the *PHO5* promoter in yeast. *Trends Biochem Sci, 22,* 93-97.

[135] Reinke, H., Gregory, P. D. & Horz, W. (2001). A transient histone hyper-acetylation signal marks nucleosomes for remodeling at the *PHO8* promoter *in vivo*. *Mol Cell*, *7,* 529-538.

[136] Cosma, M. P., Tanaka, T. & Nasmyth, K. (1999). Ordered recruitment of transcription and chromatin remodeling factors to a cell cycle-and developmentally regulated promoter. *Cell*, *97,* 299-311.

References

1. Adam, V., Krizkova, S., Fabrik, I.,et al. (2007) Metallothionein as a new potential tumor marker. *Tumor. Biol. 28,* 43- 43.
2. Alberts, B., Bray D., Lewis J., Raff M., Roberts K. & Watson J.D. (1989) Molecular Biology of the Cell (2nd edition), Ed. Adams R.,Garland Publishing, Inc. New York & London, 1219.
3. Amiard, J. C. Amiard-Triquet, C., Barka, S., Pellerin, J. & Rainbow, P. S. (2006) Metallothioneins in aquatic invertebrates: their role in metal detoxification and their use as biomarkers. *Aquat. Toxicol. 76,* 160-202.
4. Bao, Y. & Shen, X. (2007) INO80 subfamily of chromatin remodeling complexes. *Mutat. Res. 618,* 18-29.
5. Biswas, D., Takahata, S., Xin, H., Dutta-Biswas, R., Yu, Y., Formosa, T., Stillman, D. J. (2008) A Role for Chd1 and Set2 in Negatively Regulating DNA Replication in *Saccharomyces cerevisiae. Genetics 178*(2),649-659.
6. Bjerling, P., Silverstein, R. A., Thon, G., Caudy, A.,Grewal, S. & Ekwall, K. (2002) Functional divergence between histone deacetylases in fission yeast by distinct cellular localization and in vivo specificity. *Mol. Cell. Biol. 22,* 2170-2181.
7. Brown, D. T. (2001) Histone variants: are they functionally heterogeneous? *Genome Biol*. *2*(7), 0006.1-0006.6.
8. Brownell, J. E. & Allis, C. D. (1996). Special HATs for special occasions: linking histone acetylation to chromatin assembly and gene activation. *Curr Opin Genet Dev, 6,* 176-184.

9. Brownell, J. E., Zhou, J., Ranalli, T., Kobayashi, R., Edmondson, D. G., Roth, S. Y. & Allis, C. D. (1996). *Tetrahymena* histone acetyltransferase A: a transcriptional co-activator linking gene expression to histone acetylation. *Cell, 84,* 843-851.
10. Buchman, C., Skroch, P., Welch, J., Fogel, S. & Karin, M (1989) The *CUP2* gene product, regulator of yeast metallothionein expression, is a copper-activated DNA-binding protein. *Mol Cell Biol*. *9*(9), 4091–4095.
11. Butt, T. R., Sternberg, E. J., Gorman, J. A., Clark, P., Hamer, D., Rosenberg, M. & Crooke, S. T. (1984) Copper metallothionein of yeast, structure of the gene, and regulation of expression. *Proc. Natl. Acad. Sci*. USA. *81,* 3332- 3336.
12. Butt, T. R., Sternberg, E., Herd, J. & Crooke, S. T. (1984) Cloning and expression of a yeast copper metallothionein gene. *Gene. 27*(1), 23-33.
13. Cairn, B.R., Lorch, Y., Li, Y., Zhang, M., Lacomis, L., Erdjument- Bromage, H., Tempst, P., Du, J., Laurent, B.C. & Komberg, R. D. (1996) RSC, an essential, abundant chromatin-remodeling complex. *Cell. 87*(7), 1249-1260.
14. Cairns, B.R., Erdjument-Bromage, H., Tempst, P., Winston, F. & Komberg, R. D. (1998) Two actin-related proteins are shared functional components of the chromatin-remodeling complexes RSC and SWI/SNF. *Mol. Cell*. *2*(5), 639.
15. Candau, R., Moore, P.A., Wang, L., Barlev, N., Ying, C. Y., Rosen, C. A. & Berger, S. L. (1996). Identification of human proteins functionally conserved with the yeast putative adaptors ADA2 and GCN5. *Mol Cel Biol, 16,* 593-602.
16. Clarke, A. S., Lowell, J. E., Jacobson, S. J. & Pilus, L. (1999). Esa1p is an essential histone acetyltransferase required for cell cycle progression. *Mol Cell Biol, 19,* 2515-2526.

17. Cosma, M. P., Tanaka, T. & Nasmyth, K. (1999). Ordered recruitment of transcription and chromatin remodeling factors to a cell cycle-and developmentally regulated promoter. *Cell, 97*, 299-311.
18. Cuperus, G. & Shore, D. (2002) Restoration of silencing in Saccharomyces cerevisiae by tethering of a novel Sir2- interacting protein, Esc8. *Genetics. 162*(2),633-645.
19. de Ruijter, A. J. M., van Gennip, A. H., Caron, H. N., Kemp, S. & van Kuilenburg, A. B. P. (2003) Histone deacetylases (HDACs): characterization of the classical HDAC family. *Biochem. J. 370*, 737-749.
20. Du, J., Nasir, I., Benton, B. K., Kladde, M.P. & Laurent, B.C., (1998) Sth1p, a Saccharomyces cerevisiae Snf2p/Swi2p homolog, is an essential ATPase in RSC and differs from Snf/Swi in its interactions with histones and chromatin-associated proteins. *Genetics. 150*(3), 987-1005.
21. Ebbert, R., Birkmann, A. & Schuller, H. J. (1999) The product of the SNF2/SWI2 paralogue INO80 of *Saccharomyces cerevisiae* required for efficient expression of various yeast structural genes is part of a high-molecular-weight protein complex. *Mol. Microbiol. 32*, 741-751.
22. Egli, D., Domenech, J., Selvaraj, A., Balamurugan, K., Hua, H., Capdevila, M., et al. (2006) The four members of the Drosophola metallothionein family exhibit distinct yet overlapping roles in heavy metals homeostasis and detoxification. *Genes Cell 11*, 647-658.
23. Elfring, L. K., Deuring, R., McCallum, C. M., Peterson, C. L. & Tamkun, J. W. (1994) Identification and characterization and of Drosophila relatives of the yeast transcriptional activator SNF2/SWI2. *Mol. Cell. Biol. 14*, 2225-2234.

24. Esposito, M., Konarzewska, P., Odeyale, O. & Shen, C-H. (2010). Gene-wide histone acetylation at yeast *INO1* requires the transcriptional activator Ino2p. *Biochem Biophys Res Commun, 391,* 1285-1290.
25. Fischle, W., Dequiedt, F., Hendezel, M. J.,Guenther, M. G., Lazar, M. A., Voelter, W. & Verdin, E. (2002) Enzymatic activity associated with class II HDACs is dependent on a multiprotein complex containing HDAC3 and SMRT/N-CoR. *Mol. Cell* 9, 45-57.
26. Fogel, S. & Welch, J. W. (1982) Tandem gene amplification mediates copper resistance in yeast. *Proc. Natl. Acad. Sci.* USA. 79, 5342-5346.
27. Ford, J., Odeyale, O, Eskandar, A., Kouba, N. & Shen, C-H., (2007) A SWI/SNF- and INO80-dependent nucleosome movement at the *INO1* promoter. *Biochem Biophys Res Commun. 361*, 974-979.
28. Ford, J., Odeyale, O. & Shen, C-H (2008) Activator-dependent recruitment of SWI/SNF and INO80 during *INO1* activation. *Biochem Biophys Res Commun. 373*, 602-626.
29. Fürst, P. & Hamer, D. (1989) Cooperative activation of a eukaryotic transcription factor: interaction between Cu(I) and yeast ACE1 protein. Proc. Natl. Acad. Sci. U S A. *6*(14), 5267–5271.
30. Galizia, G., Ferraraccio, F., Lieto, E., Orditura, M., Castellano, P., Imperatore, V., La Manna, G., Pinto, M., Ciardiello, F., La Mura A. & De Vita, F. (2006) p27 downregulation and metallothionein overexpression in gastric cancer patients are associated with a poor survival rate. *J. Surg. Oncol*. *93*(3), 241-252.
31. Ganggaraju, V. K. & Bartholomew, B. (2007) Mechanisms of ATP Dependent Chromatin Remodeling. *Mutat. Res.618*, 3-17.

32. Gao, L., Cueto, M. A., Asselbergs, F. & Atadja, P. (2002) Cloning and functional characterization of HDAC11, a novel member of the human histone deacetylase family. *J. Biol. Chem. 277*, 25748-25755.
33. Gelbart, M. E., Rechsteiner, T., Richmond, T. J. & Tsukiyama, T. (2001) Interactions of Isw2 chromatin remodeling complex with nucleosomal arrays: analyses using recombinant yeast histones and immobilized templates. *Mol. Cell. Biol. 21*(6), 2098-2106.
34. Georgakopoulos, T. & Thireos, G. (1992) Two distinct yeast transcriptional activators require the function of the GCN5 protein to promote normal levels of transcription. *EMBO J. 11*, 4145–4152.
35. Graziano, V., Gerchman, S. E., Schneider, D. K. & Ramakrishnan, V.(1994). Histone H1 is located in the interior of the chromatin 30-nm filament. *Nature 368*, 351–354.
36. Grune, T., Brzeski, J., Eberhatwr, A., Clapier, C.R., Becker, P. B. & Muller, C.W. (2003) Crystal structure and functional analysis of a nucleosome recognition module of the remodeling factor ISWI. *Mol.Cell. 12*(2), 449-460.
37. Gu, W. & Roeder, R. G. (1997). Activation of p53 sequence-specific DNA binding by acetylation of the p53 C-terminal domain. *Cell, 90*, 595-606.
38. Hawthorne, D.C. & Mortimer, R.K. (1960) Chromosome Mapping in Sacchromyces: Centromere- Linked Genes. *Genetics. 45*(8),1085-1110.

39. Hottiger, T., Kuhla, J., Pohlig, G., Furst, P., Spielmann, A., Garn, M., Haemmerli, S. & Heim, J. (1995) 2-μm vectors containing the *Saccharomyces cerevisiae* metallothionein gene as a selectable marker: Excellent stability in complex media, and high-level expression of a recombinant protein from a *CUP1*-promoter-controlled expression cassette in *cis.Yeast, 11*, 1-14.

40. Hubbert, C., Guardiola, A., Shao, R., Kawaguchi, Y., Ito, A., Nixon, A., Yoshida, M., Wang, X. F. & Yao, T. P. (2002) HDAC6 is a microtubule-associated deacetylase. *Nature* 417, 455-458.

41. Jacobson, R. H., Ladumer, A. G., King, D. S. & Tjian, R. (2000). Structure and function of a human TAFII250 double bromodomain module. *Science, 288,* 1422-1425.

42. Jensen, L. T., Howard, W. R., Strain, J. J., Winge, D. R. & Culotta, V. C. (1996) Enhanced effectiveness of copper ion buffering by *CUP1* metallothionein compared with CRS5 metallothionein in *Saccharomyces cerevisiae*. *J. Biol. Chem. 271*(31), 18514-18519.

43. Karin, M., Najarian, R., Haslinger, A., Valenzuela, P. & Wech, J. (1983). Primary structure and transcription of an amplified genetic locus: The *CUP1* locus of yeast.Proc. *Natl. Acad. Sci. USA. 81,* 337-341.

44. Kelly, T. J., Qin, S., Gottschling, D. E. & Parthun, M. R. (2000). Type B histone acetyltransferase Hat1p participates in telomeric silencing. *Mol Cell Biol, 20,* 7051-7058.

45. Kim, J. H., Saraf, A., Florens, L., Washburn, M. & Workman, J. L. (2010) Gcn5 regulates the dissociation of SWI/SNF from chromatin by acetylation of Swi2/Snf2. *Genes Dev. 24*(24), 2766-2771.

46. Kim, Y., Mclaughlin, K., Linstrom, T., Tsukiyama, D. J. & Clark, D. J. (2006) Activation of *Saccharomyces cerevisiae HIS3* results in Gcn4p-dependent, SWI/SNF-dependent mobilization of nucleosomes over the entire gene. *Mol. Cell. Biol*. *26*, 8607-8622.

47. Kreb, J. E., Fry, C. J., Samuels, M. L. & Peterson, C. L. (2000). Global role for chromatin remodeling enzymes in mitotic gene expression. *Cell, 102,* 587-598.

48. Kuo, M.-H., Broenell, J. E. Sobel, R. E., Ranalli, T. A., Cook, R. G., Edmonoson, D. G., Roth, S. Y. & Allis, C. D. (1996). GCN5p, a yeast nuclear histone acetyltransferase, acetylates specific lysine in histone H3 and H4 that differ from deposition-related acetylation sites. *Nature, 383,* 269-272.

49. Lancher, M., O' Sulliva, R. J. & Jenuwein, T. (2003). An epigenetic road map for histone lysine methylation. *J Cell Sci, 116,* 2117-2124.

50. Lee, K.K., Prochasson, P., Florens, L., Swanson, S.K., Washburn, M.P. & Workman, J.L. (2004) Proteomic analysis of chromatin-modifying complexes in Saccharomyces cerevisiae identifies novel subunits. *Biochem. Soc. Trans. 32*(6), 899-903.

51. Longworth, M. S. & Laimins, L. A. (2006) "Histone deacetylase 3 localizes to the plasma membrane and is a substrate of Src". *Oncogene 25* (32), 4495–500.

52. Luger, K. (2003) Structure and dynamic behavior of nucleosomes. *Curr. Opin. Genet. Dev.13*, 127-135.

53. Luger, K., Mader, A. W., Richmond, R. K., Sargent, D. F. & Richmond, T. J. (1997) Crystal structure of the nucleasome core particle at 2.8A resolution. *Nature* 389, 251-260.

54. Luger, K. & Richmond, T. J., (1998) DNA binding within the nucleosome core. *Curr. Opin. Struct. Biol. 8*(1), 33-40.

55. Margueron, R., Trojer, P. & Reinberg, D. (2005). The key to development: interpreting the histone code? *Curr Opin Genet Dev*, *15*, 163-176.

56. Marmorstein, R. (2001). Protein Modules that manipulate histone tails for chromatin regulation. *Nat Rev Mol Cell Biol*, *2*, 422-431.

57. Mateescu, B., England, P., Halgand, F., Yaniv, M. & Muchardt, C. (2004). Tethering of HP1 proteins to chromatin is relieved by phosphoacetylation of histone H3. *EMBO Rep*, *5*, 490-496.

58. McGhee, J. D. & Felsenfeld G. (1980) Nucleosome Structure. *Ann. Rev. Biochem.*, *49*, 1115-1156.

59. Mellor, J. & Morillon, A., (2004) ISWI complexes in *Saccharomyces cerevisi*ae *Biochem Biophys Acta*. *1677*(1-3), 100-112.

60. Meloni, G., Faller, P. & Vasák, M. (2007) Redox silencing of copper in metal-linked neurodegenerative disorders: reaction of Zn7metallothionein-3 with Cu2+ ions. *J. Biol. Chem*. *282*(22), 16068-16078.

61. Meloni, G., Sonois, V., Delaine, T., Guilloreau, L., Gillet, A., Teissié, J., Faller, P. & Vasák, M. (2008) Metal swap between Zn7-metallothionein-3 and amyloid-beta-Cu protects against amyloid-beta toxicity. *Nat. Chem. Biol. 4*(6), 366-372.

62. Mizzen, C. A., Yang, X. J., Kokubo, T., Brownell, J. E., Bannister, A. J., Owen-Hughes, T., Workman, J., Wang, L., Berger, S. L., Kouzarides, T., Nakatani, Y. & Allis, C. D. (1996). The TAF(II)250 subunits of TFIID has histone acetyltransferase activity. *Cell*, *87*, 1261-1270.

63. Mohrmann, L. & Verrijzer, C.P. (2005) Composition and functional specificity of SWI2/SNF2 class chromatin remodeling complexes. *Biochim Biophy Acta*. *1681*, 59-73.

64. Morrison, A. J., Highland, J., Krogan, N. J., Arbel-Eden, A., Greenblatt, J. F., Haber, J. E. & Shen, X. (2004) INO80 and gamma-H2AX interaction links ATP-dependent chromatin remodeling to DNA damage repair. *Cell. 119*,767–775.

65. Muchardt, C. & Yaniv, M. (1999) ATP-dependent chromatin remodelling: SWI/SNF and Co. are on the job. *J Mol Biol*. *293*(2), 187-198.

66. Ng, H. H., Xu, R. M., Zang, Y. & Struhl, K. (2002). Ubiquitination of histone H2B by Rad6 is required for Dot1-medated methylation of histone H3 lysine 79. *J Biol Chem*, *277*, 34655-34657

67. Nishioka, K., Rice, J. C., Sarma, K., Erdjument-Bromzge, H., Werner, J., Wang, Y., Chuikov, S., Valenzuela, P., Tempst, P., Steward, R., Lis, J. T., Allis, C. D. & Reinberg, D. (2002). PR-Set7 is a nucleosome-specific methyltransferase that modifies lysine 20 of histone H4 and is associated with silent chromatin *Mol Cell, 9,* 1201-1213.

68. Noma, K. I., Allis, C. D. & Grewal, S. I. S. (2001) Transitions in distinct histone H3 methylation patterns are the heterochromatin domain boundaries. *Science* 293, 1150-1155.

69. O'Carroll D, et al. (2000) Isolation and characterization of Suv39H2, a second histon H3 methyltransferase gene that displays testis-specific expression. *Mol. Cell. Biol. 20*,9423-9433.

70. Ogryzko, V. V., Schiltz, R. L., Russanova, V., Howard, B. H. & Nakatani, Y. (1996). The transcriptional coactivators p300 and CBP are histone acetyltransferases. *Cell, 87,* 953-959.

71. Parthun, M. R. (2007). Hat1: the emerging cellular roles of a type B acetyltransferase. *Oncogene, 26,* 5319-5328.

72. Peterson, C. L. & Laniel, M. C. (2004). Histones and histone modifications. *Curr Biol, 14,* R546- R551.

73. Petrlova, J., Blastik, O., Prusa, R., et al. (2006) Determination of metallothionein content in patients with brest and colon cancer, and malignant melanoma. *Klin. Onkol*. 19, 138-142.

74. Poveda, A., Pamblanco, M., Rafrov, S., Tordera, V., Srernglanz, R. & Sendra, R. (2004). Hif1 is component of yeast histone acetyltransferacse b, a complex mainly localized in the nucleus. *J Biol Chem, 279,* 16033-16043.

75. Pray-Grant, M.G., Daniel, J.A., Schieltz, D., Yates, J. R. & Grant, P. A. (2005) Chd1 chromodomain links histone H3 methylation with SAGA- and SLIK-dependent acetylation. *Nature* 433, 434-438.

76. Quana, A. S., Buschbeck, M. & Croce, L. Di. (2006). Chromatin structure and epigenetics. *Biochemical Pharmacology, 72,* 1563-1569.

77. Rea, S., Eisenhaber, F., O'Carrol, D., Strahl, B. D., Sun, Z. W., Schmid, M., Opravil, S., Mechtler, K., Ponting, C. P., Allis, C. D. & Jenuwein, T. (2000). Regulation of chromatin structure by site-specific histone H3 methyltransferases. *Nature, 406,* 593-599.

78. Reinke, H., Gregory, P. D. & Horz, W. (2001). A transient histone hyper-acetylation signal marks nucleosomes for remodeling at the *PHO8* promoter *in vivo*. *Mol Cell*, *7,* 529-538.

79. Roth, S. Y., Denu, J. M. & Allis, C. D. (2001). Histone Acetyltransferases. *Annu Rev Biochem, 70,* 81-120.

80. Sambrook, J., Fritsch, E. F. & Maniatis, T. (1989) Molecular Cloning: a laboratory manual. 2nd ed. N.Y., Cold Spring Harbor Laboratory, Cold Spring Harbor Laboratory Press, 1659 p. ISBN 0-87969-309-6.

81. Santos-Rosa, H., Schneider, R., Bannister, A. J., Sherriff, J., Bernstein, B. E., Emre, N. C., Schreiber, S. L., Mellor, J. & Kouzarides, T. (2002). Active genes are tri-methylated at K4 of histone H3. *Nature, 419,* 407-411.

82. Sato, M. & Bremner, I. (1993) Oxygen free radicals and metallothionein. *Free. Rad. Biol. 14*, 325-337.

83. Schwaish M. A. & Strul, K. (2007) The Swi/Snf complex is important for histone eviction during transcription activation and RNA Ploymerase II elongation in vivo. *Mol. Cell. Biol. 27* (20) 6987-6995.

84. Sengupta, N. & Seto, E., (2004). "Regulation of histone deacetylase activities". *J. Cell. Biochem. 93* (1), 57–67.

85. Shen, C.-H., Leblanc, B.P., Altfieri, J. A. & Clark, D. J. (2001). Remodeling of yeast *CUP1* chromatin involves activator-dependent repositioning of nucleosomes over the entire gene and flanking sequences. *Mol. Cell. Biol*. *21*, 534-547.

86. Shen, C-H., Leblance, B. P., Alfieri, J.A. & Clark, D. J. (2001). Remodeling of yeast *CUP1* chromatin involves activator-dependent repositioning of nucleosomes over the entire gene and flanking sequences. *Mol Cell Biol, 21,* 534-547.

87. Shen, C-H.,Leblanc, B. P., Neal, C., Akhaven, R. & Clark, D. J. (2002). Targeted histone acetylation at the yeast *CUP 1* promoter requires the transcriptional activator, the TATA boxes, and the putative histone acetylase encoded by *SPT10*. *Mol Cell Biol*, *22*, 6406-6416.

88. Shen, X., Mizuguchi, G., Hamiche, A. & Wu, C. (2000) A chromatin remodelling complex involved in transcription and DNA processing. *Nature 406*,541–544.

89. Smith, E. R., Belote, J. M., Schiltz, R. L., Yang, X. J., Moore, P. A., Berger, S. L., Nakatani, Y. & Allis, C. D. (1998). Cloning of Drosophila GCN5: conserved features among metazoan GCN5 family members. *Nucleic Acids Res, 26,* 2948-2954.

90. Spencer, T. E., Jenster, G., Burcin, M. M., Allis, C. D., Zhou, J., Mizzen, C. A., McKenna, N. J., Onate, S. A., Tsai, S. Y., Tasai, M. J. & O'Maley, B. W. (1997). Steroid receptor coactivator-1 is a histone acetyltransferase. *Nature, 389,* 194-198.

91. Sterner, D. E. & Berger, S. L. (2000). Acetylation of Histones and Transcription-Related Factors. *Microbio Mole Biol Rev, 64,* 435-459.

92. Stockdale, C., Flaus, A., Ferreira, H. & Owen-Hughes, T. (2006) Analysis of Nucleosome Repositioning by Yeast ISWI and Chd1 Chromatin Remodeling Complexes. *J. Biol. Chem. 281*(24), 16279-16288.

93. Sudarsanam, P., Cao, Y., Wu, L., Laurent, B. C. & Winston, F. (1999) The nucleosome remodeling complex, Snf/Swi, is required for the maintenance of transcription in vivo and is partially redundant with the histone acetyltransferase, Gcn5. *EMBO. J. 18*(11), 3101-3106.

94. Svaren, J. & Ho rs, W.(1997). Transcription factor vs. nucleosomes: regulation of the *PHO5* promoter in yeast. *Trends Biochem Sci, 22,* 93-97.

95. Szczypka, M. S. & Thiele, D. J (1989) metallothionein gene transcription. A cysteine-rich nuclear protein activates yeast *Mol. Cell. Biol. 9*(2),421-429.

96. Tachibana, M., Sugimoto, K., Fukushima, T. & Shinkai, Y. (2001). Set domain containing protein, G9a, is a novel lysine-preferring mammalian histone methyltransferase with hyperactivity and specific selectivity to lysines 9 and 27 of histone H3. *J Biol Chem, 276,* 25309-25317.

97. Thiele, D. J. (1988) ACE1 regulates expression of the *Saccharomyces cerevisiae* metallothionein gene. *Mol. Cell Biol*. *8*(7), 2745-2752.

98. Thoma, F., Koller, T. & Klug, A., (1979). Involvement of histone H1 in the organization of the nucleosome and of the salt-dependent superstructures of chromatin. *J. Cell Biol. 83*, 403–427.

99. Tremethick, D. J.,(2007) Higher order structures of chromatin: the elusive 30nm fiber. *Cell.128*,651-154

100. Tsukiyama, T. (2002) The in vivo functions of ATP-dependent chromatin-remodeling factors. *Nat Rev Mol Cell Biol. 3*,422-429.

101. Tsukiyama, T., Palmer, J., Landel, C.C., Shiloach, J., Wu C., (1999) Characterization of the imitation switch subfamily of ATP-dependent chromatin-remodeling factors in Saccharomyces cerevisiae1, *Genes Dev. 13*(6),686-697.

102. Tsukiyama, T. & Wu C., (1997) Chromatin remodeling and transcription. Curr Opin *Genet Dev*. *7*(2),182-191.

103. Utley, R. T., Ikeda, K., Grant, P. A., Cote, J., Steger, D. J., Eberharter, A., John, S. & Workman, J. L. (1998). Transcriptional activators direct histone acetyltransferase complexes to nucleosomes. *Nature*, *98,* 498-502.

104. van Attikum, H., Fritsch, O., Hohn, B. & Gasser, S. M. (2004) Recruitment of the INO80 complex by H2A phosphorylation links ATP-dependent chromatin remodeling with DNA double-strand break repair.*Cell 119*,777–788.

105. Wang, H. Cao, R., Xia, L., Erdjument-Bromzge, H., Borchres, C., Tempst, P. & Zhang, Y. (2001) Lysine methylation within the globular domain of histone H3 by Dot1 is important for telomeric silencing and Sir protein association *Mol Cell*, *8*, 1207-1217

106. Wang, H., Huang, Z. Q., Xia, L., Feng, Q., Erdjument-Bromzge, H., Strahl, B. D., Briggs, S. D., Allis, C. D., Wong, J., Tempst, P. & Zhang, Y.(2001). ethylationof histone H4 at arginine 3 facilitating transcriptional activation by nuclear hormone receptor. *Science*, *298*, 853-857.

107. Vary, J.C., Gangaraju, V. K., Oin, J., Landel, C.C., Kooperberg, C., Bartholomew, B. & Tsukiyama, T., (2003) Yeast Isw1p forms two separable complexes in vivo. *Mol. Cell. Biol. 23*(1), 80-91

108. Weinlich, G. (2009) Metallothionein-overexpression as a prognostic marker in melanoma. G. Ital. Dermatol. Venereol. *144*(1), 27-38.

109. Weinlich, G., Eisendle, K., Hassler, E., et al. (2006) Metallothionein – overexpression as a highly significant prognostic factor in melanoma: aprospective study on 1270 patients. *Brit. J. Cancer. 94*, 835- 841.

110. Venters, B.J., Pugh, B. F. (2009) How eukaryotic genes are transcribed. *Cir Rev Biochem Mol Biol. 44* (2-3),117-141

111. Wenzheng Zhang, W., Bone, J. R., Edmondson, D. G., Turner, B. M. & Roth, S. Y. (1998). Essential and redundant functions of histone acetylation revealed by mutation of target lysines and loss of the Gcn5p acetyltransferase. *EMBO J*, *17*, 3155-3167.

112. Viarengo, A. & Nott, J. A. (1993) echanism of heavy metal action homeostasis in marine invertebrates. *Camp. Biochem. Phsiol. Part C 104*, 335-372.

113. Viarengo, A. (1989) Heavy metal in marine invertebrate: mechanisms of regulation and toxicity at the cellular level. *CRC Crit. Rev. Aquat. Sci*. *1*, 295-317.

114. Wu, W.H., Alami, S., Luk, E., Wu, C.H., Sen, S., Mizuguchi, G., Wei, D. & Wu, C. (2005) Swc2 is a widely conserved H2AZ-binding module essential forATP-dependent histone exchange, *Nat. Struct. Mol. Biol*. *12*, 1064–1071

115. Xu, W., Edmondson, D. G. & Roth, S. Y. (1998). Mammalian GCN5 and P/CAF acetyltransferases have homologous amino-terminal domain important for recognition of nucleosomal substrates. *Mol Cell Biol, 18,* 5659-5669.

116. Yamamoto, T. & Horikoshi, M. (1997). Novel substrate specificity of the histone acetyltransferase activity of HIV-1-Tat interactive protein Tip60. *J Biol Chem, 272,* 30595-30598.

117. Yang L, et al. (2002) Molecular cloning of ESET, a novel histone H3 specific methyltransferase that interacts with ERG transcription factor. *J. Biol. Chem. 277*,148-152

118. Yang, X-J. (2004). The diverse super family of lysine acetyltransferases and their roles in leukemia and other diseases. *Nucleic Acid Res,* 32, 959-976.

119. Zhang, J-G., Liu, X-Y., He, X-P., Guo, X-N., Lu, Y. & Zhang, B. (2011) Improvement of acetic acid tolerance and fermentation performance of Saccharomyces cerevisiae by disruption of the FPS1 aquaglyceroporin gene. *Biotechnol Lett* 33, 277–284.